Aus dem Institut für Anatomie und Zellbiologie
der Philipps-Universität Marburg
Abteilung Molekulare Neurowissenschaften
Direktor: Professor Dr. med. E. Weihe

Pathway-specific expression of calcitonin receptors in hypothalamic and brain stem nuclei regulating food intake and transcriptomic changes in hypothalamic orexin neurons after fasting

Inaugural Dissertation
zur Erlangung des Doktorgrades der Humanbiologie
(Dr. rer. physiol.)

dem Fachbereich Humanmedizin
der Philipps-Universität Marburg
vorgelegt

von
Ailing Ji
aus Henan, V. R. China

Marburg 2005

Angenommen vom Fachbereich Humanmedizin
der Philipps-Universität Marburg am 22. 07. 2005
Gedruckt mit Genehmigung des Fachbereichs
Dekan: Prof. Dr. med. Bernhard Maisch
Referent: Prof. Dr. med. Eberhard Weihe
Korreferent: Prof. Dr. Karlheinz Voigt

CONTENTS

1. Introduction

1.1 The control of food intake by the central nervous system

Food intake is highly regulated. Despite the fact that composition and amount of food that we eat varies considerably from one meal and one day to the next, the cumulative energy intake is matched to energy expenditure with great precision when measured over a period that spans many meals (Schwartz et al. 2000). Disorders of food intake lead to obesity, a major risk factor for developing cardiac disease and type 2 diabetes mellitus (Broberger and Hokfelt 2001), or lead to anorexia in the course of chronic pathophysiological processes including cancer and infectious disease (Plata-Salaman 2000). Both are associated with increased mortality. Recently, there has been a tremendous increase in our understanding of how the brain senses energy deficit and excess. The homeostatic regulatory systems are located mainly in the hypothalamus and brain stem (Berthoud 2004). Here, peptidergic neurons are found which serve as recipients of hormonal and nerval signals from the gastrointestinal tract, adipose tissue and other peripheral organs. These peptidergic cell populations project reciprocally to many other regions (Broberger and Hokfelt 2001). A multitude of neurotransmitters and peptidergic neuromodulators participate in these hypothalamic and brain stem "feeding pathways" and exert powerful effects on food intake.

A milestone in the understanding of the neuropeptidergic regulation of body weight and food intake was the discovery of leptin, a hormone/cytokine produced by adipocytes that mediates satiety signals to the hypothalamus causing a reduction in food intake and loss of body weight (Zhang et al. 1994). Leptin circulates at levels proportional to body fat content and enters the CNS in proportion to its plasma levels (Schwartz et al. 1996). Administration of leptin directly into the brain reduces food intake (Campfield et al. 1995). Other hormones have opposite effects such as ghrelin, which is released from the stomach and sends orexigenic signals to the brain producing appetite and increased food intake (Inui 2001) resulting in weight gain (Tschop et al. 2000). The anorexigenic hormone amylin, which belongs to the calcitonin peptide family, is secreted from the endocrine pancreas and contributes to feeding-related changes of neuronal activity in the brain stem (Riediger et al. 2004). However, its precise role and sites of action in the brain stem and in the hypothalamus are less well studied. The current model of the hypothalamus and brain stem circuitry

involved in the action of peripheral signals on feeding-regulatory circuitry is illustrated in Fig. 1.

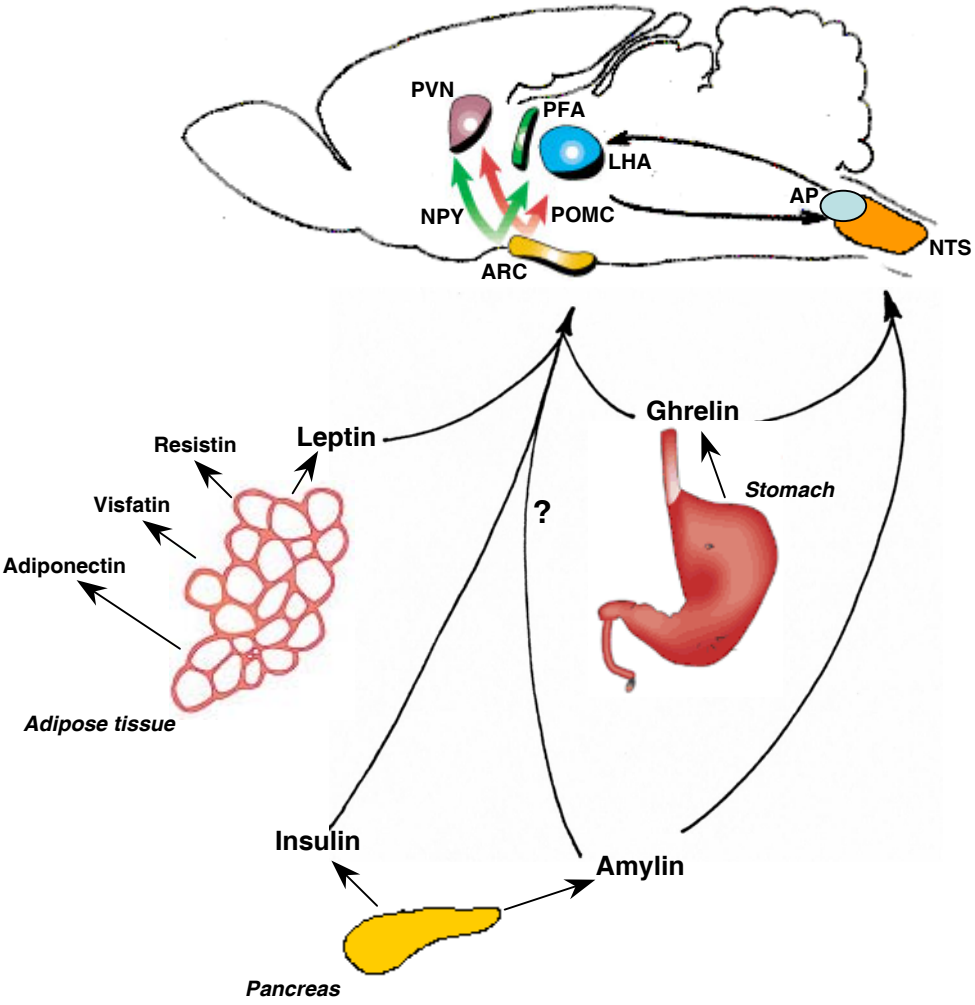

Fig. 1 A model of the action of peripheral signals on feeding-regulatory circuitry

Peripheral signals related to long-term energy stores are produced by adipose tissue (leptin) and the pancreas (insulin). Leptin and insulin reduces food intake by acting on hypothalamic pathways, which originate in the arcuate nucleus (ARC) of the hypothalamus and project to the paraventricular nucleus (PVN) and the lateral hypothalamic area (LHA). Ghrelin is released mainly from the stomach to increase appetite and food intake by acting on hypothalamic neurons and the nucleus of the solitary tract (NTS) of the brain stem. The NTS of the brain stem plays an important role in mediating the anorectic effect of the pancreatic hormone amylin, which is co-secreted with insulin from the pancreas in response to food ingestion. The involvement of higher brain centers, especially hypothalamic structures, in the regulation of the anorectic effect of amylin remains to be investigated. A number of adipocyte-derived hormones adiponectin, resistin and visfatin are found to play an important role in the regulation of food intake and energy expenditure. Adiponectin increases insulin sensitivity. By contrast, resistin induces insulin resistance in obesity. Visfatin stimulates glucose uptake by adipocyte and

muscle cells and decreases blood glucose levels. (Modified after Schwartz et al. 2000 and Badman and Flier 2005).

1.1.1 Feeding-related nuclei of the rodent hypothalamus

The hypothalamus is the area of the diencephalon ventral to the hypothalamic sulcus. It is involved in a variety of functions including the control of anterior pituitary function through secretion of hypothalamic releasing factors (Murakami et al. 1991), control of brain stem and spinal cord autonomic centers related to cardiovascular (Michelini 2001), respiratory (Kc et al. 2002), and gastrointestinal functions (Grill and Kaplan 2001), control of body temperature (Boulant 2000), wakefulness and sleep (Hagan et al. 1999), and regulation of feeding behavior through hypothalamic satiety and feeding centers (Broberger and Hokfelt 2001).

The mammalian hypothalamus consists of several nuclei involved in the regulation of food intake, including the arcuate nucleus (ARC), the paraventricular nucleus (PVN), the lateral hypothalamic area (LHA), the ventromedial nucleus (VMH), and the dorsomedial nucleus (DMH) (see Fig. 1) (Schwartz et al. 2000). The involvement of the hypothalamus in the regulation of feeding behavior was first shown in lesion studies (Hetherington and Ranson 1940) and in electrical stimulation experiments. These studies led to the development of the "Dual Center Model" for regulation of feeding, in which the medial part of the hypothalamus, in particular the VMH, was regarded as the "satiety centre", and the LHA as the "feeding centre". The "Dual Center Model" was based on the ability of electrical stimulation of the VMH to suppress food intake, and of bilateral VMH lesions to induce hyperphagia and obesity. Conversely, stimulation or lesioning of the LHA induced the opposite response. While these studies were strikingly precise in identifying the subregions of the hypothalamus in which circuits promote or suppress feeding, a major breakthrough in the understanding of the central regulation of feeding behavior was achieved with the identification of hypothalamic neuropeptides influencing feeding behavior such as neuropeptide Y (NPY; for review see Schwartz et al. 2000; Horvath and Diano 2004).

The arcuate nucleus (ARC), located at the bottom of the hypothalamus surrounding the third ventricle, has been implicated in the control of feeding behaviour. Damage to this region in mice resulted in a phenotype of hyperphagia and obesity (Olney 1969). At least two distinct subnuclear regions can be distinguished in the ARC, a medial part consisting of neurons that co-express the orexigenic

neuropeptides NPY and agouti-gene-related protein (AgRP), and a lateral part consisting of neurons that co-express the anorexigenic neuropeptides pro-opiomelanocortin (POMC) and cocaine- and amphetamine-regulated transcript (CART). These two neuronal populations are called ‘first order neurons’ because they express the specific receptors for the peripheral adiposity factors such as leptin, which can modulate the activity of these neurons directly, due to the lack of the blood brain barrier (BBB) in the median eminence (ME), where the nerve terminals of arcuate neurons are in direct contact with the bloodstream (Hillebrand et al. 2002). Leptin regulates body weight via interaction with specific leptin receptors (Ob-R) coupling to the JAK-STAT (Janus kinase-signal transducers and activators of transcription) pathway of signal transduction (Hakansson and Meister 1998). The majority of both NPY/AGRP and POMC/CART neurons have been found to express Ob-Rs (Cheung et al. 1997; Baskin et al. 1999). STAT3 immunoreactivity has been shown in these neurons (Hakansson and Meister 1998). Both types of neurons are regulated by leptin but in opposite directions. Leptin inhibits NPY synthesis and release (Stephens et al. 1995) and increases POMC mRNA expression (Schwartz et al. 1997). NPY neurons in the ARC are probably the primary targets mediating ghrelin-induced orexigenic effect. Ghrelin receptors have been identified on NPY neurons (Willesen et al. 1999). Peripheral administration of ghrelin induces Fos expression selectively in NPY neurons (Wang et al. 2002).

From the arcuate ncl., NPY/AGRP and POMC/CART neurons project to "second order neurons" which are located in the PVN, VMH, DMH, and LHA.

Several neuropeptides synthesized in PVN neurons reduce food intake and body weight when administered centrally. These include corticotropin-releasing hormone (CRH), also refered to as corticotropin-releasing factor (CRF), which causes anorexia and activates the sympathetic nervous system in addition to its role as a major regulator of the hypothalamic-pituitary-adrenal axis (Hotta et al. 1991); thyrotropin-releasing hormone (TRH), which reduces food intake in addition to stimulating the thyroid axis (Steward et al. 2003); and oxytocin, which reduces food intake (Verbalis et al. 1995) in addition to regulating uterine contractility (Ahn et al. 2004), milk ejection (Wakerley et al. 1990), memory peocessing (Heinrichs et al. 2004), social behavior (Keverne and Curley 2004) and autonomic functions (Mack et al. 2002).

The hypothesis that "second order neurons" involved in anabolic signaling reside within the LHA is supported by studies of melanin-concentrating hormone (MCH), an orexigenic peptide located in this brain area (Nahon 1994). Evidence that food consumption is increased by injection of MCH into the lateral ventricles of rats (Qu et al. 1996), and the discovery that MCH-knockout mice have reduced body weight and leanness due to hypophagia (Shimada et al. 1998) have suggested MCH as an orexigenic factor. Two additional peptides, termed hypocretin 1 and hypocretin 2 (de Lecea et al. 1998), also named 'orexin A and orexin B' (Sakurai et al. 1998), are expressed exclusively in the LHA. These peptides increase food intake in addition to causing generalized behavioural arousal when administered centrally (Sakurai et al. 1998; Hagan et al. 1999). The MCH gene is up-regulated in leptin-deficient *ob*/*ob* mice and leptin-insensitive *db*/*db* mice, whereas the orexin/hypocretin gene is down-regulated in these mice (Qu et al. 1996; Yamamoto et al. 1999), indicating that the MCH and orexin systems are regulated through different pathways.

The LHA is the most extensively interconnected area of the hypothalamus. Within the hypothalamus the lateral zone has reciprocal connections to the arcuate and paraventricular nuclei, and efferent projections to the dorsomedial, ventromedial and anterior hypothalamic nuclei. (Berthoud 2002). Rather than being passive recipients of information from the arcuate nucleus, these second order neurons process and transmit their input information via efferent projections to intrahypothalamic and extrahypothalamic sites. These include the hippocampal formation, extended amygdala, basal ganglia and thalamus, the midbrain and pons, the brain stem and spinal cord, allowing it to modulate many different functions from cognitive to autonomic. Most of the connections to brain stem and midbrain areas are reciprocal (Berthoud 2002).

1.1.2 Feeding-related regions of the brain stem

The brain stem is another important region in the brain to regulate food intake and body weight. All along the alimentary canal, various mechano- and chemosensors are located that transmit food and nutrition related signals via primary visceral afferents in the trigeminal (V), facial (VII), glossopharyngeal (IX), or vagus nerve (X) to the brain stem (Berthoud 2002). The gastrointestinal hormone cholecystokinin (CCK) is produced by mucosal enteroendocrine cells of the duodenum and jejunum and secreted in response to the presence of food within the gut lumen (Badman and Flier

2005). It contributes to the regulation of short-term food intake and is involved in the mediation of satiety (Glatzle et al. 2001). CCK activates neurons of the nucleus of the solitary tract (NTS) via stimulation of CCK-A receptors on vagal afferent nerve fibers supplying the gastrointestinal tract, which derive from the nodose ganglion, and have monosynaptic contact with NTS neurons (Raybould et al. 1988). Visceral primary afferent signaling is, however, not the only mode of communication between the gut and brain stem. Besides activating vagal afferent nerve fibers, circulating CCK may also act on CCK-A receptors in the area postrema (AP), a region of the brain stem that has a leaky blood-brain barrier and monosynaptic connection to the NTS (Glatzle et al. 2001).

The AP/NTS region of the brain stem plays an important role in the control of food intake (Hyde and Miselis 1983). This region receives nervous input from peripheral satiety signals via splanchnic and vagal afferents and hormonal input as well. Due to the lack of the blood brain barrier, receptors in this region can be reached directly by respective ligands circulating in the blood. The brainstem is sufficient for the integration of taste and gastrointestinal signals that co-determine the size of meals in the short term. However, if the brainstem is isolated from forebrain influences it is not sufficient for ingestive responses to systemic/metabolic signals that affect food intake over the long term (Grill and Kaplan 2001). The communication between hypothalamic pathways and the caudal brain stem, responding to meal-related satiety signals, is essential for the long-term regulation of energy homeostasis.

1.2 Neuropeptides in the control of food intake and energy balance

1.2.1 Orexigenic and anorexigenic peptides

Over the past few years numerous novel signaling molecules, most of them, that affect food intake and that are critical for normal energy homeostasis have been identified when injected i.c.v. or in specific hypothalamic regions. These neuropeptides, listed in table 1, can be divided into orexigenic peptides which refer to molecules that promote increased energy intake, and anorexigenic peptides which cause the opposite.

Table 1 Neuropeptides implicated in the control of energy homeostasis

Neuropeptide	Treatment	Food intake	Reference
Orexigenic			
NPY	PVN injection	↑	(Stanley et al. 1986)
AgRP	CNS administration	↑	(Small et al. 2003)
MCH	i.c.v. injection	↑	(Qu et al. 1996)
Orexin A	i.c.v. administration	↑	(Haynes et al. 1999)
Orexin B	i.c.v. administration	↑/-	(Edwards et al. 1999)
Galanin	PVN injection	↑	(Kyrkouli et al. 1990)
Ghrelin	i.c.v. injection	↑	(Nakazato et al. 2001)
Anorexigenic			
α-MSH	third ventricle administration	↓	(McMinn et al. 2000)
β-MSH	i.c.v. injection	↓	(Kask et al. 2000)
CART	i.c.v. injection	↓	(Kristensen et al. 1998)
CRH	i.c.v. administration	↓	(Hotta et al. 1991)
TRH	third ventricle administration	↓	(Steward et al. 2003)
Oxytocin	i.c.v. administration	↓	(Verbalis et al. 1995)
Neurotensin	i.c.v. administration	↓	(Luttinger et al. 1982)
CCK	Intraventricular administration	↓	(Figlewicz et al. 1989)
GLP1	i.c.v. administration	↓	(Turton et al. 1996)
Bombesin	fourth ventricle administration	↓	(Ladenheim and Ritter 1988)
Calcitonin	third ventricle administration	↓	(Plata-Salaman and Oomura 1987)
Amylin	third ventricle administration	↓	(Rushing et al. 2000)
CGRP	PVN injection	↓	(Dhillo et al. 2003)

1.2.2 The calcitonin peptide superfamily

Calcitonin, CGRP, and amylin, three members of the calcitonin peptide superfamily, are potent modulators of food intake (Poyner et al. 2002). Calcitonin (CT) was initially discovered in 1962 as a novel hypocalcemic hormone (Copp and Cheney 1962), which is secreted from thyroid C-cells (Fischer and Born 1985). Tissue-specific alternative RNA splicing of the calcitonin gene results in the production of distinct mRNAs encoding calcitonin or calcitonin gene-related peptide α (αCGRP). The brain-specific gene product of the calcitonin gene is αCGRP which is expressed in a number of brain areas involved in modulating ingestive behavior (Fischer and Born 1985). There is no evidence for the biosynthesis of calcitonin in the central

nervous system. Calcitonin and CGRP induce multiple biological effects including inhibition of food intake after peripheral and central administration (Plata-Salaman and Oomura 1987; Dhillo et al. 2003).

The anorexigenic neuropeptide amylin, which is co-secreted with insulin from pancreatic islets β-cells in response to food ingestion (Butler et al. 1990) has been suggested as a physiological peripheral satiety agent to regulate short-term food intake (i.e., meal size) (Reidelberger et al. 2004). Recent studies have demonstrated that the AP/NTS region is involved in mediating the anorectic effect of amylin (Mollet et al. 2004). There is a coincidental sensitivity (94%) of AP neurons to glucose and amylin, which exert excitatory effects on these cells. The co-sensitivity of AP neurons to glucose and amylin, both increasing in response to food intake, points to the AP as an important hindbrain center for the integration of the metabolic and hormonal control of nutrient intake (Riediger et al. 2002). Lesion experiments demonstrated that neurons in the AP/NTS region are necessary for chronically elevated peripheral amylin to reduce food intake in rats. High doses of amylin, however, may be able to bypass AP/NTS region and reduce feeding by acting at other brain sites (Lutz et al. 2001). Feeding-induced amylin release activates AP neurons projecting to subsequent relay stations such as the NTS, the lateral parabrachial nucleus (LPBN) and the central nucleus of the amygdala (CeA) known to transmit meal-related signals to the forebrain. Activation of this pathway seems to coincide with an inhibition of LHA neurons (Riediger et al. 2004). However, the phenotype of these LHA neurons remains to be clarified. Although the effect of amylin on its primary target neurons in the AP has been well characterized, the involvement of higher brain centers, especially hypothalamic structures, is poorly understood.

Amylin has also been suggested to serve as a satiety signal acting within the brain to regulate long-term energy homeostasis (Rushing et al. 2000; Rushing 2003). Intracerebroventricular (icv) infusion of low doses of amylin into the 3rd ventricle potently and dose-dependently reduced food intake and body weight and body adiposity of rat (Rushing et al. 2000), while infusion of a specific amylin antagonist (AC187) into the third ventricle significantly increased food intake (Rushing et al. 2001). There is no evidence for amylin biosynthesis in the brain (Leffert et al. 1989). However, amylin immunoreactivity was found in brain areas including the hypothalamus (Skofitsch et al. 1995). Amylin can cross the blood-brain barrier suggesting that CNS amylin is derived from the circulation (Banks et al. 1995).

Binding sites for amylin are present in several brain regions including the nucleus accumbens, the area postrema, the nucleus of the solitary tract, the dorsal raphe, and the hypothalamus (Beaumont et al. 1993). The presence of amylin and its binding sites in discrete regions of the brain suggests that amylin might have a physiological function in the central nervous system.

Amylin, like the other peptides of the calcitonin superfamily bind to specific receptor complexes, which consist of a G-protein coupled receptor, calcitonin (CT) receptor or calcitonin receptor-like receptor (CRLR), associated with different receptor-activity-modifying proteins (RAMPs) (Poyner et al. 2002).

1.3 The calcitonin receptors

Calcitonin receptors belong to the "family B" of seven transmembrane domain G-protein-coupled receptors (7 TMD-GPCRs), which typically recognize regulatory peptides such as calcitonin (CT), parathyroid hormone (PTH), growth hormone releasing hormone, pituitary adenylate cyclase-activating peptide (PACAP), vasoactive intestinal peptide, glucagon, and glucagon-like polypeptide (Houssami et al. 1994). Binding of calcitonin (CT) to these receptors causes activation of membrane adenylyl cyclase (AC) and production of cAMP through the G protein G_s, promotion of polyphosphoinositide turnover and activation of protein kinase C (PKC) via G proteins of the G_q family; under certain conditions, CT inhibits AC via the G_i subclass of G proteins (Chakraborty et al. 1991; Chabre et al. 1992; Force et al. 1992; Orcel et al. 2000).

The human calcitonin receptor was cloned in 1992 (Gorn et al. 1992). Multiple isoforms of the human calcitonin receptor have been described to be generated by differential RNA processing (Albrandt et al. 1995; Poyner et al. 2002). The best characterized splice variants of the human CT receptor gene differ by the presence ($CT_{(b)}$ receptor) or absence ($CT_{(a)}$ receptor) of 16 amino acids in the first intracellular loop. The human CT receptor isoforms have also been referred to as hCTR1 ($CT_{(b))}$ and hCTR2 ($CT_{(a)}$), respectively (Poyner et al. 2002). The two isoforms display similar ligand affinity. However, unlike the $CT_{(a)}$ receptor, the $CT_{(b)}$ receptor is poorly internalized and has altered coupling to G proteins. Loss of G_q-mediated responses and attenuation of G_s-mediated signaling has been observed upon stimulation of $CT_{(b)}$ receptor (Moore et al. 1995).

Two rat calcitonin receptor isoforms were identified in 1993 (Albrandt et al. 1993; Sexton et al. 1993). Historically known as C1a and C1b receptor (Poyner et al. 2002), they are now referred to as $CT_{(a)}$ and $CT_{(b)}$ according to the nomenclature recommendation of the IUPHAR (International Union of Pharmacology). The difference between the two isoforms is in the presence of a 111-bp insert in $CT_{(b)}$ corresponding to a 37-amino acid insert in the predicted second extracellular domain (Sexton et al. 1993). The functional consequence of this insertion is altered ligand-binding kinetics and receptor specificity, but does not affect the ability of the receptor to couple to multiple intracellular signaling pathways (Houssami et al. 1994).

An orphan receptor with 50 and 55% overall identity to the respective calcitonin receptors was identified in 1993 in rat (Njuki et al. 1993) and in 1995 in human (Fluhmann et al. 1995) and named calcitonin receptor-like receptor (CRLR). In 1998 it was identified as a specific receptor for CGRP or for adrenomedullin, depending on its association with distinct members of a new family of single transmembrane domain proteins, designated receptor-activity-modifying proteins (RAMPs) (McLatchie et al. 1998).

1.4 Receptor-activity-modifying proteins

The RAMP family of proteins comprises three members, RAMP1, RAMP2, and RAMP3. Rat RAMP1, RAMP2, and RAMP3 share 72%, 69% and 85% homology with their respective human homologues. RAMPs are required to transport GPCRs to the plasma membrane. This was first shown by McLatchie and coworkers for CRLR. RAMP1 enables CRLR to behave as a CGRP receptor. RAMP2 and RAMP3 are required for the CRLR to recognize adrenomedullin (AM) (McLatchie et al. 1998; Muff et al. 1998; Muff et al. 2001; Muff et al. 2003).

The CT receptor does not require RAMP to bind and respond to calcitonin, but in association with RAMPs it can function as amylin or as CGRP receptor (Christopoulos et al. 1999; Muff et al. 1999). Detailed analysis of the receptor specificity of CTR/RAMPs has been performed mainly in *in vitro* systems (Tilakaratne et al. 2000). Several possible combinations between CT receptor variants and RAMPs exist. *In vitro* all three RAMPs will interact with $CT_{(a)}$ and $CT_{(b)}$ receptors to generate amylin receptors. The $CT_{(b)}$/RAMP2 displays greater affinity to amylin than that of $CT_{(a)}$/RAMP2 depending on the host cell environment (Tilakaratne

et al. 2000). The high affinity for rat amylin and markedly reduced affinity for αCGRP is characteristic for $hCT_{(a)}$/RAMP3 (Christopoulos et al. 1999). Amylin receptors with varying affinity for CGRP have been observed in competition binding studies in rat brain (van Rossum et al. 1994).

The possible combinations of the ligand-CT receptor/RAMPs complex are illustrated schematically in Fig. 2.

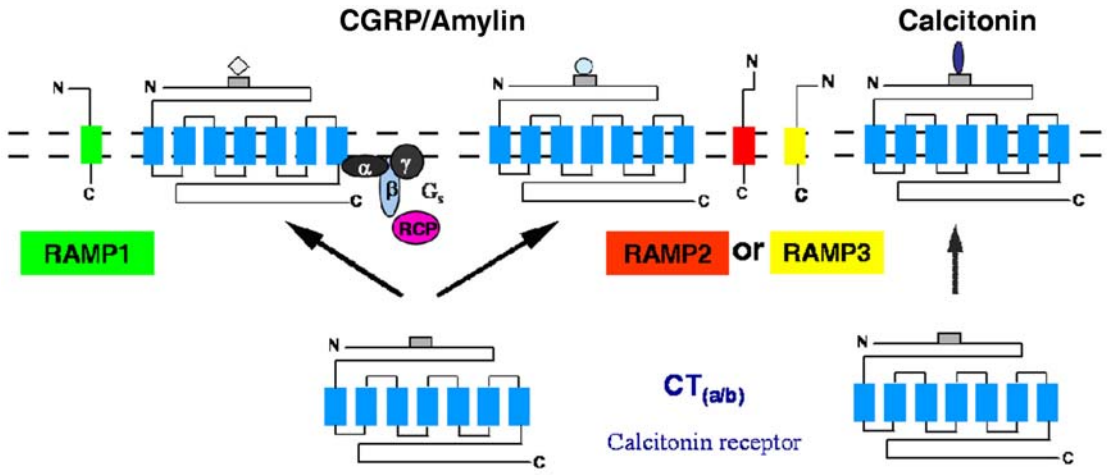

Fig. 2 Schematic diagram of the ligand-CT receptor/RAMPs complex

The calcitonin receptor does not require association with RAMPs in order to respond to calcitonin, but it can interact with RAMPs to form amylin and amylin/CGRP receptors (Modified after McLatchie et al. 1998).

The distinct molecular complexes of the CT receptor and the RAMPs are known as AMY1, AMY2, and AMY3 receptors. Splice variants of the CT receptor can be accommodated in this scheme by use of letters: $AMY_{1(a)}$, $AMY_{1(b)}$, etc, (see table 2) (Poyner et al. 2002). Unknown tissue factors clearly play an important part in determining the pharmacological properties of any given CT receptor/RAMP combination. Thus, this classification may be subject to further refinement.

Table 2 Summary of nomenclature for the calcitonin receptor isoforms / RAMPs complex

Molecular constituents	Proposed nomenclature
$CT_{(a)}$ + RAMP1	$AMY_{1(a)}$
$CT_{(a)}$ + RAMP2	$AMY_{2(a)}$
$CT_{(a)}$ + RAMP3	$AMY_{3(a)}$
$CT_{(b)}$ + RAMP1	$AMY_{1(b)}$
$CT_{(b)}$ + RAMP2	$AMY_{2(b)}$
$CT_{(b)}$ + RAMP3	$AMY_{3(b)}$

1.5 Distribution of rat calcitonin receptor isoforms

Calcitonin receptors are found widely expressed in various tissues including osteoclasts, kidney, skeletal muscle, lung, placenta, primary breast cancers, and brain (Nicholson et al. 1986; Sexton et al. 1993; Lafond et al. 1994; Albrandt et al. 1995; Gillespie et al. 1997).

Molecular studies using PCR revealed that $CT_{(b)}$ has a more restricted distribution, being primarily localized to the central nervous system, specifically the nucleus accumbens, hypothalamus, and brainstem, while the $CT_{(a)}$ isoform is more widely distributed (Sexton et al. 1993). Apart from the CNS, $CT_{(a)}$ is also expressed in the kidney (Sexton et al. 1993), skeletal muscle and lung (Albrandt et al. 1993). In vitro autoradiography demonstrated that brain regions displaying $CT_{(a)}$, but little or no $CT_{(b)}$, binding sites include the nucleus of the solitary tract and the area postrema. Nuclei expressing exclusively $CT_{(b)}$ receptors have not been identified yet (Hilton et al. 1995).

Immunohistochemistry was used to characterize the expression of CT receptors in rat brain at the protein level (Becskei et al. 2004). However, the antibodies employed could not distinguish between different CT isoforms. In situ hybridization was employed to demonstrate the expression of CT receptor genes in rat (Sheward et al. 1994; Tolcos et al. 2003; Barth et al. 2004) and mouse brain (Nakamoto et al. 2000). However, a detailed analysis of the pathway and neuron-specific distribution of the $CT_{(a)}$ and $CT_{(b)}$ isoforms in specific brain structures and nuclei and in phenotype-identified neurons has not been performed.

1.6 Aims

Since little is known on the pathway-specific expression and role of calcitonin receptors in the brain and its regulatory centers for food intake and energy expenditure, it was the main aim of this thesis to identify and compare the distribution of $CT_{(a)}$ and $CT_{(b)}$ isoforms and associated receptor complexes (RAMPs) in the rat brain with special emphasis on the feeding centers in the hypothalamus and brain stem and phenotype-identified neurons therein in order to characterize cellular and molecular mechanisms underlying CT-receptor mediated signaling in brain feeding pathways and beyond. The specific aims were the following:

1. **Comparison of gene expression of calcitonin receptor isoform expression in rat brain**

   To determine the expression patterns of the $CT_{(a)}$ and $CT_{(b)}$ calcitonin receptor isoforms, their mRNA expression was investigated in specific brain structures and nuclei with particular focus on regions which are involved in the regulation of food intake and energy expenditure by employing RT-PCR, laser capture microdissection (LCM) in combination with RT-PCR, and in situ hybridization (ISH).

2. **Cell-specific expression of calcitonin receptor isoforms in phenotype-identified hypothalamic and brain stem neurons involved in the regulation of food intake**

   To elucidate whether CT receptor isoforms could play a role in the central regulation of food intake, their mRNA expression was investigated by dual in situ hybridization for coexistence with neuropeptides with proven relevance in the control of food intake. In the hypothalamus, NPY, POMC, CART, CRH, TRH, MCH and especially hypocretin/orexin neurons were tested for coexpression of CT receptor isoforms. In the area postrema, TRH neurons were characterized with respect to their content of CT receptor isoforms. This strategy should reveal the specific cellular sites of CT receptor function in relation to food intake.

3. **Identification of CT receptor/RAMPs complexes in hypocretin/orexin neurons**

   In order to further elucidate the possible functional significance of CT receptor isoforms in hypothalamic hypocretin/orexin neurons, these neurons were tested for their content of receptor-activity-modifying proteins (RAMP 1, 2, 3) in relation to CT receptor isoforms by dual in situ hybridization.

4. **Identification of CGRP terminals on orexin neurons**

   Based on the hypothesis that CGRP could act as an endogenous ligand for CT receptors on orexin neurons, double immunohistochemistry for CGRP and orexin was performed to find out whether CGRP terminals target orexin neurons.

5. **Identification of classical neurotransmitters in orexin neurons**

   To determine whether orexin neurons are glutamatergic or GABAergic, they were tested for co-expression with the vesicular glutamate transporter VGLUT2 as a marker of glutamatergic neurotransmission, and with the biosynthetic enzyme for the inhibitory neurotransmitter GABA, GAD67, as a marker for GABAergic neurotransmission, respectively.

6. **Pilot microarray analysis of differential gene expression in orexin neurons after fasting**

   To identify novel candidate genes for the regulation of food intake in hypothalamic neurons suspected to express CT receptors, transcriptomic changes of orexin neurons after fasting were investigated by combining LCM with microarray analysis. Due to limitations of time and costs, validation of fasting-induced gene regulation had to be apriori restricted to one newly identified candidate gene. Semi-quantitative in situ hybridization was envisaged as validation strategy to prove fasting-induced regulation of a chosen candidate gene.

2 Materials and methods

2.1 Materials

2.1.1 Equipment

β-γ Detector LB122 Berthold	Amersham, Braunschweig
Biofuge	Heraeus, Hanau
Centrifuge 5403	Eppendorf, Hamburg
CM 3050 Kryostat	Leica, Nussloch
DNA-Engine PTC-200	MJ Research, Watertown, USA
Gene Amp PCR System 9700	Perkin Elmer, Foster City, USA
Gel Doc 1000	BioRad, Hercules, USA
HM 500 OM Kryostat	Microm, Walldorf
Hybridization oven	Bachofer, Reutlingen
MCID M5 Image analysis system	Imaging Research, St. Catharines, Canada
MicroPulser^{TM} Electroporation Apparatus	BioRad, Hercules, USA
Microscope AX 70	Olympus Optical, Hamburg, Germany
PixCell II Laser Capture Microdissection System	Arcturus, San Diego, USA
Power supply units	BioRad, Hercules, USA
Ultrospec 3000 UV/Visible Spectrophotometer	Pharmacia, Freiburg
Wallac 1410, Liquid Scintillation Counter	Pharmacia, Freiburg
Confocal Microscope	Olympus Optical, Hamburg, Germany
Hybridization Oven 640	Affymetrix, Santa Clara, USA
Fluidics Station 400	Affymetrix, Santa Clara, USA
GeneArray Scanner	Affymetrix, Santa Clara, USA

2.1.2 Chemicals and reagents

Acetic acid	Riedel-deHaën, Seelze
Acetic anhydride	Sigma-Aldrich, Steinheim
Acetylated Bovine Serum Albumin (BSA) solution (50 mg/ml)	Invitrogen, Karlsruhe
Agar	Fluka, Buchs
Agarose	Invitrogen, Karlsruhe
Albumin bovine Fraction V, pH7.0	Serva, Heidelberg
Ammonium persulfate	Serva, Heidelberg
Ampicillin	Sigma-Aldrich, Steinheim
Antibiotic-Antimycotic (100 x)	Invitrogen, Karlsruhe

5-bromo-4-chloro-3-indolyl-phosphate-4-toluidine salt (BCIP)	Roche, Mannheim
Boric acid	Merck, Darmstadt
Bromphenol blue sodium salt	Serva, Heidelberg
Calcium Chloride	Merck, Darmstadt
Chloroform	Roth, Karlsruhe
Citric acid monohydrate	Merck, Darmstadt
Control Oligo B2, 3 nM	Affymetrix, Santa Clara, USA
Copper (II) acetate	Merck, Darmstadt
Cresyl violet acetate	Fluka, Buchs
D19 developer	Kodak, New Haven, USA
Denhardt's Reagent (50 x)	Sigma-Aldrich, Steinheim
DePeX	Serva, Heidelberg
Deoxynucleoside triphosphate (dNTP)	Roche, Mannheim
Dextransulfate (Na-Salt)	Fluka, Buchs
3,3 diaminobenzidine tetrahydrochloride (DAB)	Sigma-Aldrich, Steinheim
Digoxigenin RNA Labeling Mix	Roche, Mannheim
Dimethylformamide	Fluka, Buchs
Dimethyl sulfoxide (DMSO)	Merck, Darmstadt
Dithiothreitol (DTT)	Roche, Mannheim
Diethyl pyrocarbonate (DEPC)	Roche, Mannheim
Ethanol	Riedel-deHaën, Seelze
Ethidium bromide	Roth, Karlsruhe
Ethylene diaminetetraacetic acid (EDTA)	Merck, Darmstadt
FluorSave™ Reagent	Calbiochem, San Diego
Formamide	Fluka, Buchs
Formaldehyde, 37%	Merck, Darmstadt
GeneChip Eukaryotic Hybridization Control Kit (contains Control cRNA and Control Oligo B2)	Affymetrix, Santa Clara, USA
Glacial acetic acid	Merck, Darmstadt
Glycerol	Merck, Darmstadt
Glycine	Roth, Karlsruhe
Guanidine hydrochloride	Roth, Karlsruhe
Herring Sperm DNA	Promega, Mannheim
Hydrogen peroxide 30% H_2O_2	Merck, Darmstadt
(2-Hydroxyethyl)-1-piperazineethanesulphonic acid (HEPES)	Roth, Karlsruhe
Isopropanol	Merck, Darmstadt
Isopentane (2-methyl butane)	Fluka, Buchs
Isopropylthio-β-D-galactoside (IPTG)	Applichem, Darmstadt

KAISER'S glycerol gelatin	Merck, Darmstadt
K5, Autoradiography emulsion	Ilford, London, UK
Ketanest 50	Parke-Davis, Freiburg
Liquemin N 25000 (Heparin-Natrium)	Roche, Mannheim
β-mercaptoethanol	Sigma, St. Louis
MES Free Acid Monohydrate SigmaUltra	Sigma-Aldrich, Steinheim
MES Sodium Salt	Sigma-Aldrich, Steinheim
Methanol	Merck, Darmstadt
Na2-EDTA	Merck, Darmstadt
NaOH	Merck, Darmstadt
Natriumcitrate Dihydrate	Merck, Darmstadt
NBT (4-Nitroblue - Tetrazol - chloride)	Roche, Mannheim
Nickel	Fluka, Buchs
NLS (normal lamb serum)	GIBCO, Karlsruhe
NorthernMax Pre/Hybridization Buffer	Ambion, Austin, USA
NTB2, Autoradiography emulsion	Eastman Kodak, Rochester, NY
NTP (nucleoside triphosphate)	Roche, Mannheim
Phenol/chloroform/isopropanol(25 : 24 : 1)	Roth, Karlsruhe
Picric acid desensitized, contains 30% water	Merck, Darmstadt
RNase inhibitor	MBI Fermentas, St.Leon-Rot, Germany
Roenteroll, developer for X-ray film	Tetenal, Norderstedt
Rompun 2%	Bayer, Leverkusen
Rotiphorese Gel 30	Roth, Karlsruhe
R-Phycoerythrin Streptavidin	Molecular Probes
SDS (Sodium dodecyl sulfate)	Roth, Karlsruhe
Sodium acetate	Roth, Karlsruhe
Sodium azide	Merck, Darmstadt
Sodium acetate	Merck, Darmstadt
Sodium chloride	Merck, Darmstadt
Sonicated salmon sperm DNA	Invitrogen, Karlsruhe
Superfix, Fixer for X-ray film	Tetenal, Norderstedt
TEMED, tetramethyl ethylene diamine	Roth, Karlsruhe
Tissue-Tek O.C.T compound	Sakura, Zoetwerwounde, Netherlands
Triethanolamine (TEA)	Sigma-Aldrich, Steinheim
3-(Triethoxysilyl) propylamine	Merck, Darmstadt
Tris (hydroxymethyl) aminomethane	Roth, Karlsruhe
Triton X-100	Sigma-Aldrich, Steinheim
TRIzol	Invitrogen, Karlsruhe
tRNA	Roche, Mannheim
Tryptone Peptone	DIFCO, Detroit, USA

Tween 20	Merck, Darmstadt
X-gal	peQLab, Erlangen
Xylene Cyanole FF	Sigma, St. Louis, USA
Xylol	Merck, Darmstadt
Yeast extract	DIFCO, Detroit, USA

2.1.3 Buffers and solutions

DEPC-treated H_2O

10% (v/v) DEPC in ethanol was diluted in H_2O to 0.1% (v/v).
incubated at 37°C overnight with shaking and autoclaved

20 x SSC (pH 6.3-6.4)

3 M NaCl
0.3 M sodium citrate
By 1:10 dilution pH 7.05

Denhardt´s reagent

1% (w/v) Ficoll 400
1% (w/v) polyvinylpyrrolidone
1% (w/v) bovine serum albumin

10 x PBS (100 mM, pH 6.75):

1.53 M NaCl
77 mM Na_2HPO_4
23 mM NaH_2PO_4
by 1 x PBS (10 mM) pH 7.3-7.4

50mM PBS (pH 7.45)

9.5 mM NaH_2PO_4
40.5 mM Na_2HPO_4
153 mM NaCl

Bouin Hollande fixative solution

Stock solution

25g copper (II) acetate dissolved in ddH_2O
add 60g picric acid into the solution and dissolve it
add ddH_2O to 1 L
filter, save in 4°C

Working solution

100 part Bouin Hollande stock solution
10 part 37% formaldehyde
1 part acetic acid
prepare prior to use

10 mM Sodium citrate buffer (pH 6.0)

Solution 1

0.1 M citric acid monohydrate

Solution 2

0.1 M sodiumcitrate dihydrate

mix 54 ml solution 1 and 246 ml solution 2

add 2700 ml ddH_2O to 3000 ml, pH 6.0

ABC complex

1 drop (50 µl) solution A + 1 drop (50 µl) solution B

in 2.5 ml 1%BSA/PBS

preincubation for 30 min at RT prior to use

DAB working solution

prepare DAB working solution prior to use: add 100 mg DAB in 800 ml 50 mM PBS buffer

filter the solution into the vessel which is covered with tin foil

Nickel enhancement

prepare Nickel enhancement prior to use: add 100 mg DAB and 600 mg Nickel sequentially in 800 ml 50 mM PBS buffer

mix completely

filter the solution into the vessel which is covered with tin foil

TE buffer(pH 8.0)

10 mM Tris (pH 8.0),

1 mM EDTA (pH 8.0)

TAE buffer(pH 8.0):

40 mM Tris-acetate

2 mM EDTA (pH 8.0)

10 x HEPES-EDTA-buffer

200 mM HEPES (Sigma)

10 mM Na_2-EDTA

pH 7.8, adjust with NaOH

filter and autoclave

RNA sample buffer

1 ml 10 x HEPES-EDTA-Buffer

5 ml Formamide

1.6 ml 37% Formaldehyde

RNA loading buffer

50% glycerol

0.5% Bromophenol blue

0.5% Xylene Cyanol

RNA gel electrophoresis buffer

1 x HEPES-EDTA-Buffer

6% Formaldehyde

In situ hybridization buffer

600 mM NaCl

10 mM Tris-HCl pH 7.5

1 mM EDTA-Na_2

0.05% (w/v) tRNA

1 x Denhardt´s

10% (w/v) Dextransulphate

100 µg/ml Sonicated Salmon Sperm DNA

50% (v/v) Formamide

20 mM DTT

Cresyl violet stain

0.5% cresyl violet

60 mM sodium acetate

340 mM acetic acid in ddH_2O

RNase buffer

10 mM Tris-HCl pH 8.0

0.5 M NaCl

1 mM EDTA

40 µg/ml RNase A (10 mg/ml in ddH_2O stocking solution)

1 U/ml RNase T1 (500,000 U/ml stocking solution)

4% phosphate-buffered Formaldehyde

Solution 1

40 g (60 g) paraformaldehyde (PFA)

500 ml (750 ml) ddH_2O (preheat water and cool to 50 - 55°C)

add concentrated NaOH slowly until solution clears

Solution 2

100 ml (150 ml) 10 x PBS

400 ml (600 ml) ddH2O

mix both solutions together and cool to RT

adjust pH with concentrated HCl to 7.3 - 7.4

filter the solution and store at 4°C

0.4% Triton X-100/PBS

prepare 0.4% Triton X-100 solution in 1 x PBS

TEA buffer (pH 8.0)

6.65 ml Triethanolamine

493 ml ddH_2O

adjust the pH to 8.0 with HCl

Digoxigenin detection buffers

Buffer 1

100 mM Tris-HCl, pH 7.5

150 mM NaCl

dissolved in ddH2O

Buffer 2

100 mM Tris-HCl, pH 9.5

100 mM NaCl

50 mM $MgCl_2$

dissolved in ddH_2O

Blocking buffer

10% NLS (normal lamb serum)

0.01% Triton X-100

dissolved in buffer 1

Chromogen solution

10 ml buffer 2

45 µl NBT (4-Nitroblue-Tetrazol-chloride)

35 µl BCIP (5-bromo-4-chloro-3- indolyl-phosphate)

12 x MES Stock (1.22 M MES, 0.89 M Na^+)

70.4 g MES free acid monohydrate

193.3 g MES Sodium Salt

800 ml of molecular biology grade water

mix and adjust volume to 1000 ml

adjust pH to 6.5 - 6.7

filter through a 0.2 µm filter

2 x Array hybridization buffer

(Final 1 x concentration is 100 mM MES, 1 M Na^+, 20mM EDTA, 0.01% Tween 20)

for 50 ml, add

8.3 ml of 12 x MES Stock

17.7 ml of 5 M NaCl

4.0 ml of 0.5 M EDTA

0.1 ml of 10% Tween 20

19.9 ml of water

store at 2°C to 8°C and shield from light

20 x SSPE buffer

3 M NaCl

0.2 M NaH_2PO_4

0.02 M EDTA

Washing and staining buffers for microarray

Wash A: non-stringent wash buffer (6 x SSPE, 0.01% Tween 20)

for 1000 ml, add

300 ml of 20 x SSPE

1.0 ml of 10% Tween 20

699 ml of water

filter through a 0.2 µm filter

Wash B: stringent wash buffer (100 mM MES, 0.1 M Na^+, 0.01% Tween 20)

for 1000 ml, add

83.3 ml of 12 x MES Stock Buffer

5.2 ml of 5 M NaCl

1.0 ml of 10% Tween 20

910.5 ml water

filter through a 0.2 µm filter

store at 2°C to 8°C and shield from light

2 x Staining buffer (Final 1 x concentration: 100 mM MES, 1 M Na^+, 0.05% Tween 20)

for 250 ml, add

41.7 ml of 12 x MES Stock Buffer

92.5 ml of 5 M NaCl

2.5 ml of 10% Tween 20

113.3 ml water

filter through a 0.2 µm filter

store at 2°C to 8°C and shield from light

10 mg/ml goat IgG stock

resuspend 50 mg in 5 ml 150 mM NaCl

store at 4°C

2.1.4 Animals

Wistar rats (200-225g, male) were purchased from Charles River (Sulzfeld, Germany).

2.1.5 Radioactive nucleotides

[α-^{35}S] UTP (1000 Ci/mmol)	Amersham Biosciences, Freiburg
[α-^{35}S] CTP (1000 Ci/mmol)	Amersham Biosciences, Freiburg
[α-^{35}S] dATP (1000 Ci/mmol)	Amersham Biosciences, Freiburg

2.1.6 Kits

ABC Kit Vectastain PK-6100	Vector, Burlingame, CA
Advantage 2 PCR Kit	BD Biosciences Clontech, USA
Avidin/Biotin Blocking Kit	Vector, Burlingame, CA
BioArray™ HighYield™ RNA Transcript Labeling Kit	Affymetrix, Santa Clara, USA
DIG Oligonucleotide Tailing Kit, 2nd Generation	Roche, Mannheim
GeneChip Sample Cleanup Module	Affymetrix, Santa Clara, USA
GeneChip T7-Oligo(dT) Promoter Primer Kit	Affymetrix, Santa Clara, USA
MessageAmp™ aRNA Kit	Ambion, Austin, Texas, USA
Poly(A)$^+$ Tract mRNA Isolation System	Promega, Mannheim
QIAGEN Plasmid Maxi Kit	QIAGEN, Hilden
QIAprep Spin Miniprep Kit	QIAGEN, Hilden
QIAquick PCR Purifiation Kit	QIAGEN, Hilden
QIAquick Nucleotide Removal Kit	QIAGEN, Hilden
QIAquick Gel Extraction Kit	QIAGEN, Hilden
RNAqueous™-Micro Kit	Ambion, Austin, Texas, USA
RNeasy Mini Kit	QIAGEN, Hilden

2.1.7 Enzymes

AatII	Roche, Mannheim
AmpliTaq Gold DNA Polymerase	Applied Biosystems, Darmstadt, Germany
DNase I (RNase free)	Roche, Mannheim
E. coli DNA Ligase	Invitrogen, Karlsruhe
E. coli DNA Polymerase I	Invitrogen, Karlsruhe
E. coli Rnase H	Invitrogen, Karlsruhe
EcoRI	New England Biolab, Schwalbach/Taunus
HindIII	New England Biolab, Schwalbach/Taunus

NcoI	New England Biolab, Schwalbach/Taunus
NdeI	New England Biolab, Schwalbach/Taunus
NotI	New England Biolab, Schwalbach/Taunus
PfuTurbo high fidelity DNA polymerase	Stratagene, La Jolla, USA
PstI	New England Biolab, Schwalbach/Taunus
RNA Polymerase (SP6, T7)	Roche, Mannheim
RNase A	Roche, Mannheim
RNase T1	Roche, Mannheim
SacII	New England Biolab, Schwalbach/Taunus
SpeI	New England Biolab, Schwalbach/Taunus
SphI	New England Biolab, Schwalbach/Taunus
Superscript II Reverse Transcriptase	Invitrogen, Karlsruhe
Taq DNA polymerase	Applied Biosystems, Foster City, USA
T4 DNA Ligase	Promega, Mannheim
T4 DNA Polymerase	Invitrogen, Karlsruhe
XbaI	New England Biolab, Schwalbach/Taunus

2.1.8 Oligonucleotides

The PCR primers were designed using the online program Primer 3 (http://www-genome.wi.mit.edu/cgi-bin/primer/primer3_www.cgi). All oligonucleotides (see table 3) were custom synthesized by MWG-Biotech (Ebersberg, Germany). The optimal annealing temperature was calculated using the primer analysis software Oligo 6 (Molecular Biology Insights, West Cascade, USA).

Table 3 List of oligonucleotides

Gene	GenBank #	Primer Name	Sequence	Annealing Tm	Product size
CART	NM_017110	rCARTF63	ccctactgctgctgctacct	56°C	698 bp
		rCARTR741	cgggttatgatgtcatctgc		
MCH	M29712	rMCHF5	ccacttctccttcggcttta	54°C	699 bp
		rMCHR683	tgcacaagtcaaagcatatca		
orexin	AF041241	rorexinF19	tccttgggtatttggaccac	59°C	512 bp
		rorexinR511	gcgaggagaggggaaagtta		
$CT_{(a)}$	L14617	$rCT_{(a)}F875$	gtgcgacgggatcctataag	54°C	270 bp
		$rCT_{(a)}R1125$	gatgatgtaaagcaagtggg		
		$rCT_{(a)}F643$	caatgccttcactcctgaca	56°C	980 bp
		$rCT_{(a)}R1603$	cttcgttgttgctgactgga		
$CT_{(b)}$	L13040	$rCT_{(b)}F723$	gcatatttttcatcataacacat	50°C	111 bp
		$rCT_{(b)}R811$	atcacttcactgtcatgagggtc		
		$rCT_{(b)}F474$	caatgccttcactcctgaca	54°C	348 bp
		$rCT_{(b)}R802$	tcatgagggtccatctttcc		
RAMP1	AB030942	rRAMP1F5	ctctgcttgccatggccctcggcctg	63°C	458 bp
		rRAMP1R435	ctacacgatgccctctgtgcgcttgctc		
RAMP2	AB030943	rRAMP2F15	caaggcgtgatggctccg	59°C	558 bp
		rRAMP2R552	ctacgcctgagcatcgccgtc		
RAMP3	AB030944	rRAMP3F10	ccatggcgaccccggcacag	60°C	490 bp
		rRAMP3R476	cattcttctagcttgccaggcacg		
GAPDH	AF106860	rGAPDHF119	cgacccttcattgacctcaactacatg	59°C	227 bp
		rGAPDHR345	ccccggccttctccatggtggtgaagac		

2.1.9 DNA and RNA size markers

1 kb DNA ladder	GIBCO, Karlsruhe
100 bp DNA ladder	GIBCO, Karlsruhe
1 kb DNA ladder	MBI Fermentas, St.Leon-Rot, Germany
100 bp DNA ladder	MBI Fermentas, St.Leon-Rot, Germany

2.1.10 Other supplies

BioMax Film	KODAK, USA
CapSure LCM Transfer Film TF-100	Arcturus, San Diego, USA
Electroporation Cuvette 1mm	Peqlab Biotechnologie, Erlangen
Eppendorf tubes	Eppendorf, Hamburg
Hyperfilm β-max	Amersham Biosciences,Freiburg
Hyperfilm MP	Amersham Biosciences,Freiburg

Micro Bio-Spin P-30 Columns	BioRad, Hercules, USA
PAP-pen	Beckman Coulter, France
Tissue-Tek Cryomold	Miles, Elkhart, USA
Glass slides	Menzel, Braunschweig, Germany

2.2 Methods

2.2.1 Animals

Animal care and procedures were conducted according to institutional guidelines. All rats were housed in clean plastic cages and maintained on a 12 h-12 h light-dark cycle at room temperature 21 ± 1°C and had *ad libitum* access to food and water.

For the fasting experiments, adult male Wistar rats (BW.200-225 g) were divided into two groups (n=3 per group). The control group rats had *ad libitum* access to food and water. The experiment group rats were fasted for 48h only with water available. After 48 h of fasting, the body weight of the rats was reduced in average 30 ± 4 g (n=3).

2.2.2 Tissue preparation

2.2.2.1 Coating of glass slides

The glass slides were first washed with detergent at 60°C for 1 h with slightly shaking. The detergent was completely removed under running water. The slides were rinsed three times with deionized water. After 45 min washing in 70% ethanol with slightly shaking, the slides were dried by baking at 60°C. After immersion in 2% 3-(Triethoxysilyl) propylamine in acetone for 30 sec, the slides were soaked 30 sec twice in acetone and twice in deionized water. Slides were then dried completely by baking overnight at 42°C.

2.2.2.2 Paraffin sections

2 Male Wistar rats were anesthetized with Ketamin (100mg/kg) and Rompun (10mg/kg) and perfused with 0.9% NaCl to wash the blood and with Bouin Hollande fixative solution to fix the tissue. Brains were removed and cut into forebrain, midbrain and hindbrain and immersed into the same fixative solution for 24-48 h with slightly shaking, then rinsed in 70% 2-propanol. Alcohol was changed daily until the fixative was completely washed out. After standard dehydration, brains were

embedded in paraffin, 7 µm sections were cut through hypothalamus. The sections were mounted on adhesive slides and stored at room temperature.

2.2.2.3 Frozen sections

The rats were killed by exposure to 100% CO_2. Brains were rapidly removed and embedded in Tissue-Tek OCT compound (Sakura, Zoeterwoude, The Netherlands) by immersion in -50°C cold 2-Methylbutane (Fluka, Seelze, Germany) on dry ice for cutting. For in situ hybridization histochemistry, 14µm thick serial coronal rat brain sections were cut on a Leica Cryostat (Leica) and thaw-mounted on adhesive slides and stored at -70°C. For laser capture microdissection, 10µm coronal sections were cut and mounted on non-coated glass slides and stored at -70°C.

2.2.3 Immunocytochemistry

2.2.3.1 Double sequential immunostaining

Double sequential immunostaining was performed on deparaffinized paraffin-embedded tissue sections (7 µm) using standard avidin-biotin-peroxidase techniques (Vectastain Elite ABC kit, Boehringer). For optimal antigen retrieval, sections were incubated in a pressure cooker (15 min at 95°C in 10 mM Na-citrate buffer, pH 6.0) and blocked by successive 30 min incubation in 5% bovine serum albumin (BSA) and avidin-biotin-blocking kit (Vectastain Elite, Boehringer). Orexin neurons were visualized with a goat-anti-rat polyclonal antibody against orexin A diluted 1:8000. Primary antibodies were applied in 1% BSA/PBS and incubated at 16°C overnight and at 37°C 2 h. Sections were washed and incubated with 1:200 donkey-anti-goat biotinylated secondary antibody (Dianova, Hamburg) for 45 min at 37°C. Immunoreactions were visualized with 3,3'-diaminobenzidine, resulting in a brown staining.

For CGRP double staining, after dehydration through a graded series of 2-propanol and in methanol/H_2O_2 solution for 30 min treatment, sections were rehydrated in a gradient series of 2-propanol and blocked with BSA and the avidin-biotin reagents to block potential nonspecific binding of the second avidin-biotin-peroxidase complex to the first avidin-biotin-peroxidase complex. CGRP was visualized with a rabbit-anti-rat polyclonal antibody against CGRP diluted 1:120.000. Primary antibodies were applied in 1% BSA/PBS and incubated at 16°C overnight and at 37°C 2 h. Sections were washed and incubated with 1:200 donkey-anti-rabbit

biotinylated secondary antibody (Dianova, Hamburg) for 45 min at 37°C. The second primary antibody was visualized by DAB/peroxidase reaction enhanced by the addition of 0.08% ammonium nickel sulfate resulting in a dark blue staining. After dehydration procedure, slides were covered with DepeX.

2.2.3.2 Double immunofluorescence

For simultaneous detection of orexin and CGRP hypothalamic sections were incubated overnight at 16°C and 2 h at 37°C with goat-anti-rat orexin A antibody diluted 1:800 together with rabbit-anti-rat CGRP antibody diluted 1:10000. Sections were incubated with 1:200 donkey-anti-rabbit biotinylated secondary antibody (Dianova, Hamburg) which interacted with the rabbit-anti-rat CGRP antibody for 45 min at 37°C, then further incubated with the mixture of 1:200 donkey-anti-goat A647 (Molecular probes, Leiden, The Netherlands) together with 1:200 Alexa A488-conjugated streptavidin (Molecular probes, Leiden, The Netherlands) for 2 h at 37°C to detect the signals of orexin A and CGRP. After 3 x 5 min washes in ddH_2O, 10 min washes in PBS, slides were covered with FluorSave™ Reagent.

Table 4 List of primary antibodies

Antigen	Dilution	Species	Source/Reference
Orexin A	1:8000[a] / 1:800[b]	Goat polycl.	Santa Cruz, California
CGRP	1:120000[a] / 1:10000[b]	Rabbit polycl.	(Rohrenbeck et al. 1999)

[a]dilution for enzymatic sequential immunostaining, [b]dilution for immunofluorescence

2.2.4 Laser capture microdissection (LCM)

2.2.4.1 Microdissection of orexin neurons

Frozen sections were rapidly transferred from -70°C without drying and fixed in 4% paraformaldehyde/PBS for 2h. Then sections were blocked by successive 30 min incubations in 5% bovine serum albumin (BSA) and avidin-biotin-blocking kit (Vectastain Elite, Boehringer). Orexin neurons were visualized with a goat-anti-rat polyclonal antibody (1:800) against orexin A (Santa Cruz, California). Primary antibodies were applied in 1% BSA/PBS and incubated at 16°C overnight and at 37°C 2 h. Sections were washed and incubated with 1:100 indocarbocyanine (Cy3)-conjugated antigoat secondary antibody (Dianova, Hamburg) at 37°C 2h, resulting in a red-orange fluorescence labeling. RNase inhibitor (40U/µl, MBI Fermentas, St. Leon-Rot, Germany) was added to the blocking buffers and the antibody solutions

(80U RNase inhibitor /ml buffer). After dehydration procedure, sections were air-dried.

Immunofluorescent labeled orexin neurons were microdissected using the laser capture microdissector (Arcturus Inc., San Diego) with CapSure™ LCM Transfer Film TF-100 caps. The following settings were used: 7.5 µm laser spot size, 65 mW pulse power, 1.2 ms pulse width, 10mV threshold voltage. After capturing, the caps were plugged into the 0.5 ml plastic tubes (Eppendorf, Köln, Germany) containing 100µl lysis buffer from RNAqueous™ Micro Kit (Ambion). The tubes were vortexed in an inverted position for 30 sec. The samples were collected by centrifugation.

2.2.4.2 Microdissection of the area postrema (AP) and of the nucleus of the solitary tract (NTS)

At the day of microdissection, frozen slides were rapidly transferred from -70°C without drying and put into 95% ethanol, 75% ethanol and 50% ethanol each for 5-7 quick dips through pre-staining fixation steps, then in 1% cresyl violet acetate made in 100% ethanol for 5min staining. The post-staining steps were 50% ethanol, 75% ethanol and 95% ethanol each 5-7 quick dips, 100% ethanol 30sec, two times xylene each 5min. Sections were air dried completely.

AP and NTS were microdissected from cresyl violet acetate stained sections using the laser capture microdissector (Arcturus Inc., San Diego) with CapSure™ LCM Transfer Film TF-100 caps using the following settings: 30 µm laser spot size, 80 mW pulse power, 4.0 ms pulse width, 90mV threshold voltage. After capturing, the caps were plugged into the 0.5ml plastic tubes (Eppendorf, Köln, Germany) containing 100µl lysis buffer from RNAqueous™ Micro Kit (Ambion). The tubes were vortexed in an inverted position for 30 sec. The samples were collected by centrifugation.

2.2.5 RNA isolation

Total RNA from different tissues was isolated using TRIzol Reagent (Invitrogen) according to the manufacturer's protocol. RNA from 320 microdissected orexin neurons and from AP and NTS of 5 sections were isolated using RNAqueous™ Micro Kit (Ambion) according to the manufacturer's protocol. RNA samples were treated with DNase I (Roche) for 30 min at 37°C and then purified with RNeasy Mini Kit (QIAGEN).

2.2.6 Reverse transcriptase polymerase chain reaction (RT-PCR)

2.2.6.1 Complementary DNA (cDNA) synthesis

cDNA was synthesized using Superscript II RNase H^- reverse transcriptase (Invitrogen) in total volume of 20 µl. DNase I treated total RNA from different tissues was incubated with oligo(dT) 12-18 (1.25 µM, Amersham Pharmacia Biotech, Freiburg, Germany) at 70°C for 10 min in a volume of 11 µl and chilled on ice for 2 min. The reaction was performed in the presence of dithiothreitol (DTT) (10 mM), reverse transcriptase (200 U), dNTPs (500 µM), the first strand buffer (Invitrogen) and incubated at 16°C for 10 min, at 42°C for 1 h and at 94°C for 5 min to inactivate the enzyme. For mock reactions the Superscript II RNase H^- reverse transcriptase was omitted. The cDNA was diluted to 50 µl by adding 30 µl PCR grade water and stored at –20°C.

2.2.6.2 Polymerase chain reaction (PCR)

All PCR reactions were performed on a GeneAmp 9700 cycler or PTC-200 cycler. For PCR amplification of rat $CT_{(a)}$ and $CT_{(b)}$ the following gene specific primers were used: rat $CT_{(a)}$ (Genebank Accession No. L14617, nt. 875-1144, 270bp), forward primer: gtgcgacgggatcctataag, reverse primer: gatgatgtaaagcaagtggg; rat $CT_{(b)}$ (Genebank Accession No. L13040, nt. 474-821, 348bp), forward primer: caatgccttcactcctgaca, reverse primer: tcatgagggtccatctttcc. Hot start PCR was performed using 5µl cDNA in a total volume of 50µl containing 1x PCR buffer, 3mM $MgCl_2$, 200µM dNTPs mixture, 0.2µM primers mixture and 1U AmpliTaq Gold™ (Applied Biosystems, Darmstadt, Germany) with the following program: 1 cycle 95°C 10 min, 10 cycles (94°C 30sec, 59°C 30sec/ -0.5°C per cycle , 72°C 30sec), 40 cycles (94°C 30sec, 54°C 30sec, 72°C 30sec) and 10 min extension at 72°C. As positive control glyceraldehydes phosphate dehydrogenase (GAPDH) was used as house keeping gene yielded a 227 bp PCR product (AF106860, nt. 119 – 345). Negative controls included RNA subjected to RT-PCR without reverse transcriptase, and PCR with water replacing cDNA. PCR products of 10 µl from each reaction were loaded and separated on 1.5% agarose gel containing ethidium bromide (EtBr). The gels were visualized under an ultraviolet transilluminator (BioRad). The PCR

products were subcloned and sequenced. The sequence identity of the PCR products was confirmed by comparison with the published sequences in Genebank.

2.2.7 Agarose gel electrophoresis

To separate DNA fragments in a size range of 100 to 10.000 bp 1.5% agarose gel was routinely used (Sambrook and Russell 2001). The appropriate amount of agarose was dissolved in 1 × TAE buffer by boiling for a few minutes in a microwave oven. When the gel solution had cooled down to about 60°C, ethidium bromide was added to a final concentration of 0.5 µg/ml. The solution was then poured into a gel mold. Suitable combs were used for generating the sample wells. The gel was allowed to harden for some 30 - 45 min. The gel was mounted in the electrophoresis chamber which was filled with 1 x TAE running buffer until the gel was just submerged. DNA samples and size standards were mixed with 0.1 volumes of 10 × loading buffer and applied to the wells. A voltage of 2 - 10 V/cm was applied until the bromophenol blue and xylene cyanol FF dyes had migrated the appropriate distance through the gel. After completion of electrophoresis gels were examined under UV transilluminator and photographed using a gel documentation system (BioRad).

2.2.8 Cloning

The QIAquick PCR Purification Kit (QIAGEN) was used to purify PCR products. The purified PCR fragments of rCART, rMCH, rNPY, rorexin, rVGLUT2, rGAD, $rCT_{(a)}$, $rCT_{(b)}$, rRAMP1, rRAMP2, rRAMP3 and rGAPDH were ligated into pGEM-T Vector (Promega), the fragment of rCRH was ligated into pGEM-3Z (Promega), the fragments of rPOMC and rTRHR2 were ligated into pcDNA3.1(+) (Invitrogen) and the fragments of rTRH and rTRHR1 were ligated into pBluescript II KS(+) (STRATAGENE). The plasmid constructs were electroporated into XL1-Blue of E. *coli* electrocompetent cells using MicroPulser™ Electroporation Apparatus (BioRad) according to manufacturer's instruction. The positive clones were amplified and the plasmids were isolated from the cells by using QIAfilter Plasmid Maxi Kit (QIAGEN) and sequenced in Sequence Laboratories (Goettingen) with universal primers T7, SP6, T3 and gene specific primers. Sequences were then confirmed by homology search using BLAST 2.0 (http://www.ncbi.nlm.nih.gov). The plasmids were linearized by different restriction enzymes as shown in table below. RNA polymerases using to produce sense or antisense RNA probes were indicated.

Table 5 List of plasmids

Gene	Insert	Enzyme	Probe	RNA polymerase
rCART	698 bp	NdeI	sense	T7
		NcoI	antisense	SP6
rNPY	440 bp	NcoI	sense	SP6
		NdeI	antisense	T7
rPOMC	433 bp	HindIII	sense	SP6
		XbaI	antisense	T7
rMCH	699 bp	NotI	sense	T7
		NcoI	antisense	SP6
rOrexin	512 bp	SphI	sense	SP6
		NdeI	antisense	T7
rTRH	800 bp	HindIII	sense	T7
		EcoRI	antisense	T3
rCRH	770 bp	EcoRI	sense	SP6
		HindIII	antisense	T7
rVGLUT2*	1060 bp	SpeI	sense	T7
		NcoI	antisense	SP6
rGAD*	841 bp		sense	T7
			antisense	SP6
$rCT_{(a)}$	980 bp	NotI	sense	T7
		AatII	antisense	SP6
$rCT_{(b)}$	111 bp	NdeI	sense	T7
		NcoI	antisense	SP6
rRAMP1	458 bp	SpeI	sense	T7
		SphI	antisense	SP6
rRAMP2	558 bp	SpeI	sense	T7
		SphI	antisense	SP6
rRAMP3	490 bp	SpeI	sense	T7
		SphI	antisense	SP6
rTRHR1*	549 bp	EcoRI	sense	T3
		HindIII	antisense	T7
rTRHR2*	1308 bp	XbaI	sense	T7
		HindIII	antisense	SP6
rGAPDH*	227 bp	SalI	sense	T7
		ApaI	antisense	SP6

*Plasmids for rVGLUT2, rGAD and rGAPDH were previously generated in the laboratory; plasmids for rTRHR1 and rTRHR2 were kindly provided by K. Bauer (Heuer et al. 2000).

2.2.9 Probes

2.2.9.1 Complementary RNA probes

In vitro transcription reactions were performed to prepare the complementary RNA probes. For preparing the GAD probes, PCR product template was prepared from the plasmid construct with T7 and SP6 primers. For preparing the other probes, plasmids containing the specific gene fragments were linearized by different restriction enzymes. In vitro transcription reactions were carried out in a volume of 10 µl contained 1 µg linearized plasmids or PCR product, 10 mM DTT (GibcoBRL), 20 U RNase inhibitor (MBI Fermentas, St.Leon-Rot, Germany), 1 x In vitro transcription buffer, 20 U RNA polymerase (Roche), 0.5 mM NTPs mixture with ^{35}S-UTP or both ^{35}S-UTP and ^{35}S-CTP (>1000 Ci/mmol, Amersham Pharmacia Biotech, Freiburg, Germany) or 1 x DIG Labeling RNA Mix with digoxigenin-11-UTP (Roche). After 90 min incubation at 37°C, 10 U RNase-free DNase I (Roche) was added into the reactions and incubated for another 15 min. After adding RNase-free water to 20 µl and 20 µl sodium carbonate buffer (pH 10.2, 80 mM $NaHCO_3$ – 120 mM Na_2CO_3) for limited hydrolysis, the reactions were incubated at 60°C for the appropriate time [t = (Lo – Lf)/ K* Lo * Lf, Lo: the cDNA length, Lf: expected length of the probes (it is 250 bp in our laboratory), K is 0.11 in our case] (Schafer et al. 1993; Schafer and Day 1995). The reactions were stopped by adding 2 µl 10% acetic acid. 28 µl RNase-free water was added and probes were purified using Micro Bio-Spin P-30 columns (BioRad).

2.2.9.2 Oligonucleotide probes

The oligonucleotide sequence of orexin, 5'-gccgctttcccagagtgaggatgcccgcggcgtggttgc cagctccgt-3' (Genebank Accession No. NM_013179, nt. 248-295, 48bp) was selected using the online program Primer 3 (http://www-genome.wi.mit.edu/cgi-bin/primer/primer3_www.cgi) considering the parameters of melting temperature, GC content, length, hairpins and length of runs and synthesized by MWG-Biotech (Ebersberg, Germany).

The design of a specific oligonucleotide probe for $CT_{(a)}$ mRNA was complicated by the fact that $CT_{(a)}$ mRNA differs from $CT_{(b)}$ only by the 111bp insert representing the alternatively spliced exon 9 (see Fig. 4). Thus, the specific

oligonucleotide probe was designed to bind to the $CT_{(a)}$ mRNA region bridging exon 8 and exon 10, but it had to be short enough making it unable to form a stable hybrid with only exon 8 or only exon 10 at the hybridization temperature. The oligonucleotide sequence of $CT_{(a)}$ is 5'-aaaaagtgcagaatcttgcaacttataggatcccgtcgcaccag gtct-3' (Genebank Accession No. L14617, nt. 868-915, 48bp).

For the [α-^{35}S]dATP labelling of the oligonucleotide probe, the Reaction Mix was prepared by adding the following reagents: 25.5 µl ddH_2O, 7.2 µl oligonucleotide (0.72 pmol/µl), 10 µl of 5 x terminal transferase buffer (Roche), 3 µl of 25 mM $CoCl_2$ (Roche), 4 µl of 10 mCi/ml [α-^{35}S]dATP (40 µCi) (Amersham) and 0.3 µl of 400 U/µl Terminal Transferase (120 U) (Roche), total reaction volume was 50 µl. The reaction was incubated for 20 min in 37°C water bath, thereafter placed on ice. 400 µl TE buffer and 2.5 µl of 20 µg/µl yeast-tRNA were added to the reaction mixture and mixed thoroughly. The labeled probe was extracted with 0.5 volume of saturated phenol and 0.5 volume of chloroform/isoamyl-alcohol (49:1), vortexed and centrifuged for 5 min at 11000 rpm. The upper phase was transferred to a new tube and washed with 1 volume of chloroform/isoamyl-alcohol (49:1) and centrifuged for 5 min at 11000 rpm. The upper phase was transferred again in another new tube. The labeled probe was precipitated with 20 µl of ice-cold 5 M NaCl and 2 volume of cold (-20°C) absolute ethanol. The tube was kept at -70°C for at least 30 min and centrifuged for 30 min at 11000 rpm. The pellet was rinsed with 500 µl of 70% cold (-20°C) ethanol and air dried and resuspended in 50 µl TE buffer containing 10 mM DTT. The incorporated radioactivity was measured in a liquid scintillation counter.

Digoxigenin-labeling of the oligonucleotide probe was prepared with DIG Oligonucleotide Tailing Kit, 2nd Generation (Roche) according to the manufacturer's protocol. the Reaction Mix was prepared by adding the following reagents: 100 pmol oligonucleotide in 9 µl, 4 µl of 5 x reaction buffer, 4 µl of 25 mM $CoCl_2$, 1 µl of 1 mM DIG-11-dUTP, 1 µl of 10 mM dATP and 1 µl of 400 U/µl terminal transferase (400 U), total reaction volume was 20 µl. The reaction was incubated for 15 min in 37°C water bath, thereafter placed on ice. 2 µl of 0.2 M EDTA (pH 8.0) was added to stop the reaction.

2.2.10 In situ hybridization (ISH)

2.2.10.1 Prehybridization

Frozen sections were removed from the freezer and air dried at room temperature for 15 min and fixed in 4°C pre-cooled 4% paraformaldehyde in phosphate-buffered-saline (PBS) for 60 min at room temperature. After three washes in 10 mM PBS (pH 7.4) for 10 min each and incubation in 0.4% Triton X-100 for 10 min, the slides were rinsed in deionized water and transferred to 0.1 M triethanolamine (pH 8.0) (Sigma). After incubation for 1 min, acetic anhydride (Sigma) was added under strong stirring to a final concentration of 0.25% (v/v) and further incubated for 10 min. The slides were washed for 10 min in 10 mM PBS (pH 7.4) and rinsed in deionized water prior to dehydration in 50% and 70% isopropanol. Finally, the slides were air-dried at room temperature for 15 min and stored at -20°C.

2.2.10.2 Hybridization

For RNA probes, in situ hybridization was performed as described previously (Schafer et al. 1993; Schafer and Day 1995), Briefly, the frozen prehybridized sections were air dried and marked. The radioactive probes were diluted to 5 x 10^4 dpm/µl (single radioactive labeling) or 1 x 10^5 dpm/µl (double radioactive labeling) in ISH buffer. Appropriate amounts of hybridization solution containing radioactive antisense or sense RNA probes were applied to the sections. Slides were coverslipped and incubated at 60°C in humid box containing 50% formamide for 16 h. Sense probes were used as nonspecific controls.

For oligonucleotide probes, the radiolabeled oligonucleotides were diluted to 4 x 10^4 dpm/µl in ISH buffer. Appropriate amounts of hybridization solution were applied to the sections. Slides were coverslipped and incubated at 42°C in humid box containing 50% formamide for 16 h.

2.2.10.3 Posthybridization

For posthybridization of sections hybridized with RNA probes, coverslips were removed by dipping in 2 x SSC and slides were washed in 2 x SSC and 1 x SSC for 20 min each at room temperature followed by incubation in pre-heated to 37°C RNase buffer (10 mM Tris-HCl pH 8.0, 0.5 M NaCl, 1 mM EDTA) containing 1 U/ml RNase

T1 and 40 µg/ml RNase A (Roche) for 30 min at 37°C and 30 min at room temperature with stirring. Slides were washed at room temperature in 1 x, 0.5 x, and 0.2 x SSC for 20 min each, at 60°C in 0.2 x SSC for 60 min and at room temperature in 0.2 x SSC and deionized water for 15 min each. The tissue was dehydrated in 50% and 70% isopropanol and then air-dried.

For posthybridization of sections hybridized with oligonucleotide probes, coverslips were removed by dipping in pre-warmed to 55°C 2 x SSC and slides were washed in 55°C 1 x SSC for 4 times, each 15 min, in room temperature 1 x SSC for 1 h and in ddH_2O for 1 min. The tissue was dehydrated in 50% and 70% isopropanol and then air-dired.

2.2.10.4 Detection

Air-dried hybridized slides were exposed to Kodak BioMax MR Film (Amersham) for an appropriate period of time. After exposure to X-ray film, the sections were coated with nuclear emulsion NTB-2 (Eastman Kodak, Rochester, NY). The coated slides were dried overnight in a dark box in the dark room. The dried slides were exposed for 3 to 42 days at 4°C. The slides were developed for 4 min in Kodak D-19 developer solution and fixed for 10 min in Tetenal Superfix25 solution (Tetenal Photowerk, Norderstedt, Germany) at room temperature. The developed slides were washed overnight in running tap water. After staining with 0.5% cresyl violet for 15 min, the slides were washed in deionized water for 3 min, once in 70% and 96% and twice in 100% isopropanol alcohol for 2 min each. After final incubation in Xylol twice for 5 min, the sections were coated with DePex and covered with glass coverslips. The sections were analyzed under an Olympus AX70 microscope (Olympus) and photographed under bright or dark field illumination.

2.2.10.5 Double in situ hybridization

For double ISH the digoxigenin labeled RNA probes were added to a final concentration of 0.5 ng/µl in the hybridization solution containing radioactive RNA probes and digoxigenin labeled oligonucleotide probes were added to 1:200 in the hybridization solution containing radioactive oligonucleotide probes. Hybridization and washing procedures were the same as described above except dehydration in alcohol was omitted. For the detection of non-radioactive hybrids, the slides were

incubated for 1 h with blocking-buffer (buffer 1 containing 10% normal lamb serum, 0.01% Triton X-100). After rinsing in buffer 1, the slides were incubated with 1:1000 diluted antibody (alkaline phosphatase-conjugated anti-DIG Fab fragments in 1:10 diluted blocking buffer by buffer 1) overnight at 4°C and 1 h at 37°C. Excessive antibody was removed by washing in buffer 1 for 10 min twice. Slides were equilibrated in buffer 2 (100 mM Tris-HCl, pH 9.5, 100 mM NaCl; 50 mM $MgCl_2$) prior to color reaction. The color reaction was performed using the solution containing 5-bromo-4-chloro-3-indolyl phosphate (BCIP) and nitroblue tetrazolium salt (NBT) (Roche). The color development was controlled under the microscope. After 20 min for MCH and orexin, 1 h for TRH and 2 h for CART, slides were washed in deionized water for at least one day with several changes. For detection of ^{35}S-labeled probes, the slides were dipped in K5 Emulsion (ILFORD Imaging, Mobberley Chershire, UK), which was diluted 1: 1 in water. Sections were exposed at 4°C for various times. The cellular distribution of silver grains of radioactive probes and the violet precipitate of DIG probes was studied under an AX70 light microscope (Olympus).

2.2.11 Grain counting analysis

Computer-aided grain counting was performed on autoradiograms using the microcomputer imaging device (MCID) image analysis software (Imaging Research Inc, St. Catharines, Ontario, Canada). The animals were divided into two groups, one control group and one 48 h fasted group. From three animals per group 9 sections per animal were used for grain counting analysis. The perikarya with a nucleus of each labeled orexin neurons was scanned (scan area) and silver grains were counted. Background labeling was determined in sections hybridized with the sense probes. The background labeling ranged from 2 to 7 grains per orexin perikarya. Measurements were expressed as the number of grains per cell and the grain density (grains per 100 μm^2 scan area). Differences between groups were analyzed using Statview 5.0 software program (SAS Institute Inc.). p values < 0.05 were considered statistically significant.

2.2.12 Microarray analysis

Gene expression of orexin neurons from control and fasted rats was compared using microarray analysis according to Affymetrix GeneChip Expression Analysis Technical Manual.

The Affymetrix GeneChip probe arrays are manufactured using technology that combines photolithography and combinatorial chemistry. Each oligonucleotide is located in a specific area on the array called a probe cell. Each probe cell contains hundreds of thousands to millions of copies of a given oligonucleotide. Biotin-labeled cRNA targets derived from the mRNA of an experimental sample are hybridized to nucleic acid probes attached to the solid support. The hybridized probe array is stained with streptavidin phycoerythrin conjugate and scanned by the GeneArray® Scanner. The amount of light emitted at 570 nm is proportional to the bound target at each location on the probe array. By monitoring the amount of label associated with each DNA location, it is possible to infer the abundance of each mRNA species represented (See www.affymetrix.com for current GeneChip technology references).

In the present study, GeneChip® Rat Expression 230A Array was used to analysis the regulation of gene expression associated with food intake in orexin neurons. The Rat 230A Array contains primarily probe sets against 5399 genes and 10467 ESTs.

The following major steps outline GeneChip expression analysis: target preparation, target hybridization, probe array washing, staining and scanning, data analysis.

2.2.12.1 Target preparation

2.2.12.1.1 RNA isolation from microdissected orexin neurons

A series of 10µm thick frozen brain sections from 3 fasted rats and from 3 control rats were used for LCM. After immunofluorescence staining, the orexin neurons were microdissected. Total RNA was isolated from the microdissected orexin neurons using RNAqueous^{TM} Micro Kit (Ambion) according to the manufacturer's protocol and treated with DNase I (Roche) for 30 min at 37°C. Followed the purification using RNeasy Mini Kit (QIAGEN), the RNA samples were precipitated with ethanol and resuspended in appropriate volume of nuclease-free water for RNA amplification.

2.2.12.1.2 First round RNA amplification

The first round RNA amplification was performed using MessageAmp™ aRNA Kit (Ambion) according to the manufacturer's protocol. For the first strand cDNA synthesis, 1 µl of T7 Oligo(dT) Primer was added to the RNA sample, the nuclease-free water was used to bring the volume to 12 µl. The mixture was incubated at 70°C for 10 min in the PCR machine with heated lid, then placed on ice. In a second tube, the Reverse Transcription Master Mix was assembled by adding the following components at room temperature: 2 µl of 10 x First Strand Buffer, 1 µl of Ribonuclease Inhibitor, 4 µl of dNTP Mix and 1 µl of Reverse Transcriptase. The 8µl of the Reverse Transcription Master Mix was added to the RNA sample and incubated for 2 h at 42°C in the PCR machine with heated lid, then placed on ice.

For the second strand cDNA synthesis, the reagents were added to the first strand reaction sample in the order: 63 µl of nuclease-free water, 10 µl of 10 x Second Strand Buffer, 4 µl of dNTP Mix, 2 µl of DNA Polymerase and 1 µl of RNase H, the total volume was 100 µl. The reaction mixture was incubated for 2 h at 16°C in the PCR machine without heated lid.

Double stranded cDNA was cleaned by using the MessageAmp™ aRNA Kit (Ambion) according to the manufacturer's protocol.

In vitro transcription for cRNA amplification was made with MessageAmp™ aRNA Kit (Ambion) according to the manufacturer's protocol. The transcription reaction was prepared by adding the components at room temperature in the order shown: 16 µl of double-stranded cDNA from above, 4 µl of 75mM T7 ATP, 4 µl of 75mM T7 CTP, 4 µl of 75mM T7 GTP, 4 µl of 75mM T7 UTP and 4 µl of T7 Enzyme Mix. The reaction was incubated for 7 h at 37°C water bath with gently mixing the contents of the tube every 30-45 min during the incubation. After incubation, the template cDNA was removed from the cRNA with DNase I treatment for 30 min at 37°C. 60 µl of Elution Solution was added to the cRNA sample to bring the final volume to 100 µl.

cRNA was purified by using the MessageAmp™ aRNA Kit (Ambion) according to the manufacturer's protocol.

2.2.12.1.3 Second round RNA amplification and synthesis of biotin labelled cRNA probe

After first round RNA amplification, cRNA was precipitated and resuspended in 8 µl RNase free water in 0.5 ml microfuge tube. For the first strand cDNA synthesis, 2 µl Second Round Primers (MessageAmp^{TM} aRNA Kit, Ambion) was added to the RNA sample and incubated for 10 min at 70°C in the PCR machine with heated lid, then the sample was cooled on ice for 2 min. The master mix was prepared as follows: 4 µl 5 x First Strand Buffer (Invitrogen), 2 µl 0.1 M DTT (Invitrogen), 1 µl Ribonuclease inhibitor (40 U/µl, MBI Fermentas), 1 µl 10 mM dNTP mix and 2 µl Superscript II RNase H$^-$ reverse transcriptase (200 U/µl, Invitrogen) and mixed by pipetting up and down. The 10 µl master mix was added to the denatured RNA and primer mixture, making a final volume of 20 µl. The components were mixed thoroughly by gently pipetting up and down several times. After a brief spinning samples were collected at the bottom of the tube. Samples were incubated for 2 h at 37°C in the PCR machine with heated lid, 1 µl RNase H (2 U/µl, Invitrogen) was added to remove the RNA template and incubated for 20 min at 37°C. Samples were heated at 95°C for 5 min to inactivate the RNase H, and then chilled on ice for 2 min and spun briefly to collect the sample at the bottom of the tube.

For the second strand cDNA synthesis, 2 µl T7-Oligo (dT) promoter primer (50 µM, Affymetrix) was added to the chilled sample from the previous step and incubated for 6 min at 70°C. Samples were chilled on ice for 2 min and spun briefly to collect the sample at the bottom of the tube. The master mix was prepared as follows: 33.5 µl RNase free H2O, 15 µl 5 x Second Strand Buffer (Invitrogen), 1.5 µl 10 mM dNTP mix and 2 µl DNA Polymerase I (10 U/µl, Invitrogen) and mixed by pipetting up and down several times. The 52 µl master mix was added to the sample and incubated at 16°C for 2 h. 2 µl T4 DNA Polymerase (5 U/µl, Invitrogen) was added to the sample and incubated at 16°C for 10 min.

Double strand cDNA was cleaned by Sample Cleanup Module (Affymetrix) according to the manufacturer's protocol.

In vitro transcription for cRNA amplification and labelling was made with BioArray^{TM} HighYield^{TM} RNA Transcript Labeling Kit (Affymetrix) according to the manufacturer's protocol. The template cDNA and other reaction components were added to the tube at room temperature in the order shown: 12 µl of template cDNA, 10 µl of RNase-free water, 4 µl of 10 x HY Reaction Buffer, 4 µl of 10 x Biotin-Labeled Ribonucleotides, 4 µl of 10 x DTT, 4 µl of RNase Inhibitor Mix and 2 µl of

20 x T7 RNA Polymerase. The reaction was incubated for 4.5 h at 37°C water bath with gently mixing the contents of the tube every 30-45 min during the incubation.

Biotin-labelled cRNA was cleaned by Sample Cleanup Module (Affymetrix) according to the manufacturer's protocol.

2.2.12.1.4 Quantification and fragmentation of cRNA probe

The purified cRNA probe was diluted to 1:100 for the photometric quantification. The cRNA must be at a minimum concentration of 0.6 µg/µl. Fragment an appropriate amount of cRNA for hybridization cocktail and gel analysis. 5 x Fragmentation Buffer was supplied with the GeneChip Sample Cleanup Module. 2 µl 5 x Fragmentation Buffer was added for every 8 µl RNA plus water, the reaction was incubated for 35 min in a 94°C water bath. The Fragmentation buffer has been optimized to break down full-length cRNA to 35 to 200 base fragments by metal-induced hydrolysis. The final concentration of RNA in the fragmentation mix can range from 0.5 µg/µl to 2 µg/µl. Undiluted, fragmented sample RNA was stored at -70°C until ready to perform the hybridization.

2.2.12.2 Eukaryotic Target Hybridization

The hybridization cocktail was prepared according to the Affymetrix guidelines by mixing the following components for each target, volumes were scaled up for hybridization to multiple probe arrays. Frozen stocks of 20 x GeneChip Eukaryotic Hybridization Control were heated to 65°C for 5 min to completely resuspend the cRNA before aliquotting.

Table 6 Components of the hybridization cocktail

Component	**Standard Array**	**Final Concentration**
Fragmented cRNA	15 µg	0.05 µg/µl
Control Oligonucleotide B2 (3nM)	5 µl	50 pM
20 x Eukaryotic Hybridization Controls (bioB, bioC, bioD, cre)	15 µl	1.5, 5, 25 and 100 pM respectively
Herring Sperm DNA (10 mg/ml)	3 µl	0.1 mg/ml
Acetylated BSA (50 mg/ml)	3 µl	0.5 mg/ml
2 x Hybridization Buffer	150 µl	1 x
H_2O	To final volume of 300 µl	
Final volume	**300 µl**	

The probe array was equilibrated to room temperature immediately before use, the Hybridization Cocktail was heated to 99°C for 5 min in a heat block, meanwhile, the array was wetted by filling it through one of the septa with 200 µl 1 x hybridization buffer using a micropipettor and appropriate tips and incubated at 45°C for 10 min with rotation. The hybridization cocktail that had been heated at 99°C was transferred to a 45°C heat block for 5 min and centrifuged at maximum speed in a microcentrifuge for 5 min to remove any insoluble material from the hybridization mixture. The buffer solution was removed from the probe array cartridge and 200 µl of the clarified hybridization cocktail was filled avoiding any insoluble matter in the volume at the bottom of the tube. The probe array was placed in rotisserie box in 45°C oven with 60 rpm rotation and hybridized for 16 h.

2.2.12.3 Washing, Staining and Scanning

The washing, staining and scanning procedures were performed in the Fluidics Station 400 (Affymetrix) at the Max Planck Institute for Terrestrial Microbiology, Marburg. Antibody amplification for eukaryotic targets washing and staining procedure was used. The SAPE solution mix and antibody solution were prepared as follows:

Table 7 SAPE solution mix

Components	Volume	Final Concentration
2 x MES Stain Buffer	600.0 µl	1 x
50 mg/ml acetylated BSA	48.0 µl	2 mg/ml
1 mg/ml Streptavidin Phycoerythrin (SAPE)	12.0 µl	10 µg/ml
DI H_2O	540.0 µl	
Total	**1200 µl**	

The mixture was mixed well and divided into two aliquots of 600 µl each to be used for stains 1 and 3, respectively.

Table 8 Antibody solution mix

Components	Volume	Final Concentration
2 x MES Stain Buffer	300.0 µl	1 x
50 mg/ml acetylated BSA	24.0 µl	2 mg/ml
10 mg/ml Normal Goat IgG	6.0 µl	0.1 mg/ml
0.5 mg/ml biotinylated antibody	3.6 µl	3 µg/ml
DI H_2O	266.4 µl	
Total	**600 µl**	

After 16 h of hybridization, the hybridization cocktail was removed from the probe array, 250 µl of non-stringent wash buffer was filled in the probe array completely. Fluidics protocols were as follows:

Table 9 Fluidics protocols

	Standard Format (EukGE-WS2)
Post Hyb Wash 1	10 cycles of 2 mixes/cycle with Wash Buffer A at 25°C
Post Hyb Wash 2	4 cycles of 15 mixes/cycle with Wash Buffer B at 50°C
Stain	Stain the probe array for 10 min in SAPE solution at 25°C
Post Stain Wash	10 cycles of 4 mixes/cycle with Wash Buffer A at 25°C
2nd Stain	Stain the probe array for 10 min in antibody solution at 25°C
3rd Stain	Stain the probe array for 10 min in SAPE solution at 25°C
Final Wash	15 cycles of 4 mixes/cycle with Wash Buffer A at 30°C The holding temperature is 25°C

Completion of the wash protocols, the probe arrays were scanned at 570nm wavelength using GeneArray Scanner (Affymetrix, USA).

2.2.12.4 Microarray analysis

Data were analyzed and provided by Dr. B. Samans, an expert of microarray analysis in Dept. of Medical Biometry and Epidemiology, University Marburg.

3 Results

3.1 Gene expression analysis of calcitonin receptor isoforms in rat brain

3.1.1 RT-PCR analysis of $CT_{(a)}$ and $CT_{(b)}$ expression in rat brain

To investigate the region-specific gene expression of the two calcitonin receptor isoforms $CT_{(a)}$ and $CT_{(b)}$ in rat brain, total RNA extracts from cortex, hippocampus, thalamus, hypothalamus, cerebellum, brain stem and pituitary were analyzed by RT-PCR using isoform-specific primer pairs. As shown in Fig. 3, $CT_{(a)}$ mRNA was detected in all of the tissues examined with similar expression levels, except cortex which showed lower levels. In contrast, $CT_{(b)}$ gene expression varied between different brain regions. The strongest signals were detected in hypothalamus followed by thalamus and brain stem, hippocampus and pituitary. Very weak signals were observed in cerebellum. No PCR product for $CT_{(b)}$ could be detected in the cortex.

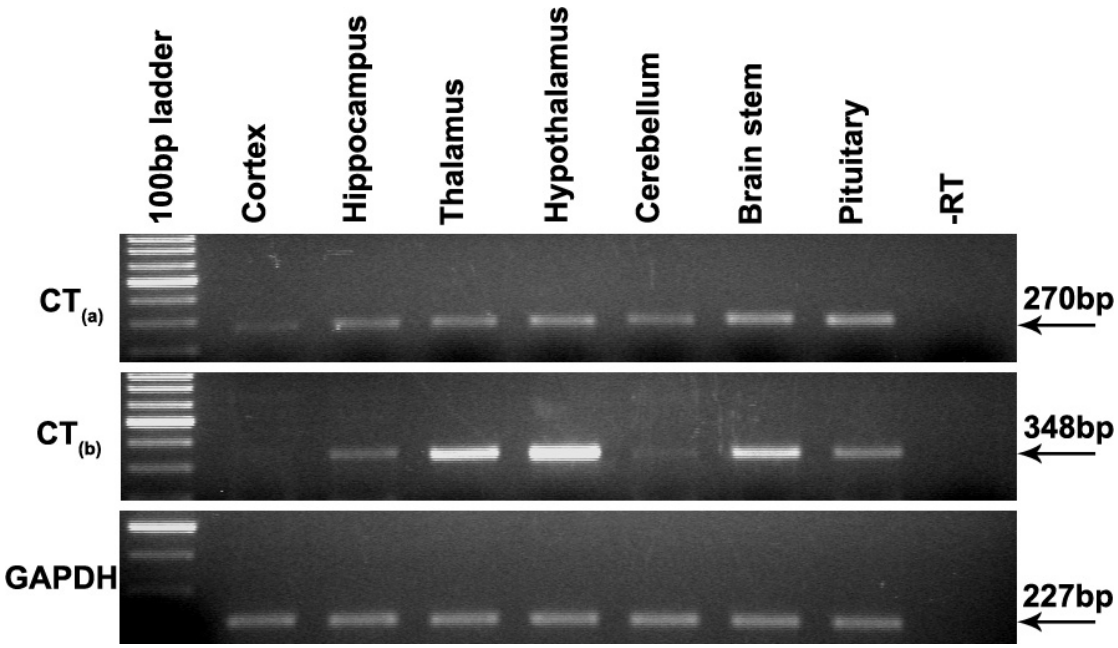

Fig. 3 RT-PCR analysis of $CT_{(a)}$ and $CT_{(b)}$ expression in rat brain

Gel electrophoresis of PCR products for $CT_{(a)}$ and $CT_{(b)}$ amplified from RNA extracts of dissected brain regions and the pituitary. A 270bp amplicon for $CT_{(a)}$ is detected in all tissues examined (upper panel). A 348bp amplicon for $CT_{(b)}$ is detected in hypothalamus, thalamus and brain stem, hippocampus, pituitary and cerebellum (middle panel). Note the lack of a specific PCR product for $CT_{(b)}$ in cerebral cortex. RT-PCR for the house-keeping gene GAPDH served as positive control (lower panel). As negative control reverse transcriptase is omitted from the cDNA synthesis of a hypothalamic RNA sample (-RT).

3.1.2 *Cellular expression patterns of calcitonin receptor mRNAs in rat brain revealed by in situ hybridization*

For comparative analysis of the regional distribution of $CT_{(a)}$ and $CT_{(b)}$ isoforms in rat brain, ISH was performed using ^{35}S-labeled cRNA probes. A $CT_{(a/b)}$ probe was generated which recognized both isoforms, while the $CT_{(b)}$ probe was designed to recognize only the $CT_{(b)}$ isoform. The isoform specificity of the probes is illustrated in Fig. 4.

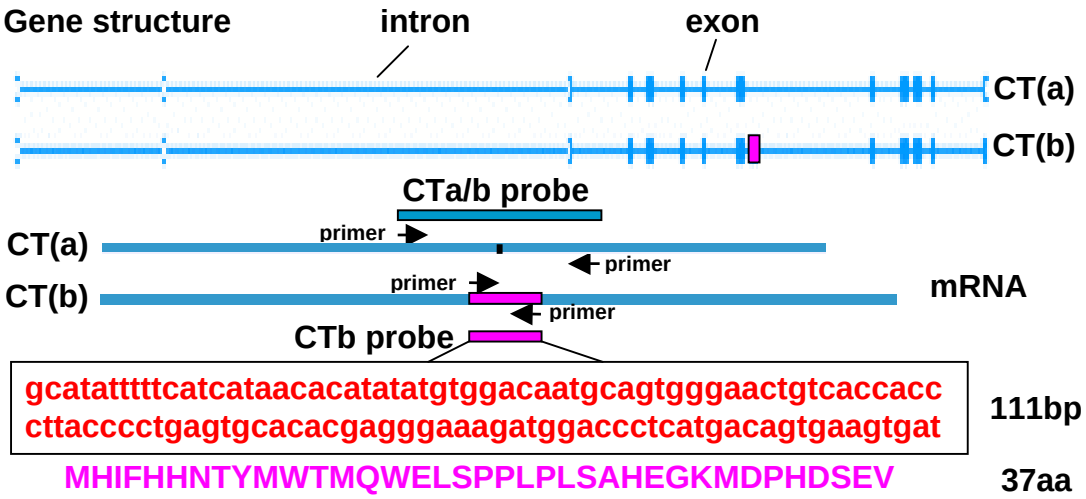

Fig. 4 Calcitonin receptor gene structure

The two rat calcitonin receptor isoforms $CT_{(a)}$ and $CT_{(b)}$ are generated by alternative splicing. Both isoforms differ in the presence of a 111bp insert (exon 9) in $CT_{(b)}$ which corresponds to a 37 amino acid insert in the predicted second extracellular domain.

Representative X-ray autoradiograms illustrate the distribution patterns of CT receptors in rat brain in Fig. 5. For a detailed analysis of cellular expression of CT receptor, hybridized slides were coated with nuclear emulsion and examined under a light microscope (Fig. 6 and Fig. 7). A subjective analysis of CT transcript levels in different brain region was performed, which is summarized in table 10.

In the telencephalon, intense hybridization signals with the $CT_{(a/b)}$ probe and the $CT_{(b)}$ probe were observed in the accumbens nucleus (Fig. 5A, Fig. 6A, Fig. 7A), lateral septal nucleus (Fig. 5B, Fig. 6B, Fig. 7B), bed nucleus of the stria terminalis (Fig. 5C, Fig. 6C, Fig. 7D) and various subdivisions of the amygdala (Fig. 5F, 5G, 5H, 5I, Fig. 6G, 6I, Fig. 7G, 7H, 7I).

In the diencephalon, CT receptor mRNAs were strongly expressed in many hypothalamic nuclei. Intense expression was detected in the septohypothalamic nucleus (Fig. 5C, Fig. 6C, Fig. 7C), the peri- and paraventricular nucleus (Fig. 5F, Fig. 6F, 6G, Fig. 7F, 7G), suprachiasmatic nucleus (Fig. 5D, Fig. 6D, Fig. 7F), as well as in the dorsomedial (Fig. 5G, Fig. 6H, Fig. 7H) and arcuate (Fig. 5H, Fig. 6I, Fig. 7I) hypothalamic nuclei. Intense to moderate expression was observed in the anterior (Fig. 5C, Fig. 6C, Fig. 7C) and lateral (Fig. 5H, Fig. 6I, Fig. 7I) hypothalamic areas. High expression levels were also present in the tuberal magnocellular nucleus (Fig. 5I), and premammillary nucleus (data not shown). Moderate signals for $CT_{(a/b)}$ probe (Fig. 5I, Fig. 6J) and low signals for $CT_{(b)}$ probe (Fig. 7J) were observed in the lateral habenular nucleus. Strong signals for $CT_{(a/b)}$ probe but not for $CT_{(b)}$ probe were observed in the subfornical organ (Fig. 5D, Fig. 6E, Fig.7E).

In the mesencephalon, intense expression of CT receptor mRNAs was observed in the dorsal raphe nucleus (Fig. 5L, Fig. 6L, Fig. 7K). Moderate expression was observed in the lateral ventral periaqueductal gray, the lateral substantia nigra and the ventral tegmental area (Fig. 5J). CT receptors were also moderately expressed in the paratrochlear nucleus, median raphe nucleus, subpeduncular, pedunculopontine and the ventral tegmental nucleus (Fig. 5K, 5L, Fig. 6K, 6L). Weak expression of $CT_{(b)}$ isoform was found in the lateral ventral periaqueductal gray, ventral tegmental area, subpeduncular tegmental nucleus and the pedunculopontine tegmental nucleus (see table 10).

In the brainstem, intense expression of CT receptor mRNAs was observed in the locus coeruleus, subcoeruleus nucleus (dorsal part), raphe magnus nucleus (Fig. 5P, Fig. 6P, Fig. 7N), area postrema and the nucleus of the solitary tract (Fig. 5R, Fig. 6R, Fig. 7O). CT receptors were moderately expressed in the dorsal and laterodorsal tegmental nucleus, lateral parabrachial nucleus, reticulotegmental nucleus of the pons (Fig. 5M, 5N, Fig. 6M, 6N, Fig. 7L, 7M), raphe obscurus nucleus, raphe pallidus nucleus and the lateral reticular nucleus (Fig. 5Q, 5R, Fig. 6Q, 6R, Fig. 7O). Signals were detectable for $CT_{(a/b)}$ probe in the dorsomedial tegmental area (Fig. 5O, Fig. 6O), parvocellular reticular nucleus, gigantocellular reticular nucleus, lateral paragigantocellular nucleus (Fig. 5Q, Fig. 6Q) and the ventral medullary reticular nucleus (Fig. 5R, Fig. 6R). In contrast, specific signals for $CT_{(b)}$ probe in these regions were undetectable.

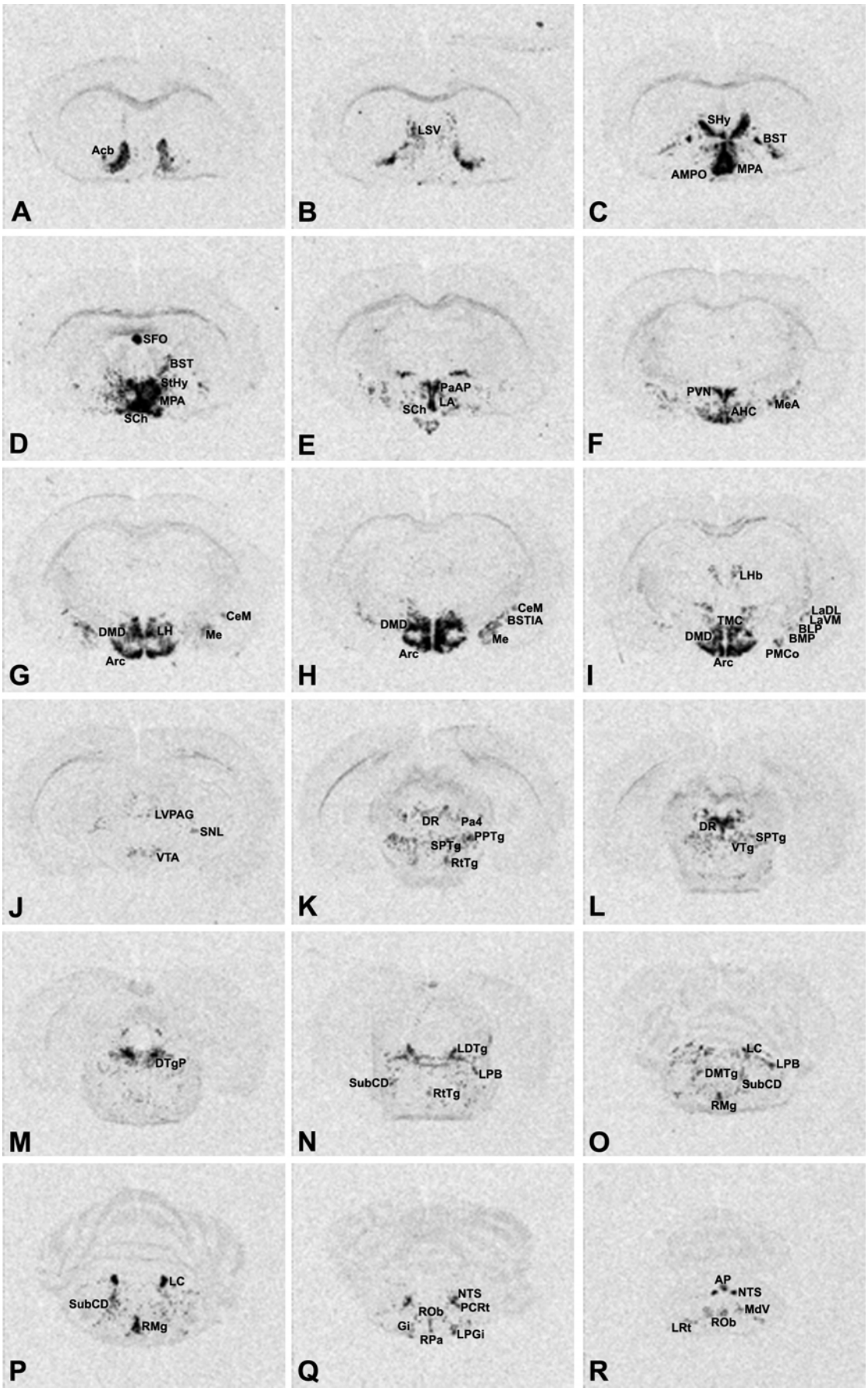

Fig. 5 Mapping of calcitonin receptor mRNA expression in rat brain

Representative X-ray film autoradiograms of coronal 14-µm-thick sections through the rat brain in rostral to caudal orientation illustrating the regional distribution of CT receptors. Consecutive brain sections are hybridized with a ^{35}S-labeled cRNA probe detecting both $CT_{(a)}$ and $CT_{(b)}$ mRNA. Acb, accumbens ncl.; AHC, anterior hypothalamic area, central; AMPO, anterior medial preoptic ncl.; AP, area postrema; Arc, arcuate hypothalamic ncl.; BLP, basolateral amygdaloid ncl., post; BMP, basomedial amygdaloid ncl., post; BST, bed nucleus of the stria terminalis; BSTIA, bed nucleus of the stria terminalis, intraamygdaloid div; CeM, central amygdaloid ncl., med div; DMD, dorsomedial hypothalamic ncl.; DMTg, dorsomedial tegmental area; DR, dorsal raphe ncl.; DTgP, dorsal tegmental ncl., pericentral; Gi, gigantocellular reticular ncl.; LA, lateroanterior hypothalamic ncl.; LaDL, lateral amygdaloid ncl., dorsolateral; LaVM, lateral amygdaloid ncl., ventromedial; LC, locus coeruleus; LDTg, laterodorsal tegmental ncl.; LH, lateral hypothalamic area; LHb, lateral habenular ncl.; LPB, lateral parabrachial ncl.; LPGi, lateral paragigantocellular ncl.; LRt, lateral reticular ncl.; LSV, lateral septal ncl.; LVPAG, lateral ventral periaqueductal gray; MdV, medullary reticular ncl., ventral; Me, medial amygdaloid ncl.; MeA, medial amygdaloid ncl., anterior; MPA, medial preoptic area; NTS, nucleus of the solitary tract; Pa4, paratrochlear ncl.; PaAP, paraventricular hypothalamic ncl., ant parvo; PCRt, parvocellular reticular ncl.; PMCo, posteromedial cortical amygdaloid ncl.; PPTg, pedunculopontine tegmental ncl.; PVN, paraventricular hypothalamic ncl.; RMg, raphe magnus ncl.; ROb, raphe obscurus ncl.; RPa, raphe pallidus ncl.; RtTg, reticulotegmental nucleus pons; SCh, suprachiasmatic ncl.; SFO, subfornical organ; SHy, septohypothalamic ncl.; SNL, substantia nigra, lateral; SPTg, subpeduncular tegmental ncl.; StHy, striohypothalamic ncl.; SubCD, subcoeruleus nucleus, dorsal; TMC, tuberal magnocellular ncl.; VTA, ventral tegmental area; VTg, ventral tegmental ncl. Exposure of X-ray film 70h.

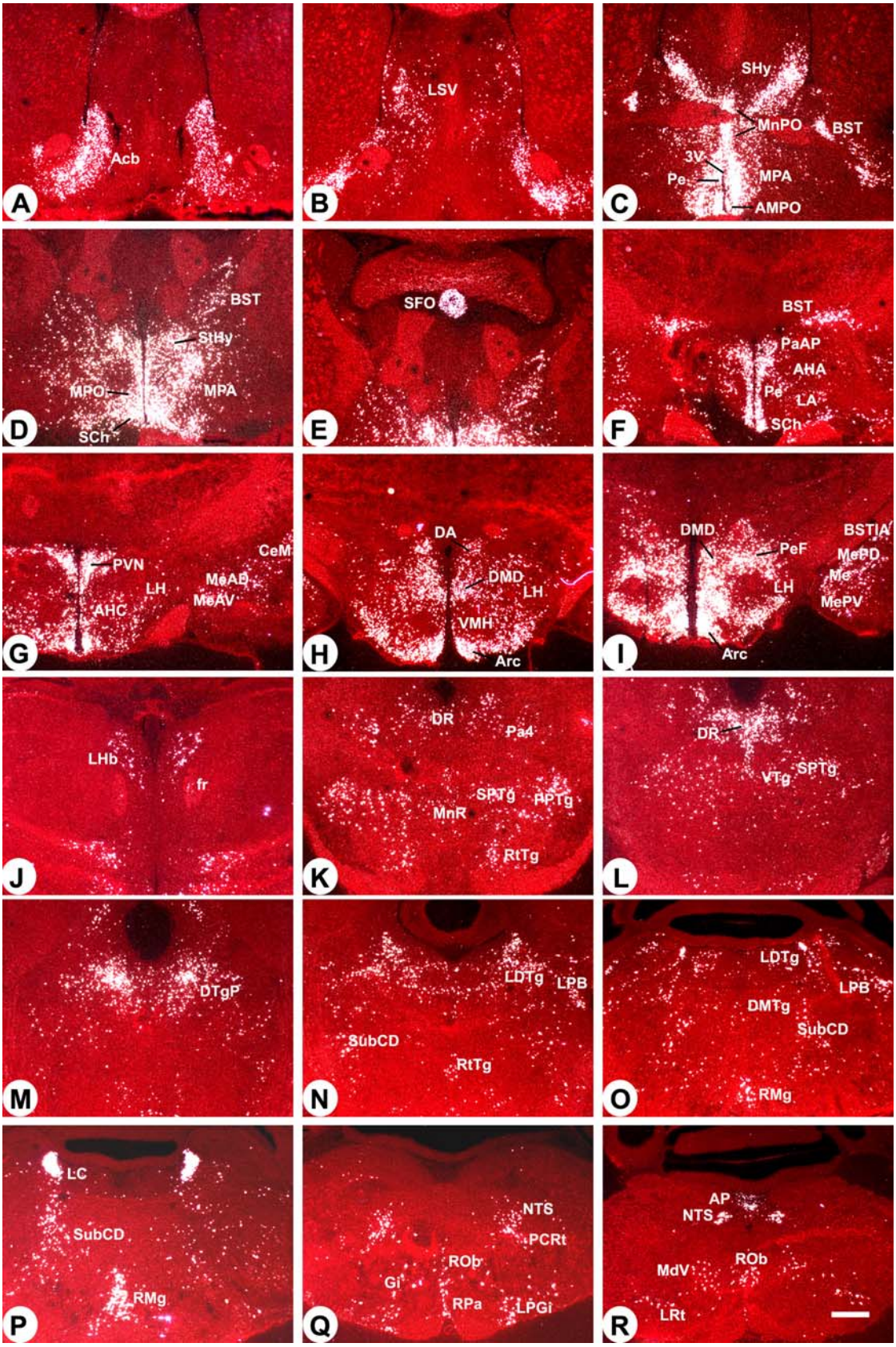

Fig. 6 Cellular distribution of calcitonin receptor mRNAs in rat brain

Representative low power microscopic darkfield autoradiograms illustrating the expression pattern of CT receptors in frozen sections through the rat brain after hybridization with ^{35}S-labeled riboprobes detecting both $CT_{(a)}$ and $CT_{(b)}$ transcripts. CT receptors are detected in Acb, accumbens ncl.; AHA, anterior hypothalamic area; AHC, anterior hypothalamic area, central; AMPO, anterior medial preoptic ncl.; AP, area postrema; Arc, arcuate hypothalamic ncl.; BST, bed nucleus of the stria terminalis; BSTIA, bed nucleus of the stria terminalis, intraamygdaloid div; CeM, central amygdaloid ncl., med div; DA, dorsal hypothalamic area; DMD, dorsomedial hypothalamic ncl.; DMTg, dorsomedial tegmental area; DR, dorsal raphe ncl.; DTgP, dorsal tegmental ncl., pericentral; fr, fasciculus retroflexus; Gi, gigantocellular reticular ncl.; LA, lateroanterior hypothalamic ncl.; LC, locus coeruleus; LDTg, laterodorsal tegmental ncl.; LH, lateral hypothalamic area; LHb, lateral habenular ncl.; LPB, lateral parabrachial ncl.; LPGi, lateral paragigantocellular ncl.; LRt, lateral reticular ncl.; LSV, lateral septal ncl.; MdV, medullary reticular ncl., ventral; Me, medial amygdaloid ncl.; MeAD, medial amygdaloid nucleus, anterodorsal; MeAV, medial amygdaloid nucleus, anteroventral; MePD, medial amygdaloid nucleus, posterodorsal; MePV, medial amygdaloid nucleus, posteroventral; MnPO, median preoptic ncl.; MnR, median raphe ncl.; MPA, medial preoptic area; MPO, medial preoptic ncl.; NTS, nucleus of the solitary tract; Pa4, paratrochlear ncl.; PaAP, paraventricular hypothalamic ncl., ant parvo; PCRt, parvocellular reticular ncl.; Pe, periventricular hypothalamic ncl.; PeF, perifornical ncl.; PPTg, pedunculopontine tegmental ncl.; PVN, paraventricular hypothalamic ncl.; RMg, raphe magnus ncl.; ROb, raphe obscurus ncl.; RPa, raphe pallidus ncl.; RtTg, reticulotegmental nucleus pons; SCh, suprachiasmatic ncl.; SFO, subfornical organ; SHy, septohypothalamic ncl.; SPTg, subpeduncular tegmental ncl.; StHy, striohypothalamic ncl.; SubCD, subcoeruleus nucleus, dorsal; VMH, ventromedial hypothalamic ncl.; VTg, ventral tegmental ncl.. 3V, third ventricle. Exposure time: 14 days. Scale bar: 200µm.

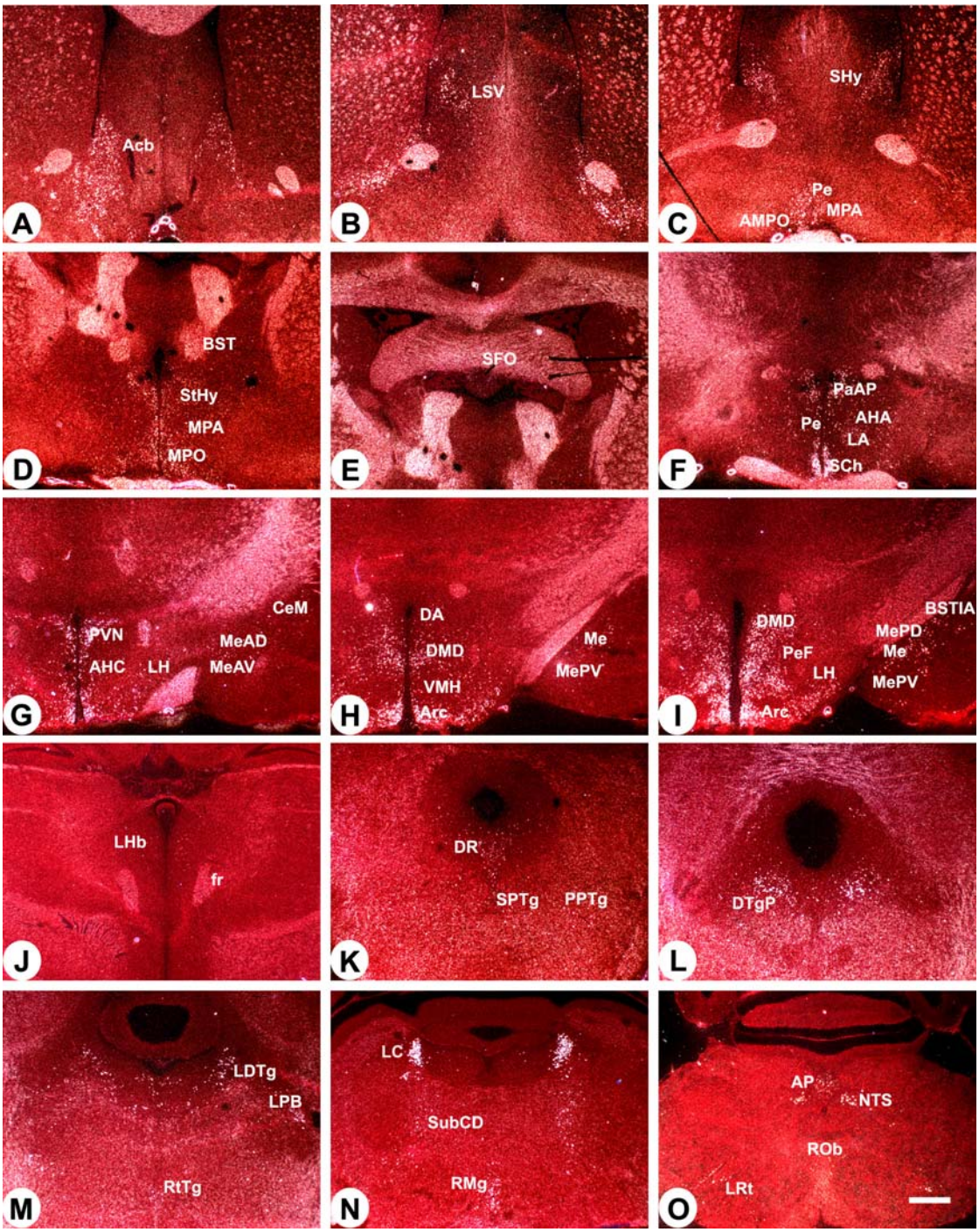

Fig. 7 Expression of $CT_{(b)}$ mRNA in rat brain

Representative low power microscopic darkfield autoradiograms illustrating the expression pattern of $CT_{(b)}$ in frozen sections through the rat brain after hybridization with ^{35}S-labeled riboprobes. $CT_{(b)}$ mRNA is detected in Acb, accumbens ncl.; AHA, anterior hypothalamic area; AHC, anterior hypothalamic area, central; AMPO, anterior medial preoptic ncl.; AP, area postrema; Arc, arcuate hypothalamic ncl.; BST, bed nucleus of the stria terminalis; BSTIA, bed nucleus of the stria terminalis, intraamygdaloid div; CeM, central amygdaloid ncl., med div; DA, dorsal hypothalamic area; DMD, dorsomedial hypothalamic ncl.; DR, dorsal raphe ncl.; DTgP, dorsal tegmental ncl., pericentral; fr,

fasciculus retroflexus; LA, lateroanterior hypothalamic ncl.; LC, locus coeruleus; LDTg, laterodorsal tegmental ncl.; LH, lateral hypothalamic area; LHb, lateral habenular ncl.; LPB, lateral parabrachial ncl.; LRt, lateral reticular ncl.; LSV, lateral septal ncl.; Me, medial amygdaloid ncl.; MeAD, medial amygdaloid nucleus, anterodorsal; MeAV, medial amygdaloid nucleus, anteroventral; MePD, medial amygdaloid nucleus, posterodorsal; MePV, medial amygdaloid nucleus, posteroventral; MPA, medial preoptic area; MPO, medial preoptic ncl.; NTS, nucleus of the solitary tract; PaAP, paraventricular hypothalamic ncl., ant parvo; Pe, periventricular hypothalamic ncl.; PeF, perifornical ncl.; PPTg, pedunculopontine tegmental ncl.; PVN, paraventricular hypothalamic ncl.; RMg, raphe magnus ncl.; ROb, raphe obscurus ncl.; RtTg, reticulotegmental nucleus pons; SCh, suprachiasmatic ncl.; SFO, subfornical organ; SHy, septohypothalamic ncl.; SPTg, subpeduncular tegmental ncl.; StHy, striohypothalamic ncl.; SubCD, subcoeruleus nucleus, dorsal; VMH, ventromedial hypothalamic ncl.. 3V, third ventricle. exposure time: 41 days. Scale bar: 200µm.

Table 10 Subjective evaluation of the regional hybridization signals obtained with the $CT_{(a/b)}$ and $CT_{(b)}$ probes in rat brain[1]

	Signals with $CT_{(a/b)}$ probe	Signals with $CT_{(b)}$ probe
Telencephalon		
Accumbens nucleus (Acb)	+++++	+++
Lateral septal nucleus (LSV)	++++	++
Bed nucleus of the stria terminalis (BST)	++++	+
Bed nu st, intraamyg div (BSTIA)	++++	++
Medial amygdaloid nu, anterior (MeA)	++++	++
Medial amyg nu, anteroventral (MeAV)	++++	++
Medial amyg nu, anterodorsal (MeAD)	++++	++
Central amyg nu, med div (CeM)	++++	++
Cent amyg nu, med, anterod (CeMAD)	++++	++
Cent amyg nu, med, posterov (CeMPV)	++++	++
Medial amygdaloid nu (Me)	++++	++
Medial amyg nu, posterodorsal (MePD)	++++	++
Medial amyg nu, posteroventral (MePV)	++++	++
Posteromed cortical amyg nu (PMCo)	++++	++
Basomedial amygdaloid nu, post (BMP)	++++	++
Basolateral amygdaloid nu, post (BLP)	++++	++
Lateral amyg nu, ventromedial (LaVM)	++++	++
Lateral amygdaloid nu, dorsolat (LaDL)	++++	++
Diencephalon		
Median preoptic nucleus (MnPO)	+++++	+
Medial preoptic area (MPA)	+++++	++
Anterior medial preoptic nu (AMPO)	+++++	+++
Septohypothalamic nu (SHy)	+++++	+++
Striohypothalamic nu (StHy)	+++++	++
Medial preoptic nu (MPO)	+++++	+++
Subfornical organ (SFO)	+++++	-
Periventricular hypoth nu (Pe)	+++++	+++
Paravent hypoth nu, ant parvo (PaAP)	+++++	+++

	Signals with $CT_{(a/b)}$ probe	Signals with $CT_{(b)}$ probe
Anterior hypoth area (AHA)	+++*	+*
Lateroanterior hypoth nu (LA)	+++*	+*
Suprachiasmatic nu (SCh)	+++++	+++
Paravent hy nu, med parvocell (PaMP)	+++++	+++
Paravenr hy nu, lat magnocell (PaLM)	+++++	+++
Paraventricular hypoth nu, vent (PaV)	+++++	+++
Anterior hypoth area, central (AHC)	+++*	+*
Dorsal hypoth area (DA)	++++	++
Dorsomedial hypothalamic nu (DMD)	+++++	+++
Ventromedial hypoth nu (VMH)	+++++	+++
Lateral hypoth area (LH)	+++*	+*
Perifornical nu (PeF)	++++*	+*
Arcuate hypoth nu (Arc)	+++++	+++
Tuberal magnocellular nu (TMC)	+++++	+++
Premammillary nu, ventral (PMV)	++++	++
Premammillary nu, dorsal (PMD)	++++	++
Lateral habenular nu (LHb)	+++*	*
Fasciculus retroflexus (fr)	+*	-
Mesencephalon		
Lateral ventral periaqueductal gray (LVPAG)	++*	*
Substantia nigra, lateral (SNL)	++*	-
Ventral tegmental area (VTA)	++*	*
Dorsal raphe nu (DR)	+++	+
Paratrochlear nu (Pa4)	++*	-
Median raphe nu (MnR)	++*	-
Subpeduncular tegmental nu (SPTg)	++*	*
Pedunculopontine tegmental nu (PPTg)	++*	*
Ventral tegmental nu (VTg)	++*	-
Brainstem		
Dorsal tegmental nu, pericentral (DTgP)	++++	++
Laterodorsal tegmental nu (LDTg)	+++*	+*
Lateral parabrachial nu (LPB)	+++*	+*
Subcoeruleus nu, dorsal (SubCD)	+++*	+*
Reticulotegmental nu pons (RtTg)	+++*	*
Dorsomedial tegmental area (DMTg)	++*	-
Locus coeruleus (LC)	+++++	+++
Raphe magnus nu (RMg)	+++++	++
Parvocellular reticular nu (PCRt)	+++*	-
Gigantocellular reticular nu (Gi)	+++*	-
Lateral paragigantocellular nu (LPGi)	+++*	-
Raphe obscurus nu (ROb)	++*	*
Raphe pallidus nu (RPa)	++*	*
Area postrema (AP)	++++	+
Nu solitary tract (NTS)	++++	+
Medullary reticular nu, ventral (MdV)	+++*	-
Lateral reticular nu (LRt)	+++*	*

For each individual probe the hybridization signal density was evaluated subjectively and ranked as follows: +++++, maximum density; ++++, very dense; +++, dense; ++, moderate; +, low; -, below detection; *, single scattered neurons.

3.2 RT-PCR analysis of $CT_{(a)}$ and $CT_{(b)}$ transcripts in the RNA extracts of microdissected area postrema (AP) and nucleus of the solitary tract (NTS)

In situ hybridization analysis revealed the expression of CT receptors in the area postrema (AP) and the nucleus of the solitary tract (NTS) of the brain stem. To investigate which isoform was expressed in these regions, LCM combined with RT-PCR analysis was performed using isoform-specific primer pairs. The area postrema (AP) and the nucleus of the solitary tract (NTS) were identified in cresyl violet stained sections (Fig. 8A, D) and laser-microdissected regions (Fig. 8C, F) (see 2.2.4.2 for details). RNA extracts from microdissected nuclei of 5 sections were pooled and subjected to one-round RNA amplification followed by RT-PCR. As shown in Fig. 8G, both calcitonin receptor isoforms of $CT_{(a)}$ and $CT_{(b)}$ were expressed in AP and NTS.

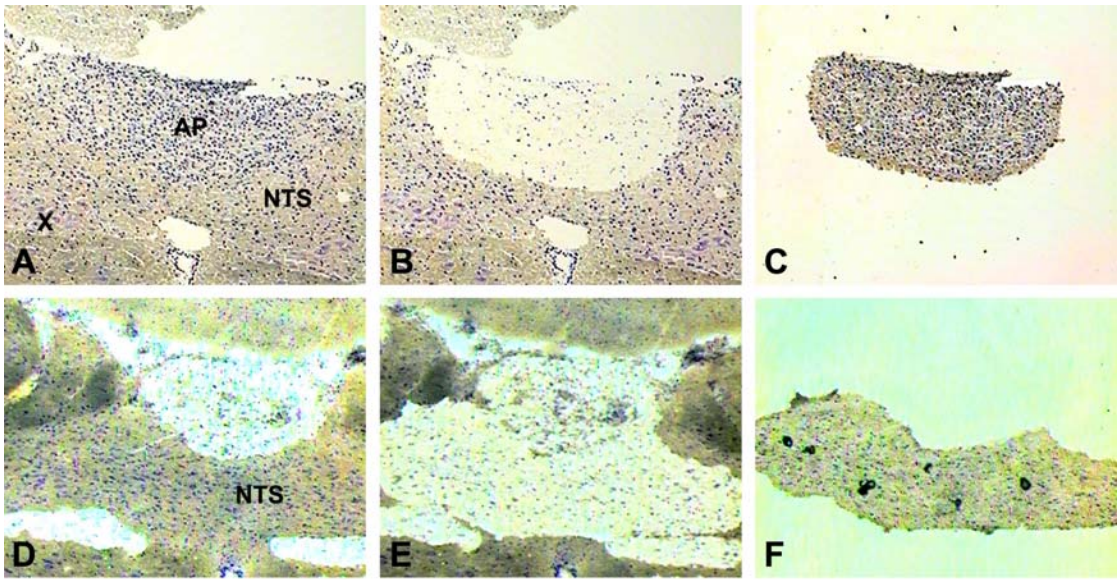

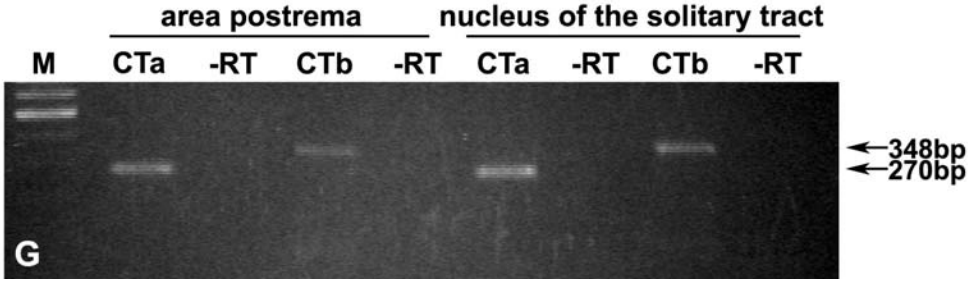

Fig. 8 RT-PCR analysis of $CT_{(a)}$ and $CT_{(b)}$ mRNA expression in microdissected area postrema and the nucleus of the solitary tract

Expression of $CT_{(a)}$ and $CT_{(b)}$ isoforms in the area postrema (AP) and the nucleus of the solitary tract (NTS) is examined by laser capture microdissection (LCM) (A-F) in combination with RT-PCR analysis (G). First, the AP is microdissected from cresyl violet acetate-stained tissue sections (A-C). LCM of the NTS (D-F) is performed after removal of the dorsal motor ncl.of vagus (X). (A, D) before microdissection, (B, E) after microdissection, (C, F) microdissected material, (G) RT-PCR analysis of amplified RNA extracts from AP and NTS microdissected from 10 sections. A 270bp fragment representing $CT_{(a)}$ mRNA and a 348bp fragment representing $CT_{(b)}$ mRNA are detected in both regions (G). Omission of reverse transcriptase (-RT) as negative control.

3.3 Expression of calcitonin receptor isoforms in phenotype-identified neurons in hypothalamus

3.3.1 Arcuate nucleus (Arc)

The expression of CT receptor isoforms in neuronal subpopulations of the arcuate ncl. characterized by their expression of the neuropeptides neuropeptide Y (NPY), pro-opiomelanocortin (POMC) or cocaine- and amphetamine-regulated transcript (CART) was investigated by dual in situ hybridization using digoxigenin-labeled probes for the neuropeptide mRNAs and radiolabeled probes for the CT receptor mRNAs. All NPY neurons exhibited positive hybridization signals with both the $CT_{(a/b)}$ probe (Fig. 9A) and the $CT_{(b)}$ probe (Fig. 9B). Since the signals with the shorter $CT_{(b)}$ probe in NPY neurons were as strong as the signals with the $CT_{(a/b)}$ probe it was concluded that NPY neurons predominantly express the $CT_{(b)}$ isoform. As summarized in table 11, 54% of POMC neurons and 48% of CART neurons were found to hybridize with the $CT_{(a/b)}$ probe (Fig. 9C, double arrows, 9E, double arrows). No hybridization signals for $CT_{(b)}$ mRNA could be detected in POMC neurons or CART neurons (Fig. 9D, 9F) suggesting that a subpopulation of POMC neurons and CART neurons express selectively the $CT_{(a)}$ isoform.

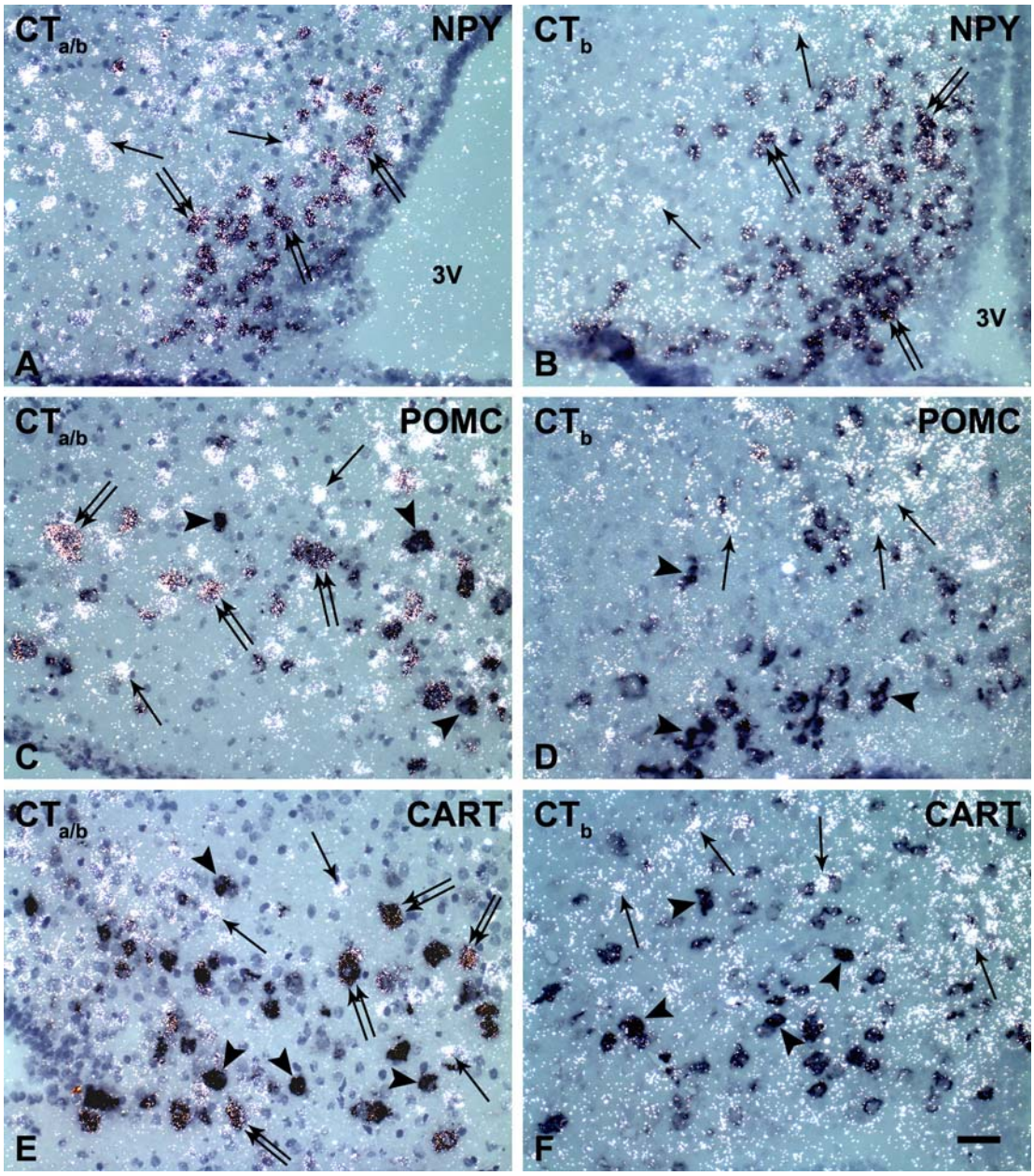

Fig. 9 Colocalization of CT receptor isoforms with NPY, POMC or CART in neurons of the arcuate nucleus

Brightfield microscopic images showing the coexpression pattern of CT receptor mRNAs with NPY (A, B), POMC (C, D) and CART (E, F), respectively, in representative sections through the arcuate nucleus of the male Wistar rats. NPY, POMC and CART transcripts are detected with digoxigenin (DIG)-labeled probes producing a dark violet reaction precipitate and CT mRNAs with ^{35}S-labeled probes represented by white grains. The Radiolabeled $CT_{(a/b)}$ riboprobe can detect both isoforms, while the radiolabeled $CT_{(b)}$ riboprobe is specific for the $CT_{(b)}$ isoform. Note both $CT_{(a/b)}$ and $CT_{(b)}$ probes label all NPY neurons (A, B, double arrows), while $CT_{(a/b)}$ signals are restricted to a subpopulation of POMC and CART neurons (C, E, double arrows). Most POMC and CART neurons do not express detectable levels of $CT_{(b)}$ mRNA (D, F) suggesting selective expression of the $CT_{(a)}$ isoform in POMC and CART

neurons. 3V, third ventricle. Exposure times: 16 days for probe $CT_{(a/b)}$, 24 days for probe $CT_{(b)}$. Scale bar in F: 50µm.

3.3.2 Paraventricular nucleus (PVN)

The expression of CT receptor isoforms in corticotropin-releasing hormone (CRH) and thyrotropin-releasing hormone (TRH) neurons in the PVN was investigated using dual in situ hybridization. As shown in Fig. 10 and table 11, 44% of CRH neurons (A, double arrows) and 23% of TRH neurons (C, double arrows) were found to express CT receptors. $CT_{(b)}$ specific transcripts were detected in about 24% of CRH neurons (B, double arrows) and 22% of TRH neurons (D, double arrows).

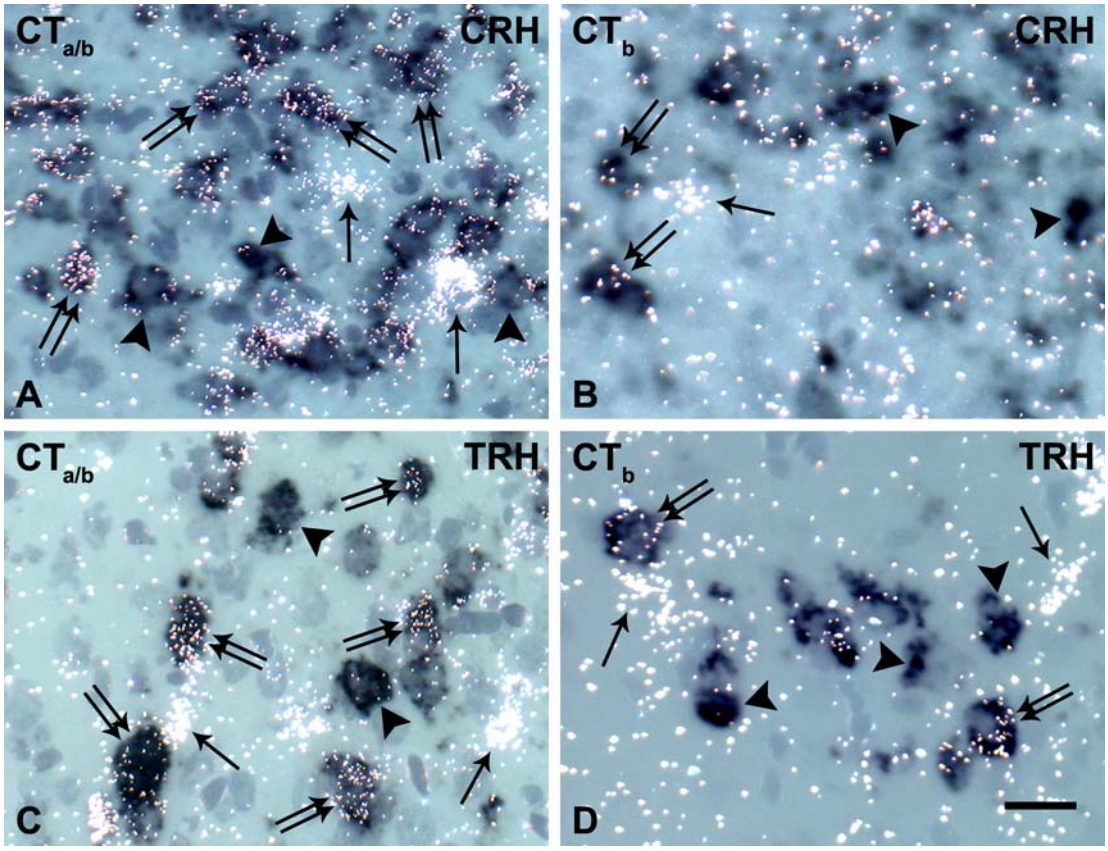

Fig. 10 Colocalization of CT receptor isoforms with CRH and TRH in neurons of the paraventricular nucleus

Representative brightfield images showing the coexpression pattern of CT receptor mRNAs with CRH (A, B) and TRH (C, D), respectively. CRH and TRH transcripts are detected with digoxigenin (DIG)-labeled probes producing a dark violet reaction precipitate and CT mRNAs with ^{35}S-labeled probes represented by white grains. Note that a subpopulation of CRH (A, double arrows) and TRH (C, double arrows) neurons exhibit a positive hybridization signal with the $CT_{(a/b)}$ probe, $CT_{(b)}$ specific signals are

found in a subpopulation of CRH (B, double arrows) and TRH (D, double arrows) neurons. Exposure times: 16 days for probe $CT_{(a/b)}$, 24 days for probe $CT_{(b)}$. Scale bar in F: 25µm.

3.3.3 Lateral hypothalamic area (LHA)

The expression of CT receptor isoforms in orexin, melanin-concentrating hormone (MCH) and cocaine- and amphetamine-regulated transcript (CART) neurons in the LHA was investigated using dual in situ hybridization. As shown in Fig. 11, all orexin neurons were found to hybridize with the $CT_{(a/b)}$ probe (Fig. 11A, double arrows). Strong signals for $CT_{(a/b)}$ were also present in another subpopulation of neurons which did not express orexin (Fig. 11A, arrows). The $CT_{(b)}$ probe labeled virtually all orexin neurons (Fig. 11B, double arrows). The signals for $CT_{(a/b)}$ in orexin neurons were weaker than those for $CT_{(b)}$ suggesting that orexin neurons predominantly express the $CT_{(b)}$ isoform. Strong signals for $CT_{(b)}$ in other than orexin neurons were not observed. Hybridization signals for CT receptor mRNAs could neither be detected in MCH neurons (Fig. 11C, 11D) nor in CART neurons (Fig. 11E, 11F) located in the lateral hypothalamic area, suggesting the lack of CT receptors in these cell types. The results are summarized in table 11.

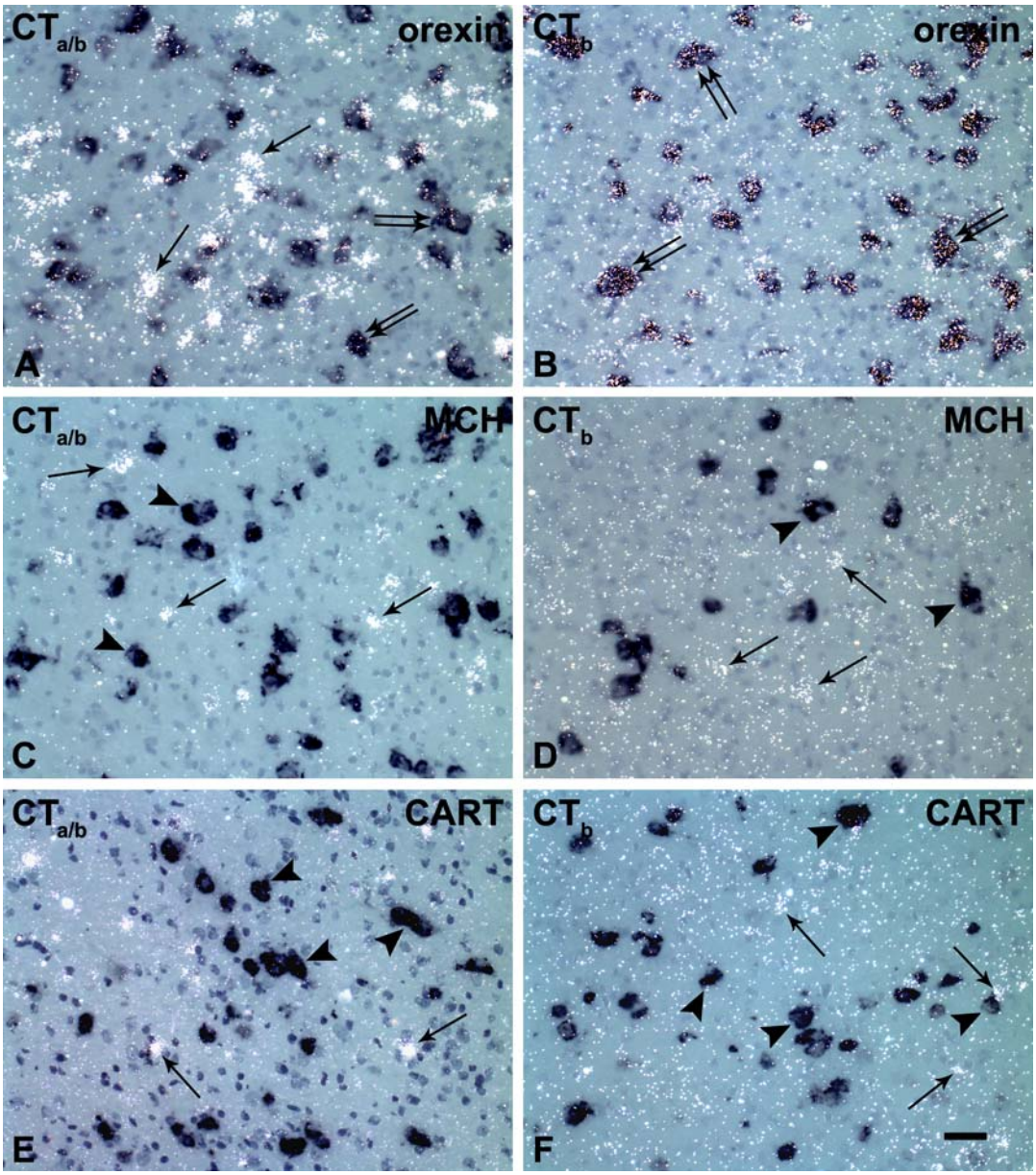

Fig. 11 Colocalization of CT receptor isoforms with orexin, MCH and CART in the lateral hypothalamic area

Representative brightfield microscopic images showing the coexpression pattern of CT receptor mRNAs with orexin (A, B), MCH (C, D) and CART (E, F), respectively. Orexin, MCH and CART transcripts are detected with digoxigenin (DIG)-labeled probes producing a dark violet reaction precipitate and CT mRNAs with ^{35}S-labeled probes represented by white grains. Note that nearly all orexin neurons (A, B, double arrows) exhibit positive hybridization signals with $CT_{(a/b)}$ probe and $CT_{(b)}$ probe, while most MCH and CART neurons (C-F, arrowheads) do not express detectable levels of CT receptor mRNAs suggesting the lack of CT receptors in these cell types. Exposure times: 16 days for probe $CT_{(a/b)}$, 24 days for probe $CT_{(b)}$. Scale bar in F: 50µm.

Table 11 Cell specific expression of $CT_{(a)}$ and $CT_{(b)}$ in peptidergic neurons relating food intake regulation in hypothalamus

Hypothalamic nucleus / area	Peptidergic phenotype	$CT_{(a/b)}$ probe	$CT_{(b)}$ probe	CT receptor isoforms	
				$CT_{(a)}$	$CT_{(b)}$
Arc	NPY	100%	100%	?	Yes
	POMC	54%*	0%	Yes	No
	CART	48%*	0%	Yes	No
PVN	CRH	44%*	24%*	?	Yes
	TRH	23%*	22%*	?	Yes
LHA	orexin	100%	100%	?	Yes
	MCH	0%	0%	No	No
	CART	0%	0%	No	No
	Unidentified neurons	100%	0%	Yes	No

*Note: To determine the coexpression of CT receptors with POMC and CART, 305 POMC neurons in 9 sections and 178 CART neurons in 7 sections from 3 control rats were counted, respectively. To determine the coexpression of CT receptors with CRH and TRH, 594 CRH neurons and 504 TRH neurons in 10 sections from 3 control rats were counted, respectively. To determine the coexpression of $CT_{(b)}$ with CRH and TRH, 442 CRH neurons and 211 TRH neurons in 7 sections from 3 control rats were counted, respectively.

3.4 Expression of calcitonin receptor isoforms in phenotype-identified neurons in brain stem

In order to clarify the cellular distribution of CT receptor isoforms in the area postrema, dual in situ hybridization analysis with CT receptor and TRH probes was performed. As shown in Fig. 12, no hybridization signals for $CT_{(a/b)}$ were observed in THR neurons in the area postrema.

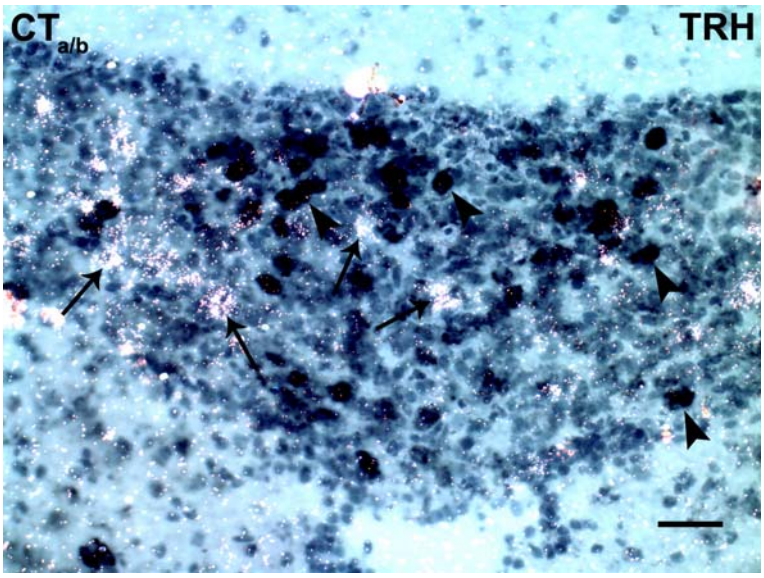

Fig. 12 Lack of calcitonin (CT) receptor expression in thyrotropin-releasing hormone (TRH) neurons of the area postrema

Representative brightfield microscopic image demonstrating that TRH neurons do not express CT receptor mRNA in the area postrema. Immunodetection of the digoxigenin-labeled TRH probe produces a dark violet reaction precipitate (arrowheads), ^{35}S-labeling for $CT_{(a/b)}$ signals is represented by white grains (arrows). Note lack of double-labeled cells. Exposure time: 16 days for probe $CT_{(a/b)}$. Scale bar: 50µm.

3.5 Identification of CT receptor isoforms in orexin neurons

3.5.1 ISH with isoform-specific oligonucleotides

To identify the CT receptor isoforms in orexin neurons, specific oligonucleotide probes for the $CT_{(a)}$ mRNA and for orexin mRNA were used to perform dual in situ hybridization. As shown in Fig. 13A, $CT_{(a)}$ was expressed in the dorsomedial hypothalamic nucleus (DMH), ventromedial hypothalamic nucleus (VMH), arcuate nucleus (ARC) and the lateral hypothalamic area (LHA). As shown in Fig. 13B, $CT_{(a)}$ was not expressed in orexin neurons.

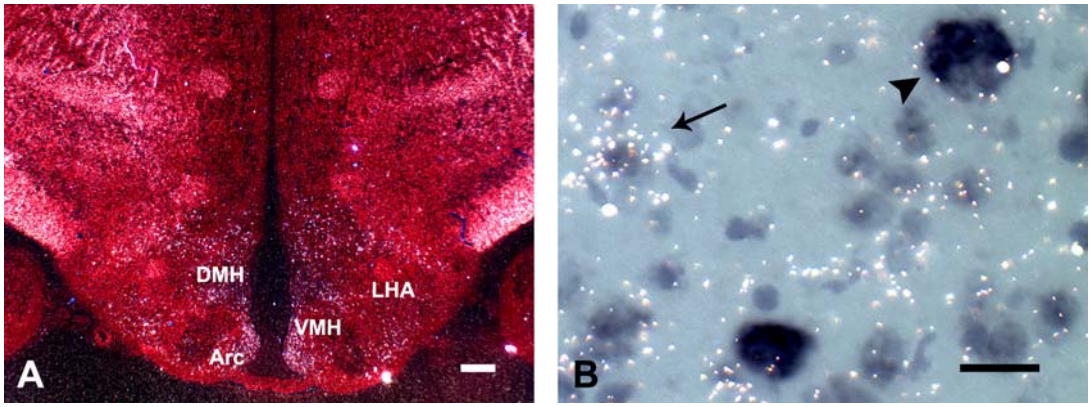

Fig. 13 Expression analysis of $CT_{(a)}$ in orexin neurons

(A) Darkfield image illustrating the expression of $CT_{(a)}$ mRNA in dorsomedial hypothalamic (DMH) nuclei, arcuate nucleus (ARC) and lateral hypothalamic area (LHA) using a ^{35}S-labeled oligonucleotide (white grains). (B) The $CT_{(a)}$ probe yields a specific hybridization signal (arrow) in a cell different from an orexin neuron, which is labeled by the dark violet reaction precipitate of the digoxigenin-labeled orexin oligo probe (arrowhead). Exposure time: 43 days for ^{35}S-labeled oligonucleotide $CT_{(a)}$ probe. Scale bar in A 100µm and in B 25µm.

3.5.2 Identification of CT receptor isoforms in microdissected orexin-immunoreactive neurons by RT-PCR

To identify the selective expression of CT receptor isoforms in orexin neurons, the method of laser capture microdissection in combination with RT-PCR was employed. Immunofluorescence-labeled orexin neurons were captured and subjected to RNA isolation and RT-PCR. As shown in Fig. 14 D, after 50 cycles of amplification only $CT_{(b)}$ was detected in orexin neurons while both $CT_{(a)}$ and $CT_{(b)}$ were detected in hypothalamus.

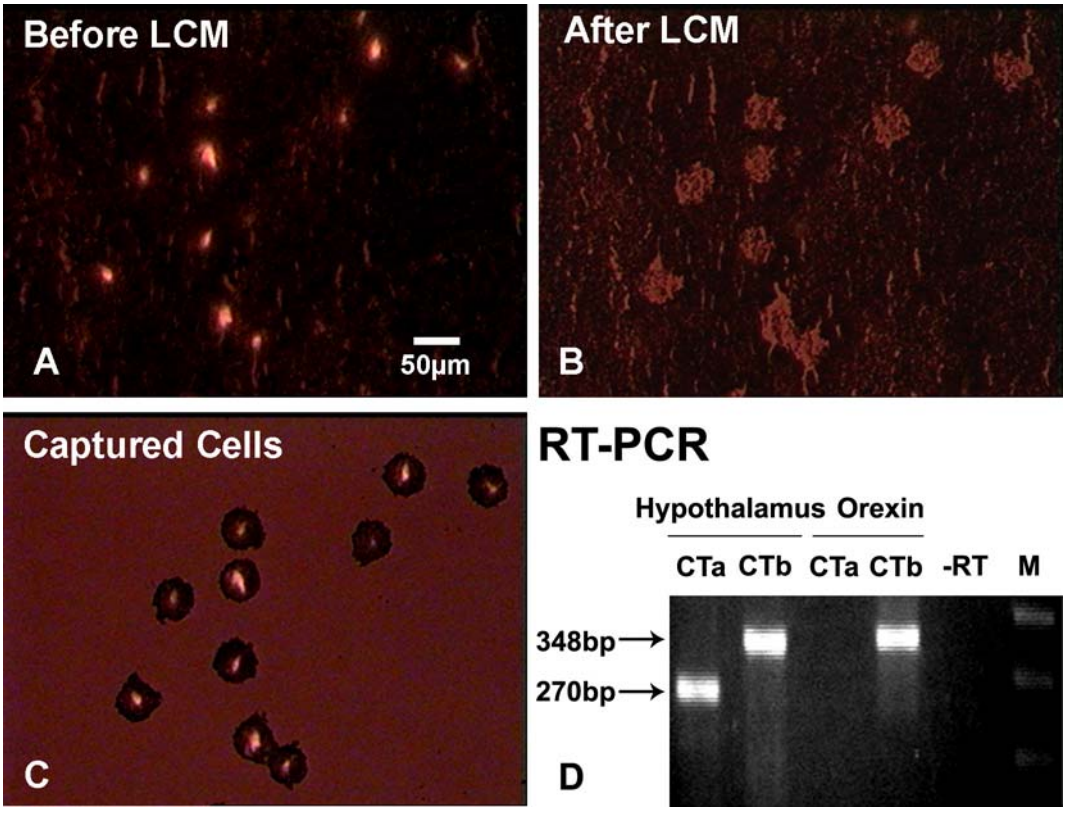

Fig. 14 Detection of $CT_{(b)}$ mRNA in microdissected orexin neurons

Immunofluorescent-labeled orexin neurons in a 10 µm thick section through rat hypothalamus, (A) before laser capture microdissection (LCM), (B) after LCM, (C) microdissected immunofluorescence-labeled orexin neurons, (D) Gel electrophoresis of PCR products for $CT_{(a)}$ and $CT_{(b)}$ amplified from RNA extracts of 32 microdissected orexin neurons and hypothalamus. In total hypothalamic extracts both the 270bp amplicon for $CT_{(a)}$ and 348bp amplicon for $CT_{(b)}$ are detected. In microdissected orexin neurons only the 348bp amplicon for $CT_{(b)}$ is detected. As negative control reverse transcriptase was omitted from the cDNA synthesis (-RT). M: DNA size marker.

3.6 Receptor-activity-modifying proteins (RAMPs) expression in orexin neurons

To investigate which of the RAMPs, that can form receptor complexes with CT receptors, are expressed in orexin neurons in situ hybridization analysis was performed. X-ray film analysis revealed strong hybridization signals for RAMP1 in the caudate putamen (CPu) (Fig. 15A), for RAMP2 in the hypothalamus (HT) (Fig. 15C), and for RAMP3 in the thalamus (Th) (Fig. 15E). The expression of RAMP isoforms in orexin neurons was investigated by dual in situ hybridization. Almost all orexin neurons were found to express RAMP2 mRNA (Fig. 15D) and RAMP3 mRNA (Fig. 15F). In contrast, Orexin neurons exhibited very low signals for RAMP1 (Fig. 15B).

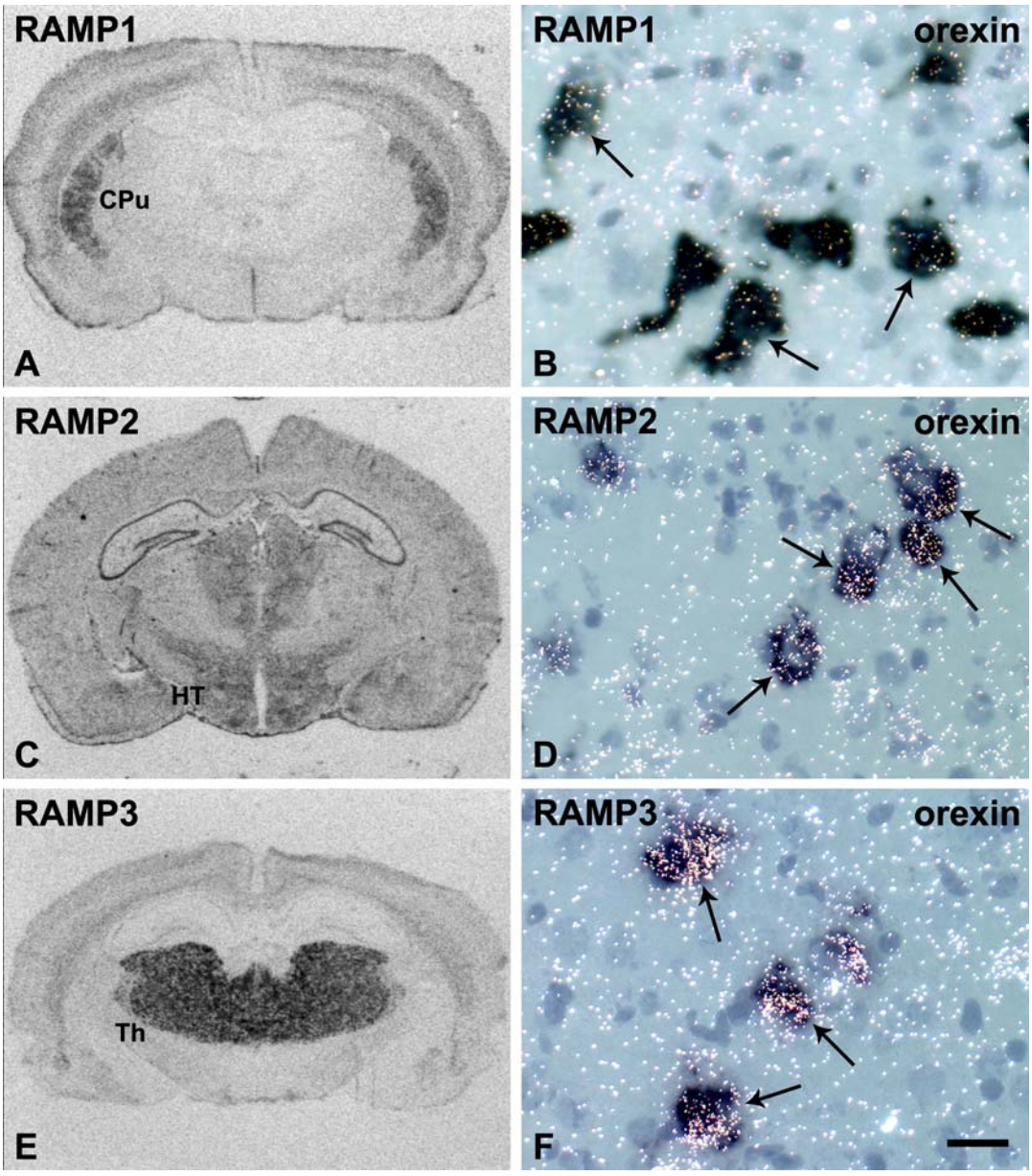

Fig. 15 Expession of RAMPs in orexin neurons

X-ray film autoradiograms of rat brain sections after ISH illustrating the region-specific distribution of RAMPs (A, C, E). Representative high resolution microscopic brightfield images of dual in situ hybridization showing the colocalization of RAMP2 mRNA (arrows in D) and RAMP3 (arrows in F) represented by white grains with orexin (violet precipitate). Very low signals for RAMP1 could be detected in orexin neurons (arrows in B). CPu, caudate putamen; HT, hypothalamus; Th, thalamus. Scale bar in F: 25µm.

3.7 Analysis of CGRP innervation on orexin neurons by immunohistochemistry

Since calcitonin and amylin, two potential ligands for CT receptor/RAMP complexes, are not expressed in brain, CGRP should be considered as the likely endogenous

ligand. Thus, the innervation of orexin neurons by CGRP fibers was examined using double-immunofluorescence staining of CGRP and orexin. Using confocal microscopy few CGRP fibers (Fig. 16 A, C green) could be detected on orexin cell bodies (Fig. 16 B, C red), suggesting the possibility that CGRP may act as endogneous ligand on orexin neurons.

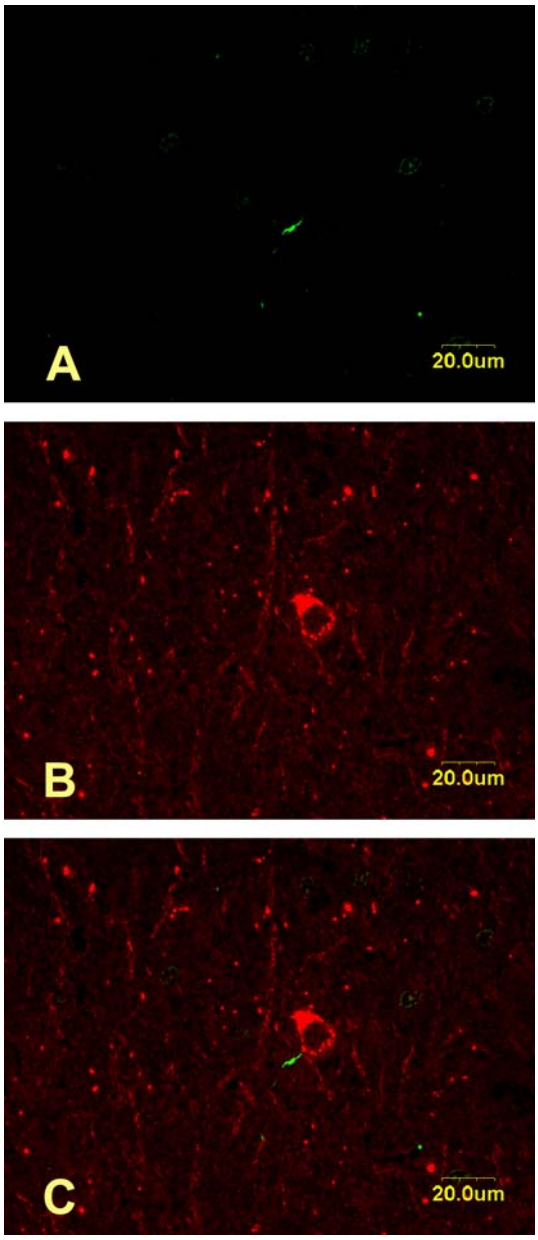

Fig. 16 Double-immunofluorescence staining of CGRP and orexin

Confocal double-immunofluorescence microscopy demonstrating a CGRP terminal (green in A and C) in close apposition to the cell body of an orexin neuron (red in B and C) in the lateral hypothalamic area.

Double immunohistochemistry of orexin and CGRP with Nickel-enhanced DAB staining was performed to examine the spatial relationship of CGRP innervation and

the orexin system in the lateral hypothalamus and the posterior paraventricular thalamic nucleus (PVP). In the lateral hypothalamus, CGRP positive terminals were detected contacting the cell bodies of orexin neurons (Fig. 17A). Furthermore, CGRP fibers with close spatial relationship to orexin fibers were observed in the posterior paraventricular thalamic nucleus (PVP) (Fig. 17B).

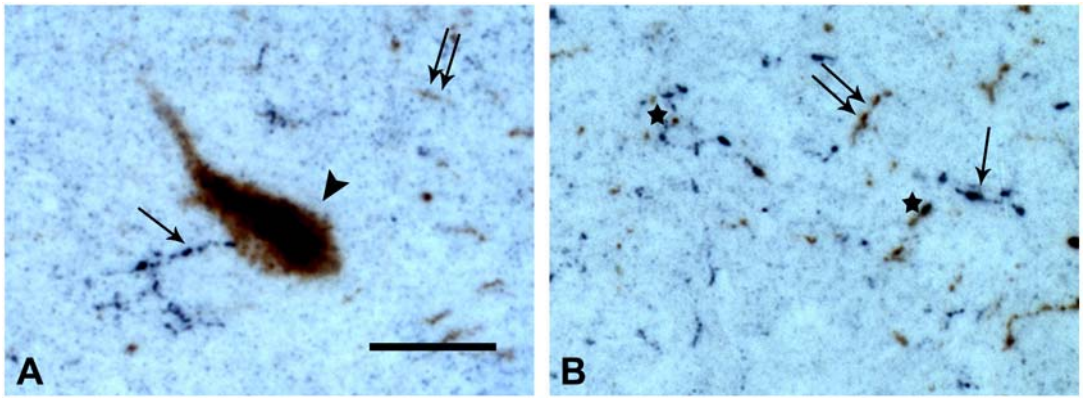

Fig. 17 Double immunohistochemistry of CGRP and orexin

High resolution brightfield images showing a dark blue CGRP fiber (arrow in A) contacting a brown orexin cell body (arrowhead in A) in the lateral hypothalamic area. In the posterior paraventricular thalamic nucleus (PVP), the dark blue CGRP fibers exhibit close spatial relationship with brown orexin fibers (stars in B). Scale bar in A: 20µm.

3.8 Characterization of the classical transmitter phenotype of orexin neurons

When the work of this thesis was started the classical transmitter used by orexin neurons had not yet been identified. Electrophysiological studies suggested that the activity of orexin neurons is autostimulated involving glutamate (Li et al. 2002). In order to clarify the classical transmitter phenotype of orexin neurons, double labeling in situ hybridization analysis was performed using VGLUT2 as a marker for the hypothalamic glutamatergic neurons and GABA synthetic enzyme glutamate decarboxylase (GAD) as the marker for GABAergic neurons. VGLUT2 and GAD67 mRNAs were found to be widely expressed through lateral hypothalamic area in agreement with previous studies (Rosin et al. 2003). Dual hybridization of frozen sections through the hypothalamus obtained from 3 animals revealed the expression of VGLUT2 mRNA in all orexin neurons (Fig. 18A, double arrows) strongly suggesting a glutamatergic phenotype of orexin neurons. Some VGLUT2 hybridization signals were also found in other neurons (Fig. 18A, single arrows). GAD67 mRNA was

detected in all of the MCH neurons indicating a GABAergic phenotype of MCH neurons (Fig. 18B, double arrows). Orexin neurons did not express GAD67 (data not shown). However, some GAD67 hybridization signals were also found in MCH-negative neurons (Fig. 18B, single arrows)

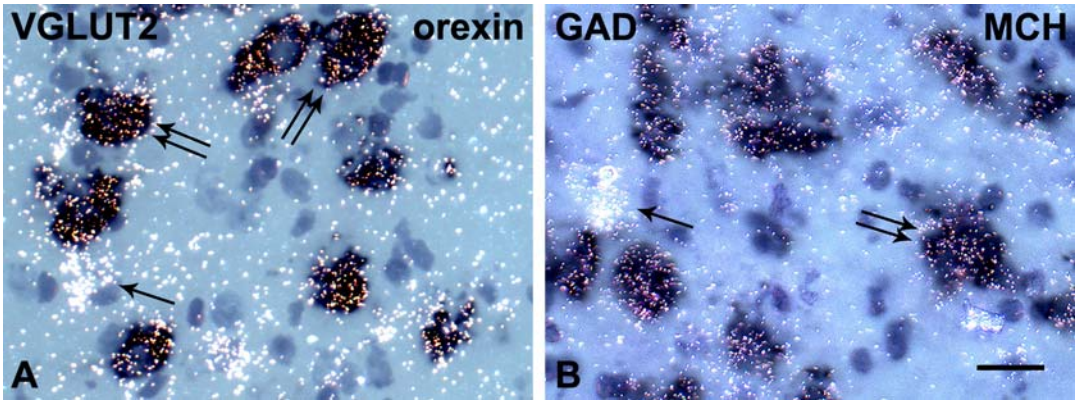

Fig. 18 Coexpression of VGLUT2 and orexin mRNA and GAD67 and MCH mRNA in hypothalamic neurons

Representative combined brightfield and darkfield images illustrating colocalization of VGLUT2 and orexin mRNA (A, double arrows) and colocalization of GAD67 and MCH mRNA (B, double arrows) in hypothalamic neurons (B, double arrows). Note strong VGLUT2 signals are present in a subpopulation of neurons which do not express orexin mRNA (A, single arrow) and strong GAD67 signals in a subpopulation of neurons which do not express MCH mRNA (B, single arrow). Orexin and MCH mRNA is detected with digoxigenin-labeled probes producing a dark violet precipitate, radioactive detection of VGLUT2 and GAD67 mRNA produces white grains under darkfield illumination. Scale bar: 25µm.

3.9 Cellular gene expression profiling of orexin neurons using LCM and microarray analysis to identify fasting-regulated genes

In order to investigate changes of the cellular transcriptome of orexin neurons after fasting and to identify novel fasting-regulated genes expressed in orexin neurons, a fasting model was used previously reported by some groups to stimulate orexin neurons (Sakurai et al. 1998).To determine the differential gene expression in fasting versus non-fasting rats, microdissected orexin neurons were subjected to microarray analysis. Immunofluorescent-labeled orexin neurons were captured from 3 rats fasted for 48h and from 3 control rats. The captured neurons were subjected to RNA isolation and RNA amplification. Two rounds of RNA amplification were necessary to obtain enough RNA from one animal for hybridizing one chip. After labeling with

biotin the cRNA probes were hybridized to the GeneChip® Rat Expression 230A Array (2.2.12) using the Affymetrix Fluidics Station in Max Planck Institute for Terrestrial Microbiology, Marburg. After target hybridization, the probe arrays were scanned. The data were analyzed and provided by Dr. B. Samans, an expert of microarray analysis in Dept. of Medical Biometry and Epidemiology, University Marburg.

Among about 5399 genes and 10467 ESTs represented on the Affymetrix RAE 230A microarray, the mRNAs of the orexin neuropeptide, calcitonin receptor, receptor-activity-modifying proteins and the vesicular glutamate transporter were detected in the RNA extracts of orexin neurons. The expression levels of these genes were unaffected after 48h fasting. The expression of these genes in orexin neurons of normal animals was also demonstrated by ISH in this thesis.

The microarray analysis of microdissected orexin neurons from rats subjected to fasting revealed 281 genes upregulated (1,32 to 2,61 fold) and 200 genes downregulated (1,32 to 2,66 fold), respectively. Enzymes, channels, receptors, neuropeptides and structural molecules were identified by comparing the microarray data with Genebank and Affymetrix gene data base.

A list of arbitrarily selected genes (table 12) that displayed upregulation (1,46 to 1,90 fold) and a list of arbitrarily selected genes (table 14) that displayed downregulation (1,45 to 1,95 fold) after fasting and that were known to be involved in the energy metabolism, signal transduction and neurotransmission have been compiled. A list of ESTs that displayed upregulation (2,61 to 1,40 fold) and a list of ESTs that displayed downregulation (2,27 to 1,40 fold) after fasting are shown in table 13 and table 15, respectively.

Table 12 Genes upregulated after 48h fasting in rat orexin neurons

Gene categories and gene titles	Affymetrix Nr.	Genebank Accession Nr.	Fold Change[1]	Biological process description[2]
Enzymes				
ATPase, Ca++ transporting, plasma membrane 1	1370050_at	NM_053311	1,80	cation transport, calcium ion transport, metabolism
aflatoxin B1 aldehyde reductase	1368121_at	NM_013215	1,46	aflatoxin metabolism
Ion channel				
chloride channel 2	1372807_at	BF402462	1,46	ion transport, chloride transport
Signal transduction				
Metallothionein	1371237_a_at	AF411318	1,78	metal ion homeostasis, zinc ion homeostasis, nitric oxide mediated signal transduction
cell adhesion molecule				
cadherin 22	1368887_at	NM_019161	1,84	cell adhesion, homophilic cell adhesion, brain development, calcium-dependent cell-cell adhesion
Neuropeptides				
arginine-glutamic acid dipeptide (RE) repeats	1371890_at	AI172033	1,90	protein-protein interaction
neuropeptide FF-amide peptide precursor	1368383_at	NM_022586	1,49	neuropeptide signaling pathway
Structural molecules				
vimentin	1367574_at	NM_031140	1,60	structural molecule activity, structural constituent of cytoskeleton, protein binding
preimplantation protein 3	1387089_at	NM_133528	1,57	protein binding
Receptors				
insulin-like growth factor 1 receptor	1368123_at	NM_052807	1,55	insulin-like growth factor receptor signaling pathway
thyrotropin releasing hormone receptor	1369751_at	M90308	1,50	thyrotropin-releasing hormone receptor activity
gamma-aminobutyric acid (GABA) B receptor, 1	1375720_at	AI171785	1,47	GABA-B receptor activity
Neurotransmission				
huntingtin-associated protein 1	1369358_a_at	AI412750	1,57	synaptic transmission, neurogenesis

[1] Fold change was determined by comparing the average gene expression levels of 3 fasted animals with that of 3 control animals.

[2] cited from affymetrix analysis data bank (https://www.affymetrix.com/analysis)

Table 13 ESTs upregulated after 48h fasting in rat orexin neurons

Affymetrix Nr.	Accession Nr.	Fold change*
1383141_a_at	AI236700	2,61
1372390_at	AI710604	2,15
1399063_at	BE105565	1,86
1375144_at	BM388843	1,83
1390284_at	BM383683	1,83
1371326_at	BI276957	1,79
1377506_at	BI289525	1,74
1374300_at	AA997139	1,70
1377522_a_at	BI294610	1,69
1373580_at	BI289991	1,69
1388519_at	BI281906	1,68
1377237_at	AI137274	1,67
1376240_at	BG378240	1,67
1373954_at	BG381520	1,67
1375912_a_at	BI285430	1,65
1372361_at	AW529931	1,61
1389137_at	AA957183	1,59
1371363_at	BI277042	1,58
1372875_at	AI408520	1,57
1376250_at	BI284814	1,56
1376922_at	AW523772	1,55
1375878_at	BE102596	1,54
1372727_at	BM384088	1,52
1371871_at	AI409731	1,50
1372265_at	AI172218	1,50
1374459_at	AI178448	1,49
1372304_at	BG378042	1,47
1373842_at	BM390718	1,40

* Fold change was determined by comparing the average gene expression levels of 3 fasted animals with that of 3 control animals.

Table 14 Genes downregulated after 48h fasting in rat orexin neurons

Gene categories and gene titles	Affymetrix Nr.	Genebank Accession Nr.	Fold Change[1]	Biological process description[2]
Enzymes				
ATP synthase, H+ transporting, mitochondrial F1 complex, epsilon subunit	1370284_at	AF010323	1,48	ATP biosynthesis, ATP synthesis coupled proton transport
Structural molecules				
collagen, type III, alpha 1	1370959_at	BI275716	1,95	skeletal development, phosphate transport, cell adhesion
nexilin	1370697_a_at	AF056034	1,60	actin filament binding
glial fibrillary acidic protein	1368353_at	NM_017009	1,56	intermediate filament-based process
Ion channel				
transient receptor potential cation channel, subfamily C, member 2	1389671_at	AW252088	1,45	cation transport, calcium ion transport, positive regulation of cytosolic calcium ion concentration
Signal transduction				
ras-like protein	1386967_at	NM_053522	1,72	small GTPase mediated signal transduction, regulation of cell shape, actin cytoskeleton organization and biogenesis
transforming growth factor beta 1 induced transcript 1	1370887_at	BI279862	1,46	response to heat

[1] Fold change was determined by comparing the average gene expression levels of 3 fasted animals with that of 3 control animals.

[2] cited from affymetrix analysis data bank (https://www.affymetrix.com/analysis)

Table 15 ESTs downregulated after 48h fasting in rat orexin neurons

Affymetrix Nr.	Accession Nr.	Fold change*
1372013_at	BG380285	2,27
1367547_at	BM388010	1,68
1372789_at	BF397881	1,59
1389560_at	BF284702	1,57
1372949_at	BG663067	1,56
1372542_at	BE113281	1,51
1388626_at	AI638949	1,50
1388611_at	AW252817	1,49
1388814_at	AI408110	1,47
1371710_at	BM391283	1,46
1374298_at	BG373455	1,45
1373754_at	AI599232	1,45

1393436_at	AI549033	1,44
1373748_at	AW532566	1,44
1376634_a_at	BE109067	1,41
1388844_at	AI102904	1,41
1375026_at	AI105369	1,40

* Fold change was determined by comparing the average gene expression levels of 3 fasted animals with that of 3 control animals.

3.10 Validation of TRH receptor expression in orexin neurons by semi-quantitative ISH

3.10.1 Characterization of TRH receptor subtypes in orexin neurons

Since TRH receptors had not been described in orexin neurons previously and since TRH was a well known anorexigenic neuropeptide, the rat TRH receptor 1 gene, upregulated 1.5 fold in the microarray after fasting, was chosen as a candidate fasting-regulated gene for further investigation. First, dual in situ hybridization was performed to demonstrate the expression of TRH receptor 1 or TRH receptor 2 in rat orexin neurons. As shown in Fig. 19, all orexin neurons were found to express TRHR1 mRNA (Fig. 19A, double arrows). However, no hybridization signals for TRHR2 could be detected in orexin neurons (Fig. 19B). These results were in agreement with the microarray data that revealed the expression of TRHR1 in orexin neurons. Moreover, no co-hybridization signals for TRHR1 and TRHR2 with MCH mRNA were observed (Fig. 19C, D) indicating that MCH neurons lack TRH receptor expression.

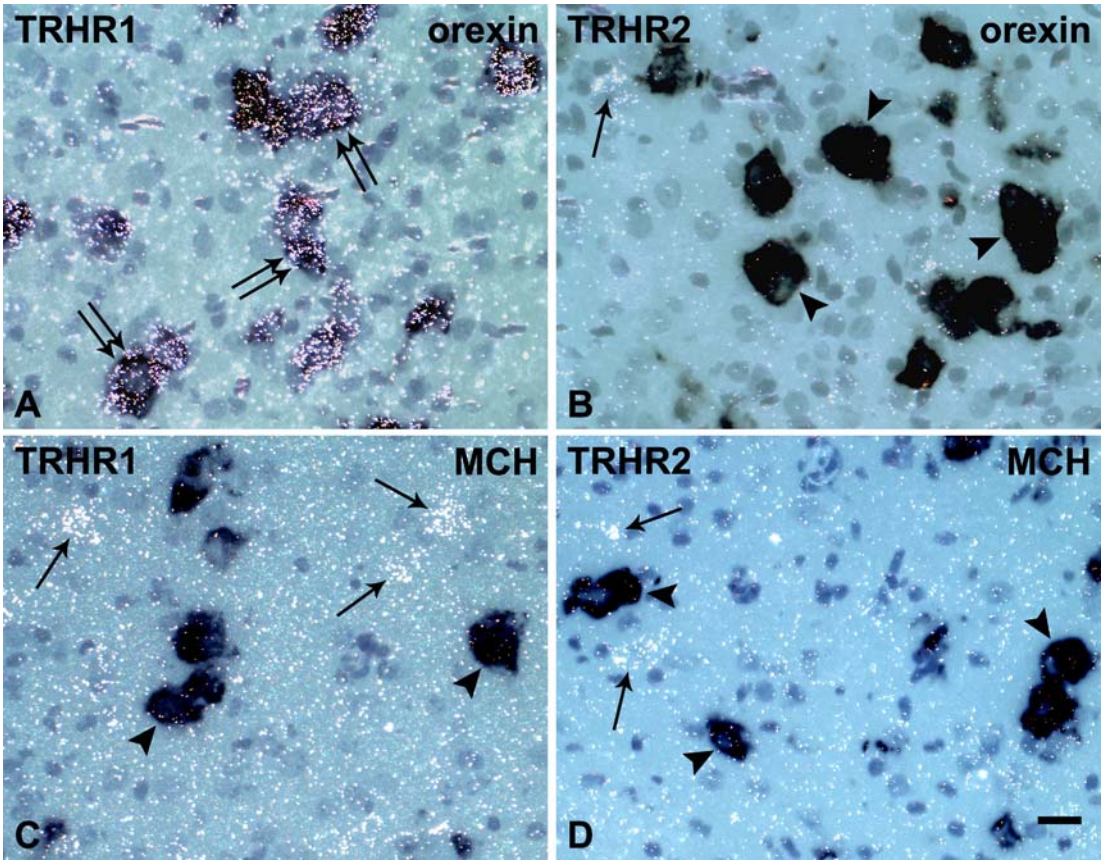

Fig. 19 Expression of TRHR1 in orexin neurons

Representative combined brightfield and darkfield images illustrating the expression of TRH-R1 in orexin neurons of control animals. All of the orexin neurons are co-labeled by the TRH-R1 and the orexin probe (A, double arrows). Orexin neurons (B, arrowheads) are negative for TRH-R2 signals (B, single arrow). MCH neurons (arrowheads in C, D) are negative for TRH-R1 signals as well as for TRH-R2 signals. Note that some MCH-negative neurons express TRHR1 or TRHR2 (single arrows in C, D). Orexin and MCH mRNA are detected with digoxigenin-labeled probes producing a dark violet precipitate. Radioactive detection of TRH-R1 and TRH-R2 mRNA produces white grains under darkfield illumination. Scale bar in D: 25µm.

3.10.2 Semi-quantitative ISH analysis of fasting-induced changes of TRHR1 mRNA in orexin neurons

In the microarray analysis the expression of TRHR1 mRNA in orexin neurons was upregulated about 1.5 fold after 48h of fasting. To confirm this result semi-quantitative image analysis of emulsion-coated autoradiograms was performed using the grain counting method (2.2.11). After an exposure time of 16 days, 27 sections from each group were subjected to grain counting. As shown in Fig. 20, the size of most orexin neurons ranged from 150µm^2 to 500µm^2. There were no significant

changes of the scan area per orexin neuron between the two groups (*p* values = 0.4) (Fig. 21A). The estimated grain counts representing TRHR1 mRNA levels per orexin neuron were increased after fasting. Of the control group 468 orexin neurons were examined for their TRHR1 expression levels. The average orexin neuron of the control group was labeled with 106 ± 2 grains. In the 48h fasted group grain counts increased to 123 ± 3 grains per orexin neuron (n= 322) (*p* values < 0.0001) (Fig. 21B). Comparing the grain density between the two groups, grain counts increased from 34 ± 1 grains per 100µm^2 scan area in the control group to 42 ± 1 grains per 100µm^2 scan area in the fasting group (*p* values < 0.0001) (Fig. 21C).

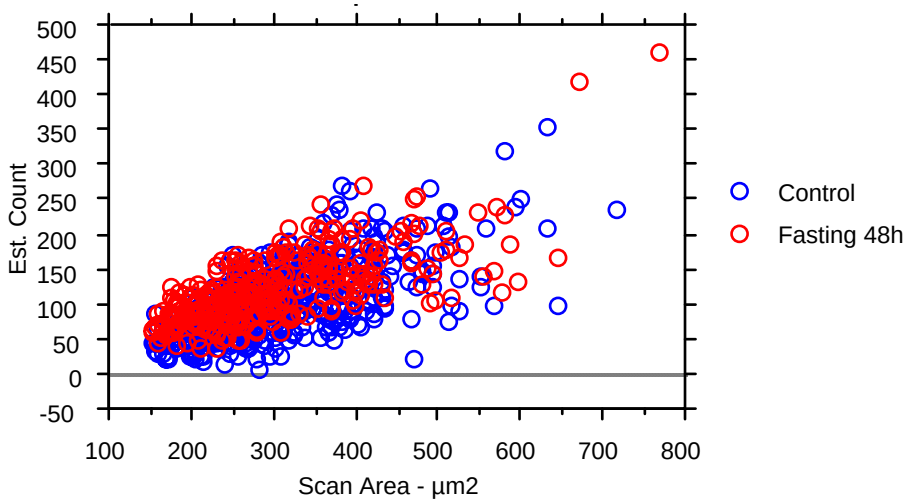

Fig. 20 Diagram of grain counts for the TRHR1 mRNA levels in orexin neurons represented by scan area

The levels of TRHR1 mRNA are represented by estimated grain counts. The orexin neurons are shown as scan area. The size of orexin neurons ranged from 150 µm^2 to 500 µm^2. Grain counts per orexin neuron are increased after fasting. Blue circles represent the cells of control animals, red circles represent the cells of fasting animals.

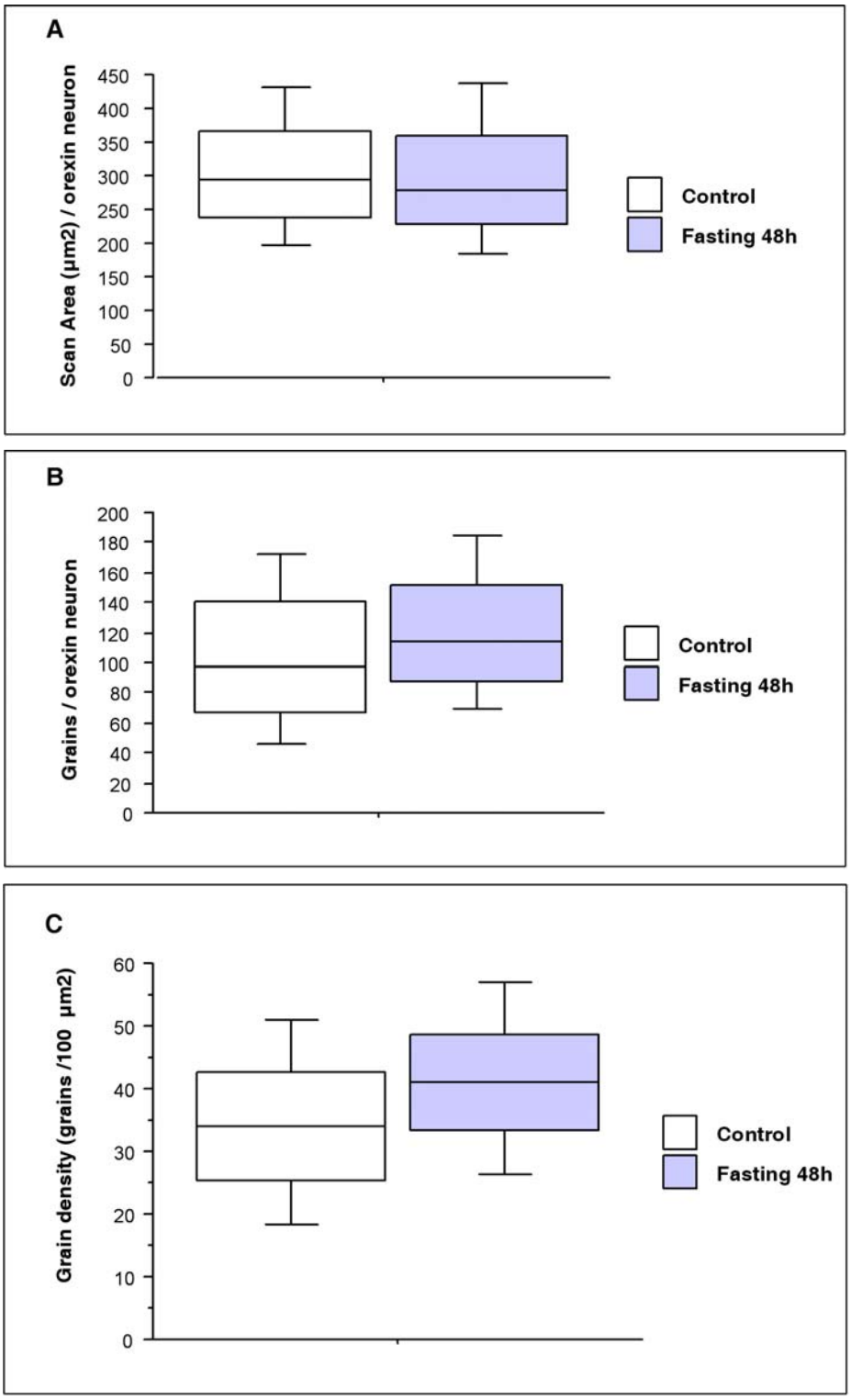

Fig. 21 Grain-counting analysis of cellular TRHR1 mRNA levels in orexin neurons

Box plot diagrams illustrating the changes of TRHR1 mRNA expression in orexin neurons after 48h fasting. Grain counting is performed on orexin neurons in 27 sections of each group. There is no significant difference of the scan area between the two groups (p values = 0.4) (A). The average number of silver grains per orexin neuron is increased 1.16 fold from 106 ± 2 grains (control group) to 123 ± 3

grains (fasting group) (p values < 0.0001) (B). The grain density is increased 1.24 fold from 34 ± 1 grains per 100μm^2 scan area in the control group to 42 ± 1 grains per 100μm^2 scan area in the fasting group (p values < 0.0001) (C).

4 Discussion

In the present study the distribution of calcitonin receptor isoforms throughout the rat brain has been investigated and their relationship to neuropeptidergic circuits in the hypothalamus and brainstem that regulate food intake and energy balance and other autonomic functions has been characterized. Furthermore, a pilot attempt was undertaken using microarray analysis to discover novel candidate genes for the regulation of food intake in orexin neurons.

The main new findings of this thesis are the following:

1) The two calcitonin receptor isoforms $CT_{(a)}$ and $CT_{(b)}$ were shown to exhibit distinct regional and cellular expression patterns throughout the rat brain that have not been reported previously. The findings provide a new basis for the understanding of CT receptor mediated signalling in major functional circuits of the brain.
2) Peptidergic hypothalamic neurons involved in the regulation of food intake as a rule express either $CT_{(a)}$ or $CT_{(b)}$ isoforms. Only occasionally, $CT_{(a)}$ and $CT_{(b)}$ are found to be coexpressed in the same neurons.
3) Orexin neurons selectively express the $CT_{(b)}$, but not the $CT_{(a)}$ isoform. The constitutive co-expression of RAMP2, RAMP3 and $CT_{(b)}$ in orexin neurons suggests that $AMY_{2(b)}$ and $AMY_{3(b)}$ receptors for amylin and/or CGRP can be expressed by orexin neurons.
4) Orexin cell bodies were found to be targeted by CGRP fibers suggesting that CGRP can act as an endogenous brain-derived ligand to directly modulate the function of orexin neurons.
5) Orexin neurons were shown to express the vesicular glutamate transporter isoform 2 (VGLUT2), but not GAD67, a marker of GABA-ergic neurons, indicating that orexin neurons are glutamatergic and use VGLUT2 to operate glutamatergic neurotransmission. This is consistent with the neuroexcitatory function of orexin neurons.
6) Microarray analysis of microdissected orexin neurons from rats subjected to fasting revealed 281 genes upregulated (1,32 to 2,61 fold) and 200 genes downregulated (1,32 to 2,66 fold), respectively. These regulated genes are regarded as novel candidate genes for the regulation of food intake or other

functions in orexin neurons. Among the upregulated genes was TRHR1. The fasting-induced upregulation of TRHR1 in orexin neurons revealed by microarray analysis was successfully validated by quantitative ISH and suggests a specific role of TRH in orexin neurons to regulate feeding behaviour.

4.1 Comparative distribution of $CT_{(a)}$ and $CT_{(b)}$ isoforms in rat brain

4.1.1 Regions of the rat brain expressing the $CT_{(a)}$ isoform but not the $CT_{(b)}$ isoform

In regions where no expression of $CT_{(b)}$ was detectable with the specific $CT_{(b)}$ probe, the expression and distribution of the $CT_{(a)}$ isoform could be indirectly identified by using the $CT_{(a/b)}$ probe. These regions which selectively express the $CT_{(a)}$ isoform as indirectly identified with the $CT_{(a/b)}$ probe in nuclei without $CT_{(b)}$ expression included the subfornical organ, the lateral substantia nigra, the paratrochlear nucleus, the median raphe nucleus, the ventral tegmental nucleus, the parvocellular reticular nucleus, the gigantocellular reticular nucleus, the lateral paragigantocellular nucleus, and the ventral medullary reticular nucleus. In regions lacking $CT_{(b)}$, this strategy to detect the $CT_{(a)}$ isoform with the bi-specific $CT_{(a/b)}$ probe is reliable and can be expected to be more sensitive than the usage of an isoform-specific $CT_{(a)}$ oligonucleotide probe.

4.1.2 Direct detection of the $CT_{(a)}$ isoform in the hypothalamus by the newly designed $CT_{(a)}$ specific oligonucleotide probe

Since intense hybridization signals for both $CT_{(b)}$ and $CT_{(a/b)}$ probes were detected in the hypothalamus, it is obvious that the $CT_{(b)}$ isoform was expressed in this region. Since $CT_{(a)}$ specific riboprobes cannot be generated because of extensive sequence homology between $CT_{(a)}$ and $CT_{(b)}$, a $CT_{(a)}$-specific oligonucleotide probe had to be used which allowed to determine the expression of $CT_{(a)}$ directly albeit with suboptimal sensitivity. The $CT_{(a)}$ oligonucleotide probe that was newly designed in this study, only recognized the $CT_{(a)}$ isoform. In contrast, the oligonucleotide probes used by others (Barth et al. 2004) did not differentiate between $CT_{(a)}$ and $CT_{(b)}$ mRNA isoforms and, therefore, have to be judged to be unreliable to detect the $CT_{(a)}$ mRNA specifically.

Using this $CT_{(a)}$ oligonucleotide probe, $CT_{(a)}$ was found to be expressed in several hypothalamic nuclei including the dorsomedial hypothalamic nucleus (DMH), the ventromedial hypothalamic nucleus (VMH), the arcuate nucleus (ARC) and the lateral hypothalamic area (LHA) which are known as centers regulating energy homeostasis. These data are the first to unequivocally reveal and localize the $CT_{(a)}$ mRNA in these specific nuclei of the brain.

4.1.3 Distribution of the $CT_{(b)}$ isoform throughout the rat brain

For the first time, a full distribution map of $CT_{(b)}$ mRNA throughout the rat brain employing a highly sensitive ISH method with a specific $CT_{(b)}$ riboprobe was established in this thesis. Intense expression of the $CT_{(b)}$ isoform was observed in the accumbens nucleus, the lateral septal nucleus, various subdivisions of the amygdala, the anterior medial preoptic nucleus, many hypothalamic nuclei, the pericentral dorsal tegmental nucleus, the locus coeruleus, the raphe magnus nucleus, the area postrema, and the nucleus of the solitary tract.

Previous studies focused on the expression of $CT_{(b)}$ in circumventricular organs of the rat brain (Barth et al. 2004). These authors used oligonucleotide probes which are less sensitive as compared to riboprobes. They may have underestimated the abundance of $CT_{(b)}$ in the investigated areas. In the mouse brain, the expression of CT receptors was investigated previously by in situ hybridization using a $CT_{(a/b)}$ riboprobe hybridizing to both the $CT_{(a)}$ and $CT_{(b)}$ mRNAs (Nakamoto et al. 2000). These studies generated the view of an overlapping distribution of $CT_{(a)}$ and $CT_{(b)}$. No brain region or neuronal population was described to express exclusively $CT_{(b)}$ mRNA.

4.1.4 Expression of $CT_{(a)}$ and $CT_{(b)}$ isoforms in the area postrema (AP) and the nucleus of the solitary tract (NTS)

Based on in situ hybridization analysis and RT-PCR analysis of microdissected specimens of the brainstem, this study has shown for the first time the expression of both $CT_{(a)}$ and $CT_{(b)}$ in the AP and NTS and provided strong evidence against the previous reports that only $CT_{(a)}$ is expressed in AP and NTS (Hilton et al. 1995; Barth et al. 2004).

The obvious discrepancy to the previous data can be explained by the following considerations. In a previous *in vitro* receptor autoradiography study (Hilton et al. 1995), the distribution of $CT_{(a)}$ binding sites in the AP and NTS of the rat brain

was revealed by [^{125}I]human calcitonin and that of $CT_{(b)}$ binding sites in these regions was shown using [^{125}I]salmon calcitonin in the presence of unlabeled human calcitonin and rat amylin under the assumption that human calcitonin could only interact with the $CT_{(a)}$ isoform and that amylin cannot bind to calcitonin receptors, respectively. However, multiple amylin receptors are known to arise from specific associations of calcitonin receptors with the different RAMPs (Christopoulos et al. 1999; Tilakaratne et al. 2000). This implies that amylin also could bind to calcitonin receptors. Therefore, the reported absence of $CT_{(b)}$ binding sites in AP and NTS could be due to the binding of unlabeled amylin to this receptor.

That expression of $CT_{(b)}$ mRNA in the AP and NTS was undectable by ISH (Barth et al. 2004) may be due to insufficient sensitivity of oligonucleotide probes used. In fact, cRNA probes employed with ISH in the present thesis revealed that both CT receptor isoforms $CT_{(a)}$ and $CT_{(b)}$ were expressed in the AP and NTS. This was corroborated by RT-PCR analysis of microdissected neurons of the AP and NTS which demonstrated presence of both CT receptor transcripts in these regions. Therefore, the view of an exclusive expression of $CT_{(a)}$ in the AP and NTS should be dismissed.

4.2 Functional implications of calcitonin receptor isoforms in specific brain structures related to the regulation of food intake

The widespread expression of CT receptors in the rat brain as demonstrated in this thesis suggests their involvement in a variety of different brain functions. Many of the regions with expression of $CT_{(a)}$ or $CT_{(b)}$ or of both isoforms, such as the accumbens nucleus, various subdivisions of the amygdala, the brain stem, and many nuclei of the hypothalamus, have been reported to be involved in the regulation of food intake besides playing a role in the regulation of many other autonomic and limbic functions, respectively.

4.2.1 Expression of calcitonin receptor in the accumbens nucleus

Using ISH, this study has demonstrated the expression of $CT_{(b)}$ in the accumbens nucleus, especially in its shell region. This is consistent with previous RT-PCR results which revealed $CT_{(b)}$ transcripts in RNA extracts of the accumbens nucleus (Sexton et

al. 1993). In this thesis, the distribution pattern of $CT_{(b)}$ in the accumbens nucleus was demonstrated for the first time at the cellular level. Whether $CT_{(a)}$ is also expressed in the accumbens nucleus needs to be shown using $CT_{(a)}$-specific oligonucleotide probes.

Previous studies have implicated the accumbens nucleus as an important region specifically involved in the mediation of feeding behavior. Inhibition of neurons in this region by administration of excitatory amino acid antagonists (Maldonado-Irizarry et al. 1995) or GABA agonists (Stratford and Kelley 1997) elicited intense feeding in satiated rats. Receptor autoradiographic binding studies revealed the existence of high affinity binding sites for amylin and CGRP in this region (Veale et al. 1994). Infusion of amylin into the rat accumbens nucleus potently depressed motor activity and ingestive behavior (Baldo and Kelley 2001). The expression of CT receptors in this region suggests that neurons of the accumbens nucleus can be directly activated by members of the calcitonin peptide family and that CT receptors may be involved in the regulation of addictive behaviour.

4.2.2 Expression of calcitonin receptor in the amygdala

In various subdivisions of the amygdala, intense expression of $CT_{(b)}$ mRNA was observed for the first time. Whether $CT_{(a)}$ is expressed in this region remains to be shown using the $CT_{(a)}$-specific oligonucleotide probe.

The amygdala had received early attention in the field of research on food intake control because of changes in ingestive behavior following various amygdala lesions (Rolls and Rolls 1973; Schoenfeld and Hamilton 1981). Amylin binding sites have been detected in the amygdala (Christopoulos et al. 1995). It appears likely that circulating amylin modulates feeding behavior via a direct effect on brain areas such as the amygdala by acting on $CT_{(b)}$ receptor.

As the amygdala also serves other functions such as fear, aggression and regulation of cardiovascular functions (Baklavadzhyan et al. 2000; Halasz et al. 2002; Gale et al. 2004), it is reasonable to postulate that $CT_{(b)}$ mediated signaling may be important in this context, too. Under conditions with break down of the blood brain barrier as seen in encephalitic conditions (Turkulov et al. 1998), blood borne CT receptor ligands may come into playing a role besides intrinsic innervation of the amygdala by CGRP fibers (Schwaber et al. 1988).

4.2.3 Expression of calcitonin receptors in specific regions of the brain stem

Both $CT_{(a)}$ and $CT_{(b)}$ were found to be expressed in the area postrema (AP) and the nucleus of the solitary tract (NTS). This suggests that neurons of the AP/NTS can be modulated by members of the calcitonin peptide family directly. Since the AP and probably the NTS lack an effective blood-brain barrier (Luckman and Lawrence 2003), the neurons of the AP and NTS expressing the relevant receptors are accessible for primary modulation by circulating endogenous ligands such as the pancreas-derived amylin. As a partner hormone to insulin, amylin controls nutrient intake by an inhibition of food intake (Lutz et al. 1994) and gastric emptying (Reidelberger et al. 2001) mediated by the AP and NTS (Lutz et al. 1998; Riediger et al. 2004). Thermal ablation of the AP and NTS resulted in a significant reduction of the anorectic effects of amylin after i.p. injection in rats (Lutz et al. 1998). Chronic amylin infusion in AP resulted in the inhibition of food intake in rats. This inhibition was blocked by the amylin antagonist AC 187 (Mollet et al. 2004). High-affinity binding sites for [^{125}I]rat amylin have been identified in the AP and NTS (Sexton et al. 1994). Moreover, RAMP2 and RAMP3 mRNA were observed within AP and NTS regions (Barth et al. 2004). The association of human $CT_{(a)}$/$CT_{(b)}$ with RAMP2/RAMP3 seems to be essential for amylin binding in vitro (Tilakaratne et al. 2000). However, the co-localization of these components in the AP and NTS regions in the very same neurons and their functional interaction still need to be shown.

TRH mRNA-expressing neurons are localized in the area postrema and the dorsal motor nucleus of the vagus (Heuer et al. 2000). These TRH-positive neurons most likely project to the NTS whose intermediate and ventrolateral subdivisions contain many TRHR1 mRNA-positive cells (Heuer et al. 2000). TRH binding sites have also been reported in the NTS (Manaker and Rizio 1989). However, the physiological importance of the expression of TRH and TRH receptor in the dorsal vagal complex [area postrema, the dorsal motor nucleus of the vagus (NDV) and the nucleus of the solitary tract (NTS)] is not fully understood. Microinjection of TRH into the dorsal vagal complex induces dose-dependent increases in gastric acid output (Okuma et al. 1987). The results of this thesis showing that CT receptors are not expressed in TRH neurons in the AP suggest that the TRH neurons in the AP are unlikely to directly respond to the neuropeptides of the calcitonin family.

CT receptors are expressed in other brain stem regions such as the locus coeruleus (LC). Neurons in the LC have been reported to be involved in many physiological and pathophysiological processes, such as arousal, sleep, autonomic control, and hypertension (Singewald and Philippu 1998). Peptides of the calcitonin superfamily induce multiple biological effects including potent vasodilatation (Poyner et al. 2002), sleep (Slisli and de Beaurepaire 1999), and respiratory regulation (Nishi et al. 2000). Taken together, CT receptors are likely to be not only involved in the regulation of food intake, but also in many other functions.

4.3 Selective expression of CT receptor isoforms in peptidergic neurons of the rat hypothalamus

This study has demonstrated for the first time that peptidergic hypothalamic neurons involved in the regulation of food intake as a rule express either $CT_{(a)}$ or $CT_{(b)}$ isoforms. Only occasionally, $CT_{(a)}$ and $CT_{(b)}$ are found to be coexpressed in the same neurons.

4.3.1 Expression of the $CT_{(a)}$ isoform in POMC, CART and CRH neurons of the hypothalamus

The $CT_{(a)}$ isoform was found to be predominantly expressed in POMC, CART and CRH neurons of the hypothalamus. POMC, CART and CRH are anorexigenic neuropeptides. POMC, expressed in the lateral subpopulation of ARC neurons, tonically inhibits food intake via α-melanocyte stimulating hormone (α-MSH), a post-translational cleavage product of POMC, which functions as melanocortin receptor agonist (McMinn et al. 2000). Mutation or polymorphism of the MC-4R gene leads to extreme obesity in humans (Hinney et al. 2003). The expression of $CT_{(a)}$ in these anorexigenic neurons suggests that the $CT_{(a)}$ isoform may be involved in the modulation of the anorexigenic function of these peptidergic neurons. The anorexigenic peptides of the calcitonin family may directly act on the POMC/CART and CRH neurons via $CT_{(a)}$ to modulate the activation of these neurons related to the regulation of food intake.

4.3.2 Expression of $CT_{(b)}$ isoform in NPY and orexin neurons of the hypothalamus

The $CT_{(b)}$ isoform was found to be predominantly expressed in NPY and orexin neurons in this thesis. NPY is regarded as the most potent orexigenic peptide (Stanley et al. 1986; Billington et al. 1991) and the expression of NPY is modulated by leptin (Schwartz et al. 1998). Previous studies showed that amylin potently inhibits NPY-induced feeding (Morris and Nguyen 2001). Orexins are the anabolic signaling molecules (Sakurai et al. 1998). The predominant expression of $CT_{(b)}$ in these orexigenic neurons suggests that the $CT_{(b)}$ isoform may be involved in the modulation of the orexigenic function of these peptidergic neurons. The anorexigenic peptides of the calcitonin family may directly act on NPY and orexin neurons via $CT_{(b)}$ to modulate the activation of these neurons related to the regulation of food intake.

4.3.3 Expression of $CT_{(b)}$ isoform in TRH neurons of the paraventricular nucleus of the hypothalamus

This study has demonstrated the expression of $CT_{(b)}$ in a subpopulation of TRH neurons in the PVN. TRH neurons are heterogeneous and elicit a variety of neuropharmacological effects. They are widely distributed throughout the brain (Heuer et al. 2000). In the hypothalamus, TRH neurons are located in the PVN, basal part of the anterior and lateral hypothalamus, perifornical area and dorsomedial nucleus of the hypothalamus (Kawano et al. 1991). TRH has been implicated in the control of food intake (Suzuki et al. 1982; Steward et al. 2003). Central administration of TRH reduces food intake (Steward et al. 2003). Fasting decreases the expression of proTRH mRNA in the PVN (Blake et al. 1991). The expression of $CT_{(b)}$ in TRH neurons of PVN suggests that the $CT_{(b)}$ isoform may be involved in the modulation of the anorexigenic function of the TRH neurons in the PVN.

However, TRH neurons in different regions of the hypothalamus may have different functions. For example, TRH has been reported to be involved in the pathophysiology of narcolepsy. Two stabilized TRH analogs (CG3703 and TA0910) significantly increase wakefulness and decrease sleep in narcoleptic canines (Nishino et al. 1997). The peptides of the calcitonin family have also been found to affect the sleep cycles (Slisli and de Beaurepaire 1999). It is unclear whether the TRH neurons in other than the PVN area express the CT receptors and modulate mutiple functions

of the peptides of the calcitonin family. These questions remain to be further investigated.

4.3.4 Differences of ligand-binding kinetics and receptor specificity of $CT_{(a)}$ and $CT_{(b)}$ isoforms

The $CT_{(a)}$ and $CT_{(b)}$ isoforms have different ligand-binding kinetics and receptor specificity. In previous competition binding studies, while both receptor isoforms bind to salmon calcitonin with high affinity, only the $CT_{(a)}$ receptor interacts with human calcitonin (Hilton et al. 1995). Calcitonin receptors in man and rodents have the highest affinity and efficacy for calcitonin peptides (Poyner et al. 2002). In association with RAMPs, calcitonin receptors can function as amylin or as CGRP receptors (Christopoulos et al. 1999; Muff et al. 1999). *In vitro* all three RAMPs will interact with $CT_{(a)}$ and $CT_{(b)}$ receptors to generate amylin receptors, while the $CT_{(b)}$/RAMP2 displays greater affinity to amylin than that of $CT_{(a)}$/RAMP2 depending on the host cell environment (Tilakaratne et al. 2000). Amylin receptors with varying affinity for CGRP have been observed in competition binding studies in rat brain (van Rossum et al. 1994). These may arise from interaction of CT receptors with different RAMPs. In order to clarify the ligands of the CT receptor isoforms in the peptidergic neurons of the hypothalamus, the coexpression patterns of the RAMPs with CT receptor isoforms in orexin neurons have been investigated.

4.4 Functional implications of $CT_{(b)}$ isoform expression in orexin neurons

4.4.1 Expression of $AMY_{2(b)}$ and $AMY_{3(b)}$ receptors in orexin neurons

For the first time, this study has shown that the $CT_{(b)}$ isoform, but not the $CT_{(a)}$ isoform, and RAMP2 and RAMP3 are expressed in virtually all orexin neurons in the LHA. The coexpression of $CT_{(b)}$ with RAMP2 and RAMP3 in orexin neurons as demonstrated in this thesis suggests that the amylin receptor subtypes $AMY_{2(b)}$ and $AMY_{3(b)}$ are expressed in orexin neurons.

Orexin neuropeptides are anabolic signaling molecules. Intracerebroventricular (icv) administration of orexin A consistently stimulates food intake, but that of orexin B has such effects only on occasions. Both orexin A and orexin B peptides stimulate food intake significantly less than NPY but to a similar extent as MCH (Edwards et al.

1999). The expression of $AMY_{2(b)}$ and $AMY_{3(b)}$ receptors in the orexin neurons suggests that peptides of the anorexigenic calcitonin family may directly act on orexin neurons to modulate the function of orexin neurons related to food intake.

4.4.2 Amylin is a possible ligand for $AMY_{2(b)}$ or $AMY_{3(b)}$ receptors in orexin neurons

Previous studies reported that the expression of orexin, but not that of MCH, is downregulated by intraperitoneal injection of amylin (Barth et al. 2003). Neurons in the LHA were inhibited in response to food intake and intraperitoneal administration of amylin (Riediger et al. 2004). The present study has demonstrated that important molecular components necessary for the amylin binding are expressed in orexin neurons, which makes them one of the primary CNS targets for circulating amylin. Previous studies reported that amylin acts as a physiological peripheral satiety agent to regulate short-term food intake (Morley et al. 1995; Arnelo et al. 1996; Reidelberger et al. 2004). Furthermore, amylin delivers adiposity signals to the brain to regulate long-term energy homeostasis (Rushing 2003).

However, amylin is not expressed in brain resident neurons and it is still unclear how amylin from the periphery may gain access to orexin neurons. One possibility is that amylin enters the brain by crossing the blood brain barrier by yet unknown transport mechanisms. Another possibility is that amylin enters the brain through the ARC of the hypothalamus or by the AP of the brain stem where the blood brain barrier is open. These questions need to be further investigated.

4.4.3 Is CGRP the brain-derived ligand for $AMY_{2(b)}$ or $AMY_{3(b)}$ receptors in orexin neurons?

Since CGRP but not amylin is expressed in brain, CGRP has to be considered as a likely brain-derived ligand for amylin receptors. In fact, double immunohistochemistry performed in this thesis has revealed that CGRP positive terminals are present in the lateral hypothalamus contacting the cell bodies and processes of the orexin neurons strongly suggesting the possibility that CGRP acts as an endogenous ligand on orexin neurons. Whether CGRP can bind to $AMY_{2(b)}$ or $AMY_{3(b)}$ or to both receptors *in vivo* to directly activate orexin neurons remains to be further investigated.

CGRP shares considerable structural and functional homology with amylin. CGRP reduces food intake after central and peripheral administration (Krahn et al. 1984; Morley et al. 1996). Peripheral CGRP is less effective than centrally administered CGRP (Krahn et al. 1984). Lesions of the AP and NTS have been shown to reduce the anorectic effects of both amylin and CGRP peptides when injected intraperitoneally (ip) (Lutz et al. 1998). However, a lesion in the AP and NTS region did not influence the anorectic effects of amylin and CGRP after administration into the lateral ventricle (Lutz et al. 1998). Therefore, calcitonin receptors/RAMPs complex in the forebrain may mediate the anorectic effects of both peptides when administered centrally.

This study has also shown that CGRP fibers form close spatial relationships with orexin fibers in the posterior paraventricular thalamic nucleus (PVP). With afferents from brainstem and hypothalamic cell groups, including the lateral hypothalamic area and efferents to limbic centers, the PVP is in a position to integrate visceral and circadian information, and to modulate limbic functions. That the PVP is involved in food intake and weight gain in rats was reported (Bhatnagar and Dallman 1999). Previous studies have shown that dense populations of orexin-containing fibers are present in the PVP, but their role is largely unknown (Date et al. 1999). The close spatial relationship of CGRP and orexin fibers in this area as shown in this thesis for the first time may suggest that these two neuropeptides cooperate in the regulation of functions of the PVP.

4.4.4 Relationship between orexin neurons and other hypothalamic peptidergic neurons

MCH is a critical regulator of feeding which acts downstream of leptin and the melanocortin system (Shimada et al. 1998). Orexin and MCH perikarya have been found in close proximity to each other, and synaptic contacts have been observed between them (Bayer et al. 2002). OX1R is expressed in MCH neurons (Backberg et al. 2002). It is likely that these two neuronal populations communicate within the LHA in an interrelated fashion. The selective expression of $CT_{(b)}$ in orexin neurons, but not in MCH neurons, suggests that peptides of the calcitonin family probably can not directly activate MCH neurons. Whether peptides of the calcitonin family could modulate the function of the MCH neurons via orexin neurons remain to be shown. CART is colocalized with MCH in this area (Broberger 1999). The lack of CT

receptors in both CART and MCH neurons as demonstrated in this thesis are in concordance with these results.

Orexin neurons have reciprocal connections to the neurons of the arcuate and paraventricular nuclei. Orexin-containing fibers are present in the paraventricular nucleus (PVN) and the arcuate nucleus (Date et al. 1999). Orexins can directly interact with NPY and POMC neurons to regulate Ca^{2+} signaling (Muroya et al. 2004). Orexin A was found to enhance food intake when injected into the paraventricular nucleus (PVN) (Dube et al. 1999). Whether peptides of the calcitonin family could modulate the function of the NPY and POMC neurons in ARC and the CRH and TRH neurons in PVN via orexin neurons remains to be shown.

4.5 Identification of a specific glutamatergic phenotype of orexin neurons

Electrophysiological studies suggested that the secretion of orexin is autostimulated via enhancing the release of glutamate from neurons in synaptic contact with orexin neurons (Li et al. 2002). However, the possibility that orexin neurons themselves release glutamate could not be excluded. In fact, glutamate immunoreactivity has been reported in orexin neurons (Li et al. 2002). However the presence of glutamate in orexin neurons does not necessarily prove that immunodetected glutamate is related to vesicular release of glutamate or to glutamate metabolism.

Like other neurotransmitters glutamate is packaged into synaptic vesicles before its release from presynaptic terminals by a vesicular transport system (Storm-Mathisen et al. 1983) Three different vesicular glutamate transporter proteins (VGLUT1-3) which transport glutamate into the synaptic vesicles represent unique markers for glutamatergic neurons (Reimer and Edwards 2004). The predominant vesicular glutamate transporter in the hypothalamus is VGLUT2 (Bai et al. 2001; Gras et al. 2002; Schafer et al. 2002; Takamori et al. 2002; Varoqui et al. 2002).

In this thesis it could be demonstrated that VGLUT2 mRNA, but not GABA synthetic enzyme glutamate decarboxylase (GAD) mRNA is expressed in all orexin neurons strongly indicating that orexin neurons have a specific VGLUT2 coded glutamatergic phenotype. These results suggest that orexin neurons themselves have the capacity for vesicular accumulation and release of glutamate implying the possibility that the released glutamate may autostimulate orexin neurons.

The finding that orexin neurons are glutamatergic is consistent with their known neuroexcitatory properties. In addition to their role in the control of energy homeostasis (Sakurai et al. 1998), orexin neurons have been implicated in other physiological functions, such as arousal maintenance (Hagan et al. 1999), analgesia (Bingham et al. 2001), endocrine function (Al-Barazanji et al. 2001), autonomic regulation (Davis et al. 2003) and the regulation of synaptic transmission and plasticity (Selbach et al. 2004). The excitatory neurotransmitter glutamate is known to be involved in these functions. Intravenous orexin administration causes a marked and sustained increase in glutamate release within the amygdala, a limbic region related to the feeding (Schoenfeld and Hamilton 1981) and sleeping (John et al. 2003). The arousal effects of orexin-A correlate with glutamate release from the locus coeruleus (Kodama and Kimura 2002). Orexin regulates motor control processes and this regulation is mediated by glutamate release in the trigeminal motor nucleus (Peever et al. 2003). The effects of orexin A on magnocellular neurones of PVN are mediated by the activation of glutamate interneurons (Follwell and Ferguson 2002). The effects of orexin B in modulating autonomic sensory signaling in the NTS are mediated by the release of glutamate in the NTS (Smith et al. 2002). The glutamatergic transmission is also reported to associate with the modulation of synaptic plasticity of orexins in the hippocampus (Selbach et al. 2004).

4.6 Possible functional implications of transcriptomic changes in orexin neurons after fasting

The pilot microarray analysis of differential gene expression in microdissected orexin neurons performed in this thesis revealed about 281 upregulated and 200 downregulated genes in orexin neurons after fasting. Among these genes, many enzymes, channels, receptors, neuropeptides and structural molecules were identified to be regulated after fasting. This study is the first to specifically assess fasting-induced gene regulation in orexin neurons.

4.6.1 Validation of the expression and upregulation of TRHR1 in orexin neurons

In principle, all regulated genes after fasting can be regarded as novel candidate genes for the regulation of food intake by orexin neurons. Among these genes, TRHR1 was

found to be expressed in orexin neurons and upregulated 1,5 fold after fasting. Using semi-quantitative in situ hybridization, the regulation of TRHR1 seen in microarray analysis has been validated in this study to amount to a 1,24-fold increase. These findings clearly indicate that the microarray approach in this thesis to test differential gene expression in microdissected neurons of rats subjected to fasting and of untreated rats was extremely powerful and accurate to reveal even very subtle changes of TRHR1 that matched changes determined by quantitative analysis with ISH. Although these changes are subtle they can be regarded to be of physiological relevance because minor changes in neuropeptide expression can have important physiological consequences (e.g. substance P, CGRP changes in primary sensory pain pathways, (Nohr et al. 1999)).

The effects of TRH are mediated by two TRH receptors, which display complementary distribution patterns in the brain (Heuer et al. 2000). It has been reported that in a subpopulation of magnocellular neurons of the lateral hypothalamic area only mRNA for TRHR1, but not for TRHR2 could be detected. Low levels of TRHR2 mRNA were observed in smaller neurons in the lateral hypothalamic area (Heuer et al. 2000). However, the phenotypes of these neurons which express TRHR1 and TRHR2 in the LHA remained unknown. The present study has demonstrated that virtually all orexin neurons in the LHA express TRHR1 but not TRHR2 mRNA. These data are the first to identify the phenotype of neurons which express TRH receptor in the lateral hypothalamic area.

Microinjection of TRH into the medial and lateral hypothalamus produces severe anorexia (Suzuki et al. 1982). The expression of TRHR1 in orexin neurons and upregulation by fasting suggests that TRH may directly act on orexin neurons via TRHR1 to modulate the activation of orexin neurons related to the regulation of food intake. Under fasting conditions, the increased expression of the TRHR1 in orexin neurons may induce an increased binding of TRH to TRHR1 to modulate the orexigenic tone.

In addition to its role in the control of energy homeostasis, TRH has been implicated in other physiological functions, including thermoregulation (Boschi and Rips 1981), respiratory and cardiovascular function (Koivusalo et al. 1979), locomotor activity (Kalivas et al. 1987), arousal (Breese et al. 1975; Horita 1998), and sleepiness (Nishino et al. 1997). Orexin neurons are known to be involved in these functions

(Date et al. 1999; Hagan et al. 1999; Davis et al. 2003). Therefore, the TRH may modulate the multiple functions of orexin neurons via TRHR1.

4.6.2 Possible functional implications of some candidate genes regulated after fasting

The present thesis has identified a number of novel candidate genes that are worth to be tested further. For example, among these genes, insulin-like growth factor I (IGF-I) receptor and gamma-aminobutyric acid (GABA) B receptor 1 were found to be expressed in orexin neurons and upregulated 1,55 fold and 1,47 fold after fasting, respectively. In fact, both genes have been found to play a role in the regulation of food intake.

The IGF-I is a potent anabolic hormone. Its concentrations in serum are increased in response to food intake and decreased in states of chronic undernutrition or when food intake is restricted (Morovat et al. 1994). Previous i*n vitro* autoradiography studies reported that the IGF-I receptor was expressed in the median eminence of the rat brain and modulated by food restriction (Bohannon et al. 1988). The binding of ^{125}I-labeled [Thr59]IGF-I in the median eminence was significantly increased in the food restricted rats due to an increase in the concentration of iodo-[Thr59]IGF-I-binding sites in the median eminence (Bohannon et al. 1988). The present thesis is the first study to identify the expression and regulation of IGF-I receptor in orexin neurons. This indicates the new concept that IGF-I may directly modulate the activity of orexin neurons. Under fasting conditions, the increased expression of the IGF-I receptor in orexin neurons may cause increased binding of the IGF-I to this receptor to modulate the orexigenic tone.

The microarray analysis for the first time revealed that GABA(B)R1 mRNA is expressed in orexin neurons. This is consistent with a previous immunoreactive study that described the GABA(B)R1 immunoreactivity in orexin neurons (Backberg et al. 2003). GABA has been reported to stimulate feeding via both ionotropic GABA(A) and metabotropic GABA(B) receptors. The functional form of the GABA(B) receptor is a heterodimer consisting of GABA(B) receptor-1 (GABA(B)R1) and GABA(B) receptor-2 (GABA(B)R2) proteins. Within the heterodimer, the GABA-binding site is localized to GABA(B)R1. A previous report that intraperitoneal and intracerebroventricular administration of the GABA(B) receptor antagonist CGP

35348 reduced food consumption in rats (Patel and Ebenezer 2004) suggests the involvement of central GABA(B) receptor in the regulation of feeding behaviour.

Orexin neurons regulate the feeding behaviour also through GABAergic circuits (Viggiano et al. 2004). Intracerebroventricular injection of orexin A increased extracellular GABA in the medial hypothalamus (Viggiano et al. 2004). The orexin neurons in the hypothalamus are densely surrounded by GABAergic nerve endings, which are likely to originate from several different sources (Backberg et al. 2003). Since the GABA(B)R1 is expressed in orexin neurons as indicated in this study, GABA may influence the release of orexins via GABA(B)R1-mediated mechanisms.

4.6.3 Possible functional implications of some candidate genes unregulated after fasting

The observation that prepro-orexin was found to be expressed in the microdissected orexin neurons indicates that the LCM-microarray strategy employed was accurate. However the orexin gene itself was not subject to fasting-induced regulation in orexin neurons.

Previous studies reported that prepro-orexin gene expression either increased (Sakurai et al. 1998) or remained unaffected after fasting (Swart et al. 2001; Tritos et al. 2001; Bertile et al. 2003). Northern blot analysis of total RNA from rat diencephalon revealed that the expression of prepro-orexin mRNA was upregulated 2.4 fold in male Wistar rats fasted for 48h (Sakurai et al. 1998). In contrast, in situ hybridization and immunohistochemistry showed that prepro-orexin mRNA levels and orexin-A immunoreactivity were unaffected in male Sprague Dawley rats fasted for 48h (Swart et al. 2001). Moreover, it has been reported that 4 days or 5-7 days food deprivation did not induce significant changes in prepro-orexin mRNA levels in male Sprague Dawley rats analyzed by in situ hybridization (Bertile et al. 2003). The expression of prepro-orexin mRNA in male C57BL/6J mice fasted for 60h was also unaffected as measured by in situ hybridization histochemistry (Tritos et al. 2001).

The reason for discrepancies between previous studies and data in this thesis are most likely due to species (mouse vs. rat) or technical differences (Northern blot analysis vs. in situ hybridization and microarray analysis). Unchanged levels of prepro-orexin mRNA after fasting would be consistent with the need to spare energy during fasting. Indeed, in transgenic mice, orexin overexpression results in decreased body weight despite increased food intake due to inappropriately increased metabolic

rate whereas orexin-deficient mice show slightly reduced body weight despite markedly reduced food intake due to decreased metabolic rate (Inui 2000).

Other genes demonstrated by ISH in this study, such as the calcitonin receptor, receptor-activity-modifying proteins and the vesicular glutamate transporter were also revealed to be expressed in orexin neurons by microarray analysis. Although the expression of these genes was not affected after fasting according to microarray analysis, the involvement of these genes in the regulation of feeding behaviour is conceivable as discussed above. The cellular and molecular mechanisms of these genes in relation to food intake, and other functions in association with orexin neurons need to be further investigated.

4.6.4 Perspectives of the data obtained by microarray analysis of microdissected orexin neurons

It was beyond the scope of this thesis to validate the regulation of all the other genes (including those appearing as ESTs) found by microarray analysis. It is obvious that further extensive experiments are required assessing gain and loss of function with the help of siRNA technologies, new knockout animals and new transgenic models overexpressing genes in question as well cell culture approaches with single cell PCR analysis to determine the functional and mechanistic roles of the various novel candidate genes in relation to food intake and other functions beyond food intake regulation. With such strategies it should be possible to unravel distinct specific functions of these candidate genes with respect to enhancing or reducing appetite, stimulating or inhibiting energy expenditure, taking part in the short- or long- term effects of food intake regulation etc. Moreover, it may be possible to determine the involvement of these genes in many other functions than regulation of energy homeostasis, e.g. regulation of arousal, sleep, autonomic control, and hypertension. It will be an enormous task to clarify the probably diverse functions of the different candidate genes in orexin neurons requiring gene by gene analysis which obviously was beyond the scope of this thesis. Nevertheless, the strategy to perform cell-specific functional transcriptomic analysis seems to be more promising than transcriptomic analysis of crude hypothalamic extracts that do not pay tribute to the vast anatomical and functional heterogeneity of hypothalamic nuclei and neurons. Implicitly, microarray analysis of the phenotype-identified cell groups in the hypothalamus and brain stem related to the regulation of food intake are likely to prove valuable to

discover, validate and functionally characterize genes with so far unknown relevance in the regulation of food intake and energy expenditure. In any case, such investigations will lead to a better understanding of the molecular, cellular and functional specificity of hypothalamic and brainstem circuits.

5 Summary

The hypothalamus and brainstem are regarded as key centers of the brain that regulate energy homeostasis including food intake. Activation of these central neuropeptidergic pathways with orexigenic or anorexigenic properties by hormonal, nerval and nutrient stimuli exerts powerful effects on food intake. Among these neuropeptides are the members of the calcitonin/CGRP family, e.g. calcitonin (CT), amylin and calcitonin gene-related peptide (CGRP), which are ligands for receptor complexes consisting of CT receptor isoforms and receptor-activity-modifying proteins (RAMPs). There is evidence that the calcitonin/CGRP family and their receptors play a role in the regulation of food intake and long-term energy homeostasis. As no systematic analysis of the distribution of CT receptor isoforms throughout the brain is available, it is not fully understood how and where the peptides of the calcitonin family and their receptors participate in these feeding circuits.

Therefore, it was the aim of this thesis to characterize the distribution of CT receptor isoforms in the rat brain and, in particular, to answer the question whether peptides of the calcitonin family can directly act on peptidergic neurons in the hypothalamus, the area postrema (AP) and the nucleus of the solitary tract (NTS). For this purpose, RT-PCR in combination with laser capture microdissection (LCM), in situ hybridization (ISH), and immunocytochemistry were employed to determine the cell-specific expression pattern of the CT receptor isoforms $CT_{(a)}$ and $CT_{(b)}$ throughout the brain and especially in nuclei of the hypothalamus and brain stem relevant for feeding behavior. With particular emphasis, the orexin neurons in the lateral hypothalamic area were investigated. In order to identify novel candidate genes involved in the regulation of food intake in the hypothalamus, orexin neurons from fasting and non-fasting rats were laser microdissected and the differential gene expression was determined by microarray analysis.

The following essential new findings and conclusions have been obtained:

1. Both $CT_{(a)}$ and $CT_{(b)}$ were found to be expressed in the rat brain. They exhibit distinct differences in their expression patterns. While $CT_{(a)}$ was found to be widely expressed throughout the brain consistent with a wide variety of functions exerted by members of the calcitonin family, $CT_{(b)}$ showed a more restricted expression pattern suggesting more limited functions for $CT_{(b)}$ mediated

neurotransmission. $CT_{(b)}$ was predominately expressed in the hypothalamus and brain stem.

2. Peptidergic hypothalamic neurons, as a rule, expressed either $CT_{(a)}$ or $CT_{(b)}$ isoforms. NPY neurons, orexin neurons and a subpopulation of TRH neurons predominately expressed the $CT_{(b)}$ isoform, while the $CT_{(a)}$ isoform was selectively expressed in a subpopulation of POMC/CART neurons and CRH neurons. CT receptors were absent from TRH neurons in the area postrema (AP).
3. Co-expression of $CT_{(b)}$ with RAMP2 and RAMP3 in orexin neurons suggests that functional amylin receptor subtypes $AMY_{2(b)}$ and $AMY_{3(b)}$ are expressed in orexin neurons. These data indicate a role of amylin and/or CGRP in the modulation of orexin neurons.
4. Double immunohistochemistry demonstrated that in the lateral hypothalamus CGRP positive terminals contact orexin neurons indicating that CGRP may act as an endogenous ligand on orexin neurons.
5. The expression of vesicular glutamate transporter 2 in virtually all of the orexin neurons in the LHA clearly indicates that orexin neurons have a glutamatergic but not a GABAergic phenotype.
6. LCM Microarray analysis of microdissected orexin neurons from animals subjected to fasting has led to the identification of 481 novel candidate genes that regulate feeding behavior at the level of orexin neurons. Among the regulated genes were thyrotropin releasing hormone receptor 1 (TRHR1), insulin-like growth factor 1 receptor, and gamma-aminobutyric acid (GABA) B receptor 1. By in situ hybridization, the regulation of TRHR1 was validated.
7. The expression of TRHR1 in orexin neurons, but not TRHR2, and the upregulation of TRHR1 mRNA after fasting suggest that TRH may influence energy homeostasis by directly acting on orexin neurons via TRHR1.

Taken together, CT receptor isoforms are likely to play an important and isoform-specific role throughout the brain and especially in feeding circuits of the hypothalamus and brain stem. As these circuits also serve other functions than regulation of energy homeostasis, e.g regulation of sleep, autonomic functions and arousal, CT receptors are probably involved in an isoform-sepcific manner to modulate such functions, too. Likewise, the genes found to be regulated in orexin neurons after fasting can be postulated to play a role beyond functions of orexin neurons related to food intake.

6 Zusammenfassung

Hypothalamus und Hirnstamm gelten als Schlüsselzentren des Gehirns für die Regulation der Energie-Homöostase einschließlich der Nahrungsaufnahme. Eine Beeinflussung seiner neuropeptidergen Schaltkreise, die sowohl orexigene als anorexigene Komponeneten haben, durch hormonelle und nervale Faktoren sowie durch Nährstoffe übt einen starken Einfluss auf die Nahrungsaufnahme aus. Vieles deutet darauf hin, dass Neuropeptide der Calcitonin/CGRP-Familie zur zentralen Regulation der Nahrungsaufnahme und des langfristigen Energiegleichgewichts beitragen. Mitglieder der Calcitonin/CGRP-Familie sind Calcitonin (CT), Amylin und "Calcitonin gene-realted peptide"(CGRP). Sie fungieren als Liganden für Rezeptor-Komplexe, die aus verschiedenen Isoformen des CT-Rezeptors und der "receptor-activity-modifying proteins" (RAMPs) bestehen. Wie und wo diese Neuropeptide und ihre Rezeptoren Schaltkreise des Essverhaltens modulieren, blieb angesichts des Fehlens systematischer Expressionanalysen bisher ungeklärt.

Deshalb war es das Ziel dieser Dissertation, die Verteilung der CT-Rezeptor-Isoformen im Rattenhirn zu charakterisieren, und insbesondere die Frage zu beantworten, ob Peptide der CT-Familie auf peptiderge Neurone des Hypothalamus, der Area postrema (AP) und des Nucleus tractus solitarii eine direkte Wirkung entfalten können. Zu diesem Zweck wurden Methoden der RT-PCR in Kombination mit Laser-Capture-Microdissektion (LCM), In situ-Hybridisierung (ISH) und Immunhistochemie (ICC) eingesetzt, um die zellspezifischen Expressionsmuster der CT-Rezeptor-Isoformen im gesamten Rattenhirn, insbesondere in den Kerngebieten des Hypothalamus und des Hirnstamms, die für das Essverhalten wichtig sind, zu bestimmen. Mit besonderer Gewichtung wurden die Orexin-Neurone in der lateralen hypothalamischen Region (LHA) untersucht. Um neue Kandidatengene zu identifizieren, die an der Regulation der Nahrungsaufnahme im Hypothalamus beteiligt sind, wurden Orexin-Neurone von Ratten mit und ohne Nahrungskarenz lasermicrodissektiert, um deren differenzielle Genexpression mittels Microarray-Analyse zu bestimmen.

Die folgenden grundlegenden Erkenntnisse wurden gewonnen und folgende Schlussfolgerungen gezogen:

1) Beide CT Rezeptor-Isoformen, $CT_{(a)}$ und $CT_{(b)}$, sind im Gehirn exprimiert mit klaren Unterschieden in ihrem Expressionsmuster. Während $CT_{(a)}$ im Rattenhirn weit

verbreitet ist, was im Einklang mit der Vielzahl an Funktionen der CT-Peptidfamilie steht, zeigt $CT_{(b)}$ ein eingeschränkteres Expressionsmuster mit bevorzugter Expression im Hypothalamus und Hirnstamm, was auf begrenzte Funktionen der $CT_{(b)}$-vermittelten Neurotransmission hindeutet. **2)** Peptiderge hypothalamische Neurone exprimieren in der Regel entweder die $CT_{(a)}$-oder die $CT_{(b)}$-Isoform. NPY-Neurone, Orexin-Neurone und eine Subpopulation der TRH-Neurone exprimieren überwiegend die $CT_{(b)}$-Isoform, während die $CT_{(a)}$-Isoform in einer Subpopulation von POMC/CART- und CRH-Neuronen exprimiert wird. Hingegen finden sich keine CT-Rezeptoren auf den TRH-Neuronen in der AP. **3)** Die Ko-expression von $CT_{(b)}$ mit RAMP2 und RAMP3 in Orexin-Neuronen weist auf die Möglichkeit der funktionellen Expression der Amylin-Rezeptorsubtypen $AMY_{2(b)}$ und $AMY_{3(b)}$ in diesem Zelltyp hin. **4)** Mit ICC-Doppelmarkierung konnte gezeigt werden, dass in der LHA CGRP-positive Endigungen Orexin-Neurone kontaktieren, was auf CGRP als möglichen endogenen Liganden hindeutet. **5)** Die Expression des vesikulären Glutamat-transporters 2 in nahezu allen Orexin-Neuronen zeigt eindeutig, dass Orexin-Neurone einen glutamatergen Phänotyp haben. **6)** Microarray-Analyse microdissektierter Orexin-Neurone von Ratten nach 48h Fasten führte zur Identifizierung 481 neuer Kandidatengene, die das Essverhalten auf zellulärer Ebene in Orexin-Neuronen möglicherweise regulieren. Darunter befanden sich der Thyreotropin-Rezeptor Typ 1 (TRHR1), "Insulin-like growth factor 1" Rezeptor, GABA (B)-Rezeptor 1. Mittels semi-quantitativer ISH wurde die Regulation von TRHR1 validiert. **7)** Die Expression von TRHR1, jedoch nicht TRHR2, und die gering erhöhten TRHR1 mRNA-Spiegel in Orexin-Neuronen nach 48stündigem Fasten weisen auf eine Rolle von TRH bei der Regulation des Energiegleichgewichts durch direkte TRHR1-vermittelte Wirkung auf Orexin-Neurone hin.

Insgesamt bedeuten die hier erzielten Ergebnisse, dass CT-Rezeptoren eine wichtige und wahrscheinlich isoform-spezifische Rolle im Gehirn spielen, insbesondere in den Schaltkreisen der Ernährungsregulation im Hypothalamus und im Hirnstamm. Da diese Schaltkreise auch anderen Funktionen dienen, wie z.B. der Regulation von Wachheit und Schlaf und weiterer vegetativer Funktionen, ist es wahrscheinlich, dass CT-Rezeptoren isoform-spezifisch auch diese Funktionen modulieren können. Ebenso kann man davon ausgehen, dass die Gene, deren Expression in Orexin-Neuronen nach Fasten verändert war, auch eine Rolle bei anderen Funktionen der Orexin-Neurone über die Regulation der Nahrungsaufnahme hinaus spielen.

7 References

Ahn, T. G., S. J. Han, Y. S. Cho, T. H. An, S. C. Pak and G. Flouret (2004). "In vivo activity of the potent oxytocin antagonist on uterine activity in the rat." In Vivo **18**(6): 763-6.

Al-Barazanji, K. A., S. Wilson, J. Baker, D. S. Jessop and M. S. Harbuz (2001). "Central orexin-A activates hypothalamic-pituitary-adrenal axis and stimulates hypothalamic corticotropin releasing factor and arginine vasopressin neurones in conscious rats." J Neuroendocrinol **13**(5): 421-4.

Albrandt, K., E. M. Brady, C. X. Moore, E. Mull, M. E. Sierzega and K. Beaumont (1995). "Molecular cloning and functional expression of a third isoform of the human calcitonin receptor and partial characterization of the calcitonin receptor gene." Endocrinology **136**(12): 5377-84.

Albrandt, K., E. Mull, E. M. Brady, J. Herich, C. X. Moore and K. Beaumont (1993). "Molecular cloning of two receptors from rat brain with high affinity for salmon calcitonin." FEBS Lett **325**(3): 225-32.

Arnelo, U., J. Permert, T. E. Adrian, J. Larsson, P. Westermark and R. D. Reidelberger (1996). "Chronic infusion of islet amyloid polypeptide causes anorexia in rats." Am J Physiol **271**(6 Pt 2): R1654-9.

Backberg, M., M. Collin, M. L. Ovesjo and B. Meister (2003). "Chemical coding of GABA(B) receptor-immunoreactive neurones in hypothalamic regions regulating body weight." J Neuroendocrinol **15**(1): 1-14.

Backberg, M., G. Hervieu, S. Wilson and B. Meister (2002). "Orexin receptor-1 (OX-R1) immunoreactivity in chemically identified neurons of the hypothalamus: focus on orexin targets involved in control of food and water intake." Eur J Neurosci **15**(2): 315-28.

Badman, M. K. and J. S. Flier (2005). "The gut and energy balance: visceral allies in the obesity wars." Science **307**(5717): 1909-14.

Bai, L., H. Xu, J. F. Collins and F. K. Ghishan (2001). "Molecular and functional analysis of a novel neuronal vesicular glutamate transporter." J Biol Chem **276**(39): 36764-9.

Baklavadzhyan, O. G., N. L. Pogosyan, A. V. Arshakyan, A. G. Darbinyan, A. V. Khachatryan and T. G. Nikogosyan (2000). "Studies of the role of the central nucleus of the amygdala in controlling cardiovascular functions." Neurosci Behav Physiol **30**(2): 231-6.

Baldo, B. A. and A. E. Kelley (2001). "Amylin infusion into rat nucleus accumbens potently depresses motor activity and ingestive behavior." Am J Physiol Regul Integr Comp Physiol **281**(4): R1232-42.

Banks, W. A., A. J. Kastin, L. M. Maness, W. Huang and J. B. Jaspan (1995). "Permeability of the blood-brain barrier to amylin." Life Sci **57**(22): 1993-2001.

Barth, S. W., T. Riediger, T. A. Lutz and G. Rechkemmer (2003). "Differential effects of amylin and salmon calcitonin on neuropeptide gene expression in the lateral hypothalamic area and the arcuate nucleus of the rat." Neurosci Lett **341**(2): 131-4.

Barth, S. W., T. Riediger, T. A. Lutz and G. Rechkemmer (2004). "Peripheral amylin activates circumventricular organs expressing calcitonin receptor a/b subtypes and receptor-activity modifying proteins in the rat." Brain Res **997**(1): 97-102.

Baskin, D. G., J. F. Breininger and M. W. Schwartz (1999). "Leptin receptor mRNA identifies a subpopulation of neuropeptide Y neurons activated by fasting in rat hypothalamus." Diabetes **48**(4): 828-33.

Bayer, L., G. Mairet-Coello, P. Y. Risold and B. Griffond (2002). "Orexin/hypocretin neurons: chemical phenotype and possible interactions with melanin-concentrating hormone neurons." Regul Pept **104**(1-3): 33-9.

Beaumont, K., M. A. Kenney, A. A. Young and T. J. Rink (1993). "High affinity amylin binding sites in rat brain." Mol Pharmacol **44**(3): 493-7.

Becskei, C., T. Riediger, D. Zund, P. Wookey and T. A. Lutz (2004). "Immunohistochemical mapping of calcitonin receptors in the adult rat brain." Brain Res **1030**(2): 221-33.

Berthoud, H. R. (2002). "Multiple neural systems controlling food intake and body weight." Neurosci Biobehav Rev **26**(4): 393-428.

Berthoud, H. R. (2004). "Mind versus metabolism in the control of food intake and energy balance." Physiol Behav **81**(5): 781-93.

Bertile, F., H. Oudart, F. Criscuolo, Y. L. Maho and T. Raclot (2003). "Hypothalamic gene expression in long-term fasted rats: relationship with body fat." Biochem Biophys Res Commun **303**(4): 1106-13.

Bhatnagar, S. and M. F. Dallman (1999). "The paraventricular nucleus of the thalamus alters rhythms in core temperature and energy balance in a state-dependent manner." Brain Res **851**(1-2): 66-75.

Billington, C. J., J. E. Briggs, M. Grace and A. S. Levine (1991). "Effects of intracerebroventricular injection of neuropeptide Y on energy metabolism." Am J Physiol **260**(2 Pt 2): R321-7.

Bingham, S., P. T. Davey, A. J. Babbs, E. A. Irving, M. J. Sammons, M. Wyles, P. Jeffrey, L. Cutler, I. Riba, A. Johns, R. A. Porter, N. Upton, A. J. Hunter and A. A. Parsons (2001). "Orexin-A, an hypothalamic peptide with analgesic properties." Pain **92**(1-2): 81-90.

Blake, N. G., D. J. Eckland, O. J. Foster and S. L. Lightman (1991). "Inhibition of hypothalamic thyrotropin-releasing hormone messenger ribonucleic acid during food deprivation." Endocrinology **129**(5): 2714-8.

Bohannon, N. J., E. S. Corp, B. J. Wilcox, D. P. Figlewicz, D. M. Dorsa and D. G. Baskin (1988). "Characterization of insulin-like growth factor I receptors in the median eminence of the brain and their modulation by food restriction." Endocrinology **122**(5): 1940-7.

Boschi, G. and R. Rips (1981). "Effects of thyrotropin releasing hormone injections into different loci of rat brain on core temperature." Neurosci Lett **23**(1): 93-8.

Boulant, J. A. (2000). "Role of the preoptic-anterior hypothalamus in thermoregulation and fever." Clin Infect Dis **31 Suppl 5**: S157-61.

Breese, G. R., J. M. Cott, B. R. Cooper, A. J. Prange, Jr., M. A. Lipton and N. P. Plotnikoff (1975). "Effects of thyrotropin-releasing hormone (TRH) on the actions of pentobarbital and other centrally acting drugs." J Pharmacol Exp Ther **193**(1): 11-22.

Broberger, C. (1999). "Hypothalamic cocaine- and amphetamine-regulated transcript (CART) neurons: histochemical relationship to thyrotropin-releasing hormone, melanin-concentrating hormone, orexin/hypocretin and neuropeptide Y." Brain Res **848**(1-2): 101-13.

Broberger, C. and T. Hokfelt (2001). "Hypothalamic and vagal neuropeptide circuitries regulating food intake." Physiol Behav **74**(4-5): 669-82.

Butler, P. C., J. Chou, W. B. Carter, Y. N. Wang, B. H. Bu, D. Chang, J. K. Chang and R. A. Rizza (1990). "Effects of meal ingestion on plasma amylin concentration in NIDDM and nondiabetic humans." Diabetes **39**(6): 752-6.

Campfield, L. A., F. J. Smith, Y. Guisez, R. Devos and P. Burn (1995). "Recombinant mouse OB protein: evidence for a peripheral signal linking adiposity and central neural networks." Science **269**(5223): 546-9.

Chabre, O., B. R. Conklin, H. Y. Lin, H. F. Lodish, E. Wilson, H. E. Ives, L. Catanzariti, B. A. Hemmings and H. R. Bourne (1992). "A recombinant calcitonin receptor independently stimulates 3',5'-cyclic adenosine monophosphate and Ca2+/inositol phosphate signaling pathways." Mol Endocrinol **6**(4): 551-6.

Chakraborty, M., D. Chatterjee, S. Kellokumpu, H. Rasmussen and R. Baron (1991). "Cell cycle-dependent coupling of the calcitonin receptor to different G proteins." Science **251**(4997): 1078-82.

Cheung, C. C., D. K. Clifton and R. A. Steiner (1997). "Proopiomelanocortin neurons are direct targets for leptin in the hypothalamus." Endocrinology **138**(10): 4489-92.

Christopoulos, G., G. Paxinos, X. F. Huang, K. Beaumont, A. W. Toga and P. M. Sexton (1995). "Comparative distribution of receptors for amylin and the

related peptides calcitonin gene related peptide and calcitonin in rat and monkey brain." Can J Physiol Pharmacol **73**(7): 1037-41.

Christopoulos, G., K. J. Perry, M. Morfis, N. Tilakaratne, Y. Gao, N. J. Fraser, M. J. Main, S. M. Foord and P. M. Sexton (1999). "Multiple amylin receptors arise from receptor activity-modifying protein interaction with the calcitonin receptor gene product." Mol Pharmacol **56**(1): 235-42.

Copp, D. H. and B. Cheney (1962). "Calcitonin-a hormone from the parathyroid which lowers the calcium-level of the blood." Nature **193**: 381-2.

Date, Y., Y. Ueta, H. Yamashita, H. Yamaguchi, S. Matsukura, K. Kangawa, T. Sakurai, M. Yanagisawa and M. Nakazato (1999). "Orexins, orexigenic hypothalamic peptides, interact with autonomic, neuroendocrine and neuroregulatory systems." Proc Natl Acad Sci U S A **96**(2): 748-53.

Davis, S. F., K. W. Williams, W. Xu, N. R. Glatzer and B. N. Smith (2003). "Selective enhancement of synaptic inhibition by hypocretin (orexin) in rat vagal motor neurons: implications for autonomic regulation." J Neurosci **23**(9): 3844-54.

de Lecea, L., T. S. Kilduff, C. Peyron, X. Gao, P. E. Foye, P. E. Danielson, C. Fukuhara, E. L. Battenberg, V. T. Gautvik, F. S. Bartlett, 2nd, W. N. Frankel, A. N. van den Pol, F. E. Bloom, K. M. Gautvik and J. G. Sutcliffe (1998). "The hypocretins: hypothalamus-specific peptides with neuroexcitatory activity." Proc Natl Acad Sci U S A **95**(1): 322-7.

Dhillo, W. S., C. J. Small, P. H. Jethwa, S. H. Russell, J. V. Gardiner, G. A. Bewick, A. Seth, K. G. Murphy, M. A. Ghatei and S. R. Bloom (2003). "Paraventricular nucleus administration of calcitonin gene-related peptide inhibits food intake and stimulates the hypothalamo-pituitary-adrenal axis." Endocrinology **144**(4): 1420-5.

Dube, M. G., S. P. Kalra and P. S. Kalra (1999). "Food intake elicited by central administration of orexins/hypocretins: identification of hypothalamic sites of action." Brain Res **842**(2): 473-7.

Edwards, C. M., S. Abusnana, D. Sunter, K. G. Murphy, M. A. Ghatei and S. R. Bloom (1999). "The effect of the orexins on food intake: comparison with neuropeptide Y, melanin-concentrating hormone and galanin." J Endocrinol **160**(3): R7-12.

Figlewicz, D. P., A. J. Sipols, D. Porte, Jr., S. C. Woods and R. A. Liddle (1989). "Intraventricular CCK inhibits food intake and gastric emptying in baboons." Am J Physiol **256**(6 Pt 2): R1313-7.

Fischer, J. A. and W. Born (1985). "Novel peptides from the calcitonin gene: expression, receptors and biological function." Peptides **6 Suppl 3**: 265-71.

Fluhmann, B., R. Muff, W. Hunziker, J. A. Fischer and W. Born (1995). "A human orphan calcitonin receptor-like structure." Biochem Biophys Res Commun **206**(1): 341-7.

Follwell, M. J. and A. V. Ferguson (2002). "Cellular mechanisms of orexin actions on paraventricular nucleus neurones in rat hypothalamus." J Physiol **545**(Pt 3): 855-67.

Force, T., J. V. Bonventre, M. R. Flannery, A. H. Gorn, M. Yamin and S. R. Goldring (1992). "A cloned porcine renal calcitonin receptor couples to adenylyl cyclase and phospholipase C." Am J Physiol **262**(6 Pt 2): F1110-5.

Gale, G. D., S. G. Anagnostaras, B. P. Godsil, S. Mitchell, T. Nozawa, J. R. Sage, B. Wiltgen and M. S. Fanselow (2004). "Role of the basolateral amygdala in the storage of fear memories across the adult lifetime of rats." J Neurosci **24**(15): 3810-5.

Gillespie, M. T., R. J. Thomas, Z. Y. Pu, H. Zhou, T. J. Martin and D. M. Findlay (1997). "Calcitonin receptors, bone sialoprotein and osteopontin are expressed in primary breast cancers." Int J Cancer **73**(6): 812-5.

Glatzle, J., M. E. Kreis, K. Kawano, H. E. Raybould and T. T. Zittel (2001). "Postprandial neuronal activation in the nucleus of the solitary tract is partly mediated by CCK-A receptors." Am J Physiol Regul Integr Comp Physiol **281**(1): R222-9.

Gorn, A. H., H. Y. Lin, M. Yamin, P. E. Auron, M. R. Flannery, D. R. Tapp, C. A. Manning, H. F. Lodish, S. M. Krane and S. R. Goldring (1992). "Cloning, characterization, and expression of a human calcitonin receptor from an ovarian carcinoma cell line." J Clin Invest **90**(5): 1726-35.

Gras, C., E. Herzog, G. C. Bellenchi, V. Bernard, P. Ravassard, M. Pohl, B. Gasnier, B. Giros and S. El Mestikawy (2002). "A third vesicular glutamate transporter expressed by cholinergic and serotoninergic neurons." J Neurosci **22**(13): 5442-51.

Grill, H. J. and J. M. Kaplan (2001). "Interoceptive and integrative contributions of forebrain and brainstem to energy balance control." Int J Obes Relat Metab Disord **25 Suppl 5**: S73-7.

Hagan, J. J., R. A. Leslie, S. Patel, M. L. Evans, T. A. Wattam, S. Holmes, C. D. Benham, S. G. Taylor, C. Routledge, P. Hemmati, R. P. Munton, T. E. Ashmeade, A. S. Shah, J. P. Hatcher, P. D. Hatcher, D. N. Jones, M. I. Smith, D. C. Piper, A. J. Hunter, R. A. Porter and N. Upton (1999). "Orexin A activates locus coeruleus cell firing and increases arousal in the rat." Proc Natl Acad Sci U S A **96**(19): 10911-6.

Hakansson, M. L. and B. Meister (1998). "Transcription factor STAT3 in leptin target neurons of the rat hypothalamus." Neuroendocrinology **68**(6): 420-7.

Halasz, J., Z. Liposits, M. R. Kruk and J. Haller (2002). "Neural background of glucocorticoid dysfunction-induced abnormal aggression in rats: involvement of fear- and stress-related structures." Eur J Neurosci **15**(3): 561-9.

Haynes, A. C., B. Jackson, P. Overend, R. E. Buckingham, S. Wilson, M. Tadayyon and J. R. Arch (1999). "Effects of single and chronic intracerebroventricular administration of the orexins on feeding in the rat." Peptides **20**(9): 1099-105.

Heinrichs, M., G. Meinlschmidt, W. Wippich, U. Ehlert and D. H. Hellhammer (2004). "Selective amnesic effects of oxytocin on human memory." Physiol Behav **83**(1): 31-8.

Hetherington, A. W. and S. W. Ranson (1940). "Hypothalamic lesions and adiposity in the rat." Anat Rec **78**: 149-72.

Heuer, H., M. K. Schafer, D. O'Donnell, P. Walker and K. Bauer (2000). "Expression of thyrotropin-releasing hormone receptor 2 (TRH-R2) in the central nervous system of rats." J Comp Neurol **428**(2): 319-36.

Hillebrand, J. J., D. de Wied and R. A. Adan (2002). "Neuropeptides, food intake and body weight regulation: a hypothalamic focus." Peptides **23**(12): 2283-306.

Hilton, J. M., S. Y. Chai and P. M. Sexton (1995). "In vitro autoradiographic localization of the calcitonin receptor isoforms, C1a and C1b, in rat brain." Neuroscience **69**(4): 1223-37.

Hinney, A., S. Hohmann, F. Geller, C. Vogel, C. Hess, A. K. Wermter, B. Brokamp, H. Goldschmidt, W. Siegfried, H. Remschmidt, H. Schafer, T. Gudermann and J. Hebebrand (2003). "Melanocortin-4 receptor gene: case-control study and transmission disequilibrium test confirm that functionally relevant mutations are compatible with a major gene effect for extreme obesity." J Clin Endocrinol Metab **88**(9): 4258-67.

Horita, A. (1998). "An update on the CNS actions of TRH and its analogs." Life Sci **62**(17-18): 1443-8.

Horvath, T. L. and S. Diano (2004). "The floating blueprint of hypothalamic feeding circuits." Nat Rev Neurosci **5**(8): 662-7.

Hotta, M., T. Shibasaki, N. Yamauchi, H. Ohno, R. Benoit, N. Ling and H. Demura (1991). "The effects of chronic central administration of corticotropin-releasing factor on food intake, body weight, and hypothalamic-pituitary-adrenocortical hormones." Life Sci **48**(15): 1483-91.

Houssami, S., D. M. Findlay, C. L. Brady, D. E. Myers, T. J. Martin and P. M. Sexton (1994). "Isoforms of the rat calcitonin receptor: consequences for ligand binding and signal transduction." Endocrinology **135**(1): 183-90.

Hyde, T. M. and R. R. Miselis (1983). "Effects of area postrema/caudal medial nucleus of solitary tract lesions on food intake and body weight." Am J Physiol **244**(4): R577-87.

Inui, A. (2000). "Transgenic approach to the study of body weight regulation." Pharmacol Rev **52**(1): 35-61.

Inui, A. (2001). "Ghrelin: an orexigenic and somatotrophic signal from the stomach." Nat Rev Neurosci **2**(8): 551-60.

John, J., M. F. Wu, T. Kodama and J. M. Siegel (2003). "Intravenously administered hypocretin-1 alters brain amino acid release: an in vivo microdialysis study in rats." J Physiol **548**(Pt 2): 557-62.

Kalivas, P. W., D. Stanley and A. J. Prange, Jr. (1987). "Interaction between thyrotropin-releasing hormone and the mesolimbic dopamine system." Neuropharmacology **26**(1): 33-8.

Kask, A., L. Rago, J. E. Wikberg and H. B. Schioth (2000). "Differential effects of melanocortin peptides on ingestive behaviour in rats: evidence against the involvement of MC(3) receptor in the regulation of food intake." Neurosci Lett **283**(1): 1-4.

Kawano, H., Y. Tsuruo, H. Bando and S. Daikoku (1991). "Hypophysiotrophic TRH-producing neurons identified by combining immunohistochemistry for pro-TRH and retrograde tracing." J Comp Neurol **307**(4): 531-8.

Kc, P., M. A. Haxhiu, F. P. Tolentino-Silva, M. Wu, C. O. Trouth and S. O. Mack (2002). "Paraventricular vasopressin-containing neurons project to brain stem and spinal cord respiratory-related sites." Respir Physiol Neurobiol **133**(1-2): 75-88.

Keverne, E. B. and J. P. Curley (2004). "Vasopressin, oxytocin and social behaviour." Curr Opin Neurobiol **14**(6): 777-83.

Kodama, T. and M. Kimura (2002). "Arousal effects of orexin-A correlate with GLU release from the locus coeruleus in rats." Peptides **23**(9): 1673-81.

Koivusalo, F., I. Paakkari, J. Leppaluoto and H. Karppanen (1979). "The effect of centrally administered TRH on blood pressure, heart rate and ventilation in rat." Acta Physiol Scand **106**(1): 83-6.

Krahn, D. D., B. A. Gosnell, A. S. Levine and J. E. Morley (1984). "Effects of calcitonin gene-related peptide on food intake." Peptides **5**(5): 861-4.

Kristensen, P., M. E. Judge, L. Thim, U. Ribel, K. N. Christjansen, B. S. Wulff, J. T. Clausen, P. B. Jensen, O. D. Madsen, N. Vrang, P. J. Larsen and S. Hastrup (1998). "Hypothalamic CART is a new anorectic peptide regulated by leptin." Nature **393**(6680): 72-6.

Kyrkouli, S. E., B. G. Stanley, R. D. Seirafi and S. F. Leibowitz (1990). "Stimulation of feeding by galanin: anatomical localization and behavioral specificity of this peptide's effects in the brain." Peptides **11**(5): 995-1001.

Ladenheim, E. E. and R. C. Ritter (1988). "Low-dose fourth ventricular bombesin selectively suppresses food intake." Am J Physiol **255**(6 Pt 2): R988-93.

Lafond, J., L. Simoneau, R. Savard and D. Lajeunesse (1994). "Calcitonin receptor in human placental syncytiotrophoblast brush border and basal plasma membranes." Mol Cell Endocrinol **99**(2): 285-92.

Leffert, J. D., C. B. Newgard, H. Okamoto, J. L. Milburn and K. L. Luskey (1989). "Rat amylin: cloning and tissue-specific expression in pancreatic islets." Proc Natl Acad Sci U S A **86**(9): 3127-30.

Li, Y., X. B. Gao, T. Sakurai and A. N. van den Pol (2002). "Hypocretin/Orexin excites hypocretin neurons via a local glutamate neuron-A potential mechanism for orchestrating the hypothalamic arousal system." Neuron **36**(6): 1169-81.

Luckman, S. M. and C. B. Lawrence (2003). "Anorectic brainstem peptides: more pieces to the puzzle." Trends Endocrinol Metab **14**(2): 60-5.

Luttinger, D., R. A. King, D. Sheppard, J. Strupp, C. B. Nemeroff and A. J. Prange, Jr. (1982). "The effect of neurotensin on food consumption in the rat." Eur J Pharmacol **81**(3): 499-503.

Lutz, T. A., E. Del Prete and E. Scharrer (1994). "Reduction of food intake in rats by intraperitoneal injection of low doses of amylin." Physiol Behav **55**(5): 891-5.

Lutz, T. A., A. Mollet, P. A. Rushing, T. Riediger and E. Scharrer (2001). "The anorectic effect of a chronic peripheral infusion of amylin is abolished in area postrema/nucleus of the solitary tract (AP/NTS) lesioned rats." Int J Obes Relat Metab Disord **25**(7): 1005-11.

Lutz, T. A., R. Rossi, J. Althaus, E. Del Prete and E. Scharrer (1998). "Amylin reduces food intake more potently than calcitonin gene-related peptide (CGRP) when injected into the lateral brain ventricle in rats." Peptides **19**(9): 1533-40.

Lutz, T. A., M. Senn, J. Althaus, E. Del Prete, F. Ehrensperger and E. Scharrer (1998). "Lesion of the area postrema/nucleus of the solitary tract (AP/NTS) attenuates the anorectic effects of amylin and calcitonin gene-related peptide (CGRP) in rats." Peptides **19**(2): 309-17.

Mack, S. O., P. Kc, M. Wu, B. R. Coleman, F. P. Tolentino-Silva and M. A. Haxhiu (2002). "Paraventricular oxytocin neurons are involved in neural modulation of breathing." J Appl Physiol **92**(2): 826-34.

Maldonado-Irizarry, C. S., C. J. Swanson and A. E. Kelley (1995). "Glutamate receptors in the nucleus accumbens shell control feeding behavior via the lateral hypothalamus." J Neurosci **15**(10): 6779-88.

Manaker, S. and G. Rizio (1989). "Autoradiographic localization of thyrotropin-releasing hormone and substance P receptors in the rat dorsal vagal complex." J Comp Neurol **290**(4): 516-26.

McLatchie, L. M., N. J. Fraser, M. J. Main, A. Wise, J. Brown, N. Thompson, R. Solari, M. G. Lee and S. M. Foord (1998). "RAMPs regulate the transport and

ligand specificity of the calcitonin-receptor-like receptor." Nature **393**(6683): 333-9.

McMinn, J. E., C. W. Wilkinson, P. J. Havel, S. C. Woods and M. W. Schwartz (2000). "Effect of intracerebroventricular alpha-MSH on food intake, adiposity, c-Fos induction, and neuropeptide expression." Am J Physiol Regul Integr Comp Physiol **279**(2): R695-703.

Michelini, L. C. (2001). "Oxytocin in the NTS. A new modulator of cardiovascular control during exercise." Ann N Y Acad Sci **940**: 206-20.

Mollet, A., S. Gilg, T. Riediger and T. A. Lutz (2004). "Infusion of the amylin antagonist AC 187 into the area postrema increases food intake in rats." Physiol Behav **81**(1): 149-55.

Moore, E. E., R. E. Kuestner, S. D. Stroop, F. J. Grant, S. L. Matthewes, C. L. Brady, P. M. Sexton and D. M. Findlay (1995). "Functionally different isoforms of the human calcitonin receptor result from alternative splicing of the gene transcript." Mol Endocrinol **9**(8): 959-68.

Morley, J. E., S. A. Farr and J. F. Flood (1996). "Peripherally administered calcitonin gene-related peptide decreases food intake in mice." Peptides **17**(3): 511-6.

Morley, J. E., J. F. Flood, S. A. Farr, H. J. Perry, 3rd, F. E. Kaiser and P. M. Morley (1995). "Effects of amylin on appetite regulation and memory." Can J Physiol Pharmacol **73**(7): 1042-6.

Morovat, A., K. A. Burton and M. J. Dauncey (1994). "Short-term regulation of plasma IGF-I concentration by food intake in young growing pigs." Horm Metab Res **26**(6): 265-9.

Morris, M. J. and T. Nguyen (2001). "Does neuropeptide Y contribute to the anorectic action of amylin?" Peptides **22**(3): 541-6.

Muff, R., W. Born and J. A. Fischer (2001). "Adrenomedullin and related peptides: receptors and accessory proteins." Peptides **22**(11): 1765-72.

Muff, R., W. Born and J. A. Fischer (2003). "Adrenomedullin selectivity of calcitonin-like receptor/receptor activity modifying proteins." Hypertens Res **26 Suppl**: S3-8.

Muff, R., N. Buhlmann, J. A. Fischer and W. Born (1999). "An amylin receptor is revealed following co-transfection of a calcitonin receptor with receptor activity modifying proteins-1 or -3." Endocrinology **140**(6): 2924-7.

Muff, R., K. Leuthauser, N. Buhlmann, S. M. Foord, J. A. Fischer and W. Born (1998). "Receptor activity modifying proteins regulate the activity of a calcitonin gene-related peptide receptor in rabbit aortic endothelial cells." FEBS Lett **441**(3): 366-8.

Murakami, M., M. Mori, Y. Kato and I. Kobayashi (1991). "Hypothalamic thyrotropin-releasing hormone regulates pituitary thyrotropin beta- and alpha-subunit mRNA levels in the rat." Neuroendocrinology **53**(3): 276-80.

Muroya, S., H. Funahashi, A. Yamanaka, D. Kohno, K. Uramura, T. Nambu, M. Shibahara, M. Kuramochi, M. Takigawa, M. Yanagisawa, T. Sakurai, S. Shioda and T. Yada (2004). "Orexins (hypocretins) directly interact with neuropeptide Y, POMC and glucose-responsive neurons to regulate Ca 2+ signaling in a reciprocal manner to leptin: orexigenic neuronal pathways in the mediobasal hypothalamus." Eur J Neurosci **19**(6): 1524-34.

Nahon, J. L. (1994). "The melanin-concentrating hormone: from the peptide to the gene." Crit Rev Neurobiol **8**(4): 221-62.

Nakamoto, H., Y. Soeda, S. Takami, M. Minami and M. Satoh (2000). "Localization of calcitonin receptor mRNA in the mouse brain: coexistence with serotonin transporter mRNA." Brain Res Mol Brain Res **76**(1): 93-102.

Nakazato, M., N. Murakami, Y. Date, M. Kojima, H. Matsuo, K. Kangawa and S. Matsukura (2001). "A role for ghrelin in the central regulation of feeding." Nature **409**(6817): 194-8.

Nicholson, G. C., J. M. Moseley, P. M. Sexton, F. A. Mendelsohn and T. J. Martin (1986). "Abundant calcitonin receptors in isolated rat osteoclasts. Biochemical and autoradiographic characterization." J Clin Invest **78**(2): 355-60.

Nishi, Y., N. Kitamura, M. Otani, E. Hondo, K. Taguchi and J. Yamada (2000). "Distribution of capsaicin-sensitive substance P- and calcitonin gene-related peptide-immunoreactive nerves in bovine respiratory tract." Anat Anz **182**(4): 319-26.

Nishino, S., J. Arrigoni, J. Shelton, T. Kanbayashi, W. C. Dement and E. Mignot (1997). "Effects of thyrotropin-releasing hormone and its analogs on daytime sleepiness and cataplexy in canine narcolepsy." J Neurosci **17**(16): 6401-8.

Njuki, F., C. G. Nicholl, A. Howard, J. C. Mak, P. J. Barnes, S. I. Girgis and S. Legon (1993). "A new calcitonin-receptor-like sequence in rat pulmonary blood vessels." Clin Sci (Lond) **85**(4): 385-8.

Nohr, D., M. K. Schafer, S. Persson, H. Romeo, F. Nyberg, C. Post, G. Ekstrom and E. Weihe (1999). "Calcitonin gene-related peptide gene expression in collagen-induced arthritis is differentially regulated in primary afferents and motoneurons: influence of glucocorticoids." Neuroscience **93**(2): 759-73.

Okuma, Y., Y. Osumi, T. Ishikawa and T. Mitsuma (1987). "Enhancement of gastric acid output and mucosal blood flow by tripeptide thyrotropin releasing hormone microinjected into the dorsal motor nucleus of the vagus in rats." Jpn J Pharmacol **43**(2): 173-8.

Olney, J. W. (1969). "Brain lesions, obesity, and other disturbances in mice treated with monosodium glutamate." Science **164**(880): 719-21.

Orcel, P., H. Tajima, Y. Murayama, T. Fujita, S. M. Krane, E. Ogata, S. R. Goldring and I. Nishimoto (2000). "Multiple domains interacting with Gs in the porcine calcitonin receptor." Mol Endocrinol **14**(1): 170-82.

Patel, S. M. and I. S. Ebenezer (2004). "The effects of intraperitoneal and intracerebroventricular administration of the GABAB receptor antagonist CGP 35348 on food intake in rats." Eur J Pharmacol **503**(1-3): 89-93.

Peever, J. H., Y. Y. Lai and J. M. Siegel (2003). "Excitatory effects of hypocretin-1 (orexin-A) in the trigeminal motor nucleus are reversed by NMDA antagonism." J Neurophysiol **89**(5): 2591-600.

Plata-Salaman, C. R. (2000). "Central nervous system mechanisms contributing to the cachexia-anorexia syndrome." Nutrition **16**(10): 1009-12.

Plata-Salaman, C. R. and Y. Oomura (1987). "Calcitonin as a feeding suppressant: localization of central action to the cerebral III ventricle." Physiol Behav **40**(4): 501-13.

Poyner, D. R., P. M. Sexton, I. Marshall, D. M. Smith, R. Quirion, W. Born, R. Muff, J. A. Fischer and S. M. Foord (2002). "International Union of Pharmacology. XXXII. The mammalian calcitonin gene-related peptides, adrenomedullin, amylin, and calcitonin receptors." Pharmacol Rev **54**(2): 233-46.

Qu, D., D. S. Ludwig, S. Gammeltoft, M. Piper, M. A. Pelleymounter, M. J. Cullen, W. F. Mathes, R. Przypek, R. Kanarek and E. Maratos-Flier (1996). "A role for melanin-concentrating hormone in the central regulation of feeding behaviour." Nature **380**(6571): 243-7.

Raybould, H. E., R. J. Gayton and G. J. Dockray (1988). "Mechanisms of action of peripherally administered cholecystokinin octapeptide on brain stem neurons in the rat." J Neurosci **8**(8): 3018-24.

Reidelberger, R. D., U. Arnelo, L. Granqvist and J. Permert (2001). "Comparative effects of amylin and cholecystokinin on food intake and gastric emptying in rats." Am J Physiol Regul Integr Comp Physiol **280**(3): R605-11.

Reidelberger, R. D., A. C. Haver, U. Arnelo, D. D. Smith, C. S. Schaffert and J. Permert (2004). "Amylin Receptor Blockade Stimulates Food Intake in Rats." Am J Physiol Regul Integr Comp Physiol.

Reimer, R. J. and R. H. Edwards (2004). "Organic anion transport is the primary function of the SLC17/type I phosphate transporter family." Pflugers Arch **447**(5): 629-35.

Riediger, T., H. A. Schmid, T. A. Lutz and E. Simon (2002). "Amylin and glucose co-activate area postrema neurons of the rat." Neurosci Lett **328**(2): 121-4.

Riediger, T., D. Zuend, C. Becskei and T. A. Lutz (2004). "The anorectic hormone amylin contributes to feeding-related changes of neuronal activity in key structures of the gut-brain axis." Am J Physiol Regul Integr Comp Physiol **286**(1): R114-22.

Rohrenbeck, A. M., M. Bette, D. C. Hooper, F. Nyberg, L. E. Eiden, B. Dietzschold and E. Weihe (1999). "Upregulation of COX-2 and CGRP expression in resident cells of the Borna disease virus-infected brain is dependent upon inflammation." Neurobiol Dis **6**(1): 15-34.

Rolls, E. T. and B. J. Rolls (1973). "Altered food preferences after lesions in the basolateral region of the amygdala in the rat." J Comp Physiol Psychol **83**(2): 248-59.

Rosin, D. L., M. C. Weston, C. P. Sevigny, R. L. Stornetta and P. G. Guyenet (2003). "Hypothalamic orexin (hypocretin) neurons express vesicular glutamate transporters VGLUT1 or VGLUT2." J Comp Neurol **465**(4): 593-603.

Rushing, P. A. (2003). "Central amylin signaling and the regulation of energy homeostasis." Curr Pharm Des **9**(10): 819-25.

Rushing, P. A., M. M. Hagan, R. J. Seeley, T. A. Lutz, D. A. D'Alessio, E. L. Air and S. C. Woods (2001). "Inhibition of central amylin signaling increases food intake and body adiposity in rats." Endocrinology **142**(11): 5035.

Rushing, P. A., M. M. Hagan, R. J. Seeley, T. A. Lutz and S. C. Woods (2000). "Amylin: a novel action in the brain to reduce body weight." Endocrinology **141**(2): 850-3.

Sakurai, T., A. Amemiya, M. Ishii, I. Matsuzaki, R. M. Chemelli, H. Tanaka, S. C. Williams, J. A. Richardson, G. P. Kozlowski, S. Wilson, J. R. Arch, R. E. Buckingham, A. C. Haynes, S. A. Carr, R. S. Annan, D. E. McNulty, W. S. Liu, J. A. Terrett, N. A. Elshourbagy, D. J. Bergsma and M. Yanagisawa (1998). "Orexins and orexin receptors: a family of hypothalamic neuropeptides and G protein-coupled receptors that regulate feeding behavior." Cell **92**(4): 573-85.

Sambrook, J. and D. W. Russell (2001). "Molecular cloning: a laboratory manual." Cold Spring Harbor Laboratory Press, Cold Spring Harbor, New York.

Schafer, M. K., H. Varoqui, N. Defamie, E. Weihe and J. D. Erickson (2002). "Molecular cloning and functional identification of mouse vesicular glutamate transporter 3 and its expression in subsets of novel excitatory neurons." J Biol Chem **277**(52): 50734-48.

Schafer, M. K.-H. and R. Day (1995). "In situ hybridization techniques to map processing enzymes." Methods in Neurosciences **23**: 16-23.

Schafer, M. K.-H., J. P. Herman and S. J. Watson (1993). "In situ hybridization histochemistry." In: Imaging Drug action in the brain (Edythe D. London, ed): 337-378.

Schoenfeld, T. A. and L. W. Hamilton (1981). "Disruption of appetite but not hunger or satiety following small lesions in the amygdala of rats." J Comp Physiol Psychol **95**(4): 565-87.

Schwaber, J. S., C. Sternini, N. C. Brecha, W. T. Rogers and J. P. Card (1988). "Neurons containing calcitonin gene-related peptide in the parabrachial nucleus project to the central nucleus of the amygdala." J Comp Neurol **270**(3): 416-26, 398-9.

Schwartz, M. W., J. C. Erickson, D. G. Baskin and R. D. Palmiter (1998). "Effect of fasting and leptin deficiency on hypothalamic neuropeptide Y gene transcription in vivo revealed by expression of a lacZ reporter gene." Endocrinology **139**(5): 2629-35.

Schwartz, M. W., E. Peskind, M. Raskind, E. J. Boyko and D. Porte, Jr. (1996). "Cerebrospinal fluid leptin levels: relationship to plasma levels and to adiposity in humans." Nat Med **2**(5): 589-93.

Schwartz, M. W., R. J. Seeley, S. C. Woods, D. S. Weigle, L. A. Campfield, P. Burn and D. G. Baskin (1997). "Leptin increases hypothalamic pro-opiomelanocortin mRNA expression in the rostral arcuate nucleus." Diabetes **46**(12): 2119-23.

Schwartz, M. W., S. C. Woods, D. Porte, Jr., R. J. Seeley and D. G. Baskin (2000). "Central nervous system control of food intake." Nature **404**(6778): 661-71.

Selbach, O., N. Doreulee, C. Bohla, K. S. Eriksson, O. A. Sergeeva, W. Poelchen, R. E. Brown and H. L. Haas (2004). "Orexins/hypocretins cause sharp wave- and theta-related synaptic plasticity in the hippocampus via glutamatergic, gabaergic, noradrenergic, and cholinergic signaling." Neuroscience **127**(2): 519-28.

Sexton, P. M., S. Houssami, J. M. Hilton, L. M. O'Keeffe, R. J. Center, M. T. Gillespie, P. Darcy and D. M. Findlay (1993). "Identification of brain isoforms of the rat calcitonin receptor." Mol Endocrinol **7**(6): 815-21.

Sexton, P. M., G. Paxinos, M. A. Kenney, P. J. Wookey and K. Beaumont (1994). "In vitro autoradiographic localization of amylin binding sites in rat brain." Neuroscience **62**(2): 553-67.

Sheward, W. J., E. M. Lutz and A. J. Harmar (1994). "The expression of the calcitonin receptor gene in the brain and pituitary gland of the rat." Neurosci Lett **181**(1-2): 31-4.

Shimada, M., N. A. Tritos, B. B. Lowell, J. S. Flier and E. Maratos-Flier (1998). "Mice lacking melanin-concentrating hormone are hypophagic and lean." Nature **396**(6712): 670-4.

Singewald, N. and A. Philippu (1998). "Release of neurotransmitters in the locus coeruleus." Prog Neurobiol **56**(2): 237-67.

Skofitsch, G., S. J. Wimalawansa, D. M. Jacobowitz and W. Gubisch (1995). "Comparative immunohistochemical distribution of amylin-like and calcitonin gene related peptide like immunoreactivity in the rat central nervous system." Can J Physiol Pharmacol **73**(7): 945-56.

Slisli, Y. and R. de Beaurepaire (1999). "Interleukin-1beta and calcitonin, but not corticotropin-releasing factor, alter sleep cycles when injected into the rat hypothalamic lateral paraventricular area." Neurosci Lett **265**(1): 29-32.

Small, C. J., Y. L. Liu, S. A. Stanley, I. P. Connoley, A. Kennedy, M. J. Stock and S. R. Bloom (2003). "Chronic CNS administration of Agouti-related protein (Agrp) reduces energy expenditure." Int J Obes Relat Metab Disord **27**(4): 530-3.

Smith, B. N., S. F. Davis, A. N. Van Den Pol and W. Xu (2002). "Selective enhancement of excitatory synaptic activity in the rat nucleus tractus solitarius by hypocretin 2." Neuroscience **115**(3): 707-14.

Stanley, B. G., S. E. Kyrkouli, S. Lampert and S. F. Leibowitz (1986). "Neuropeptide Y chronically injected into the hypothalamus: a powerful neurochemical inducer of hyperphagia and obesity." Peptides **7**(6): 1189-92.

Stephens, T. W., M. Basinski, P. K. Bristow, J. M. Bue-Valleskey, S. G. Burgett, L. Craft, J. Hale, J. Hoffmann, H. M. Hsiung, A. Kriauciunas and et al. (1995). "The role of neuropeptide Y in the antiobesity action of the obese gene product." Nature **377**(6549): 530-2.

Steward, C. A., T. L. Horan, S. Schuhler, G. W. Bennett and F. J. Ebling (2003). "Central administration of thyrotropin releasing hormone (TRH) and related peptides inhibits feeding behavior in the Siberian hamster." Neuroreport **14**(5): 687-91.

Storm-Mathisen, J., A. K. Leknes, A. T. Bore, J. L. Vaaland, P. Edminson, F. M. Haug and O. P. Ottersen (1983). "First visualization of glutamate and GABA in neurones by immunocytochemistry." Nature **301**(5900): 517-20.

Stratford, T. R. and A. E. Kelley (1997). "GABA in the nucleus accumbens shell participates in the central regulation of feeding behavior." J Neurosci **17**(11): 4434-40.

Suzuki, T., H. Kohno, T. Sakurada, T. Tadano and K. Kisara (1982). "Intracranial injection of thyrotropin releasing hormone (TRH) suppresses starvation-induced feeding and drinking in rats." Pharmacol Biochem Behav **17**(2): 249-53.

Swart, I., J. M. Overton and T. A. Houpt (2001). "The effect of food deprivation and experimental diabetes on orexin and NPY mRNA levels." Peptides **22**(12): 2175-9.

Takamori, S., P. Malherbe, C. Broger and R. Jahn (2002). "Molecular cloning and functional characterization of human vesicular glutamate transporter 3." EMBO Rep **3**(8): 798-803.

Tilakaratne, N., G. Christopoulos, E. T. Zumpe, S. M. Foord and P. M. Sexton (2000). "Amylin receptor phenotypes derived from human calcitonin receptor/RAMP coexpression exhibit pharmacological differences dependent on receptor isoform and host cell environment." J Pharmacol Exp Ther **294**(1): 61-72.

Tolcos, M., C. Tikellis, S. Rees, M. Cooper and P. Wookey (2003). "Ontogeny of calcitonin receptor mRNA and protein in the developing central nervous system of the rat." J Comp Neurol **456**(1): 29-38.

Tritos, N. A., J. W. Mastaitis, E. Kokkotou and E. Maratos-Flier (2001). "Characterization of melanin concentrating hormone and preproorexin expression in the murine hypothalamus." Brain Res **895**(1-2): 160-6.

Tschop, M., D. L. Smiley and M. L. Heiman (2000). "Ghrelin induces adiposity in rodents." Nature **407**(6806): 908-13.

Turkulov, V., N. Madle-Samardzija, A. Ilic, J. Vukadinov and G. Canak (1998). "[Herpes simplex and lymphocytic choriomeningitis viruses in infections of the central nervous system--clinical and cerebrospinal fluid characteristics]." Med Pregl **51**(9-10): 436-40.

Turton, M. D., D. O'Shea, I. Gunn, S. A. Beak, C. M. Edwards, K. Meeran, S. J. Choi, G. M. Taylor, M. M. Heath, P. D. Lambert, J. P. Wilding, D. M. Smith, M. A. Ghatei, J. Herbert and S. R. Bloom (1996). "A role for glucagon-like peptide-1 in the central regulation of feeding." Nature **379**(6560): 69-72.

van Rossum, D., D. P. Menard, A. Fournier, S. St-Pierre and R. Quirion (1994). "Autoradiographic distribution and receptor binding profile of [125I]Bolton Hunter-rat amylin binding sites in the rat brain." J Pharmacol Exp Ther **270**(2): 779-87.

Varoqui, H., M. K. Schafer, H. Zhu, E. Weihe and J. D. Erickson (2002). "Identification of the differentiation-associated Na+/PI transporter as a novel vesicular glutamate transporter expressed in a distinct set of glutamatergic synapses." J Neurosci **22**(1): 142-55.

Veale, P. R., R. Bhogal, D. G. Morgan, D. M. Smith and S. R. Bloom (1994). "The presence of islet amyloid polypeptide/calcitonin gene-related peptide/salmon calcitonin binding sites in the rat nucleus accumbens." Eur J Pharmacol **262**(1-2): 133-41.

Verbalis, J. G., R. E. Blackburn, G. E. Hoffman and E. M. Stricker (1995). "Establishing behavioral and physiological functions of central oxytocin: insights from studies of oxytocin and ingestive behaviors." Adv Exp Med Biol **395**: 209-25.

Viggiano, A., M. Monda, F. Fuccio and B. De Luca (2004). "Extracellular GABA in the medial hypothalamus is increased following hypocretin-1 administration." Acta Physiol Scand **182**(1): 89-94.

Wakerley, J. B., T. S. Juss, R. Farrington and C. D. Ingram (1990). "Role of the paraventricular nucleus in controlling the frequency of milk ejection and the facilitatory effect of centrally administered oxytocin in the suckled rat." J Endocrinol **125**(3): 467-75.

Wang, L., D. H. Saint-Pierre and Y. Tache (2002). "Peripheral ghrelin selectively increases Fos expression in neuropeptide Y - synthesizing neurons in mouse hypothalamic arcuate nucleus." Neurosci Lett **325**(1): 47-51.

Willesen, M. G., P. Kristensen and J. Romer (1999). "Co-localization of growth hormone secretagogue receptor and NPY mRNA in the arcuate nucleus of the rat." Neuroendocrinology **70**(5): 306-16.

Yamamoto, Y., Y. Ueta, Y. Date, M. Nakazato, Y. Hara, R. Serino, M. Nomura, I. Shibuya, S. Matsukura and H. Yamashita (1999). "Down regulation of the prepro-orexin gene expression in genetically obese mice." Brain Res Mol Brain Res **65**(1): 14-22.

Zhang, Y., R. Proenca, M. Maffei, M. Barone, L. Leopold and J. M. Friedman (1994). "Positional cloning of the mouse obese gene and its human homologue." Nature **372**(6505): 425-32.

8 Abbreviations

All units of measurement are abbreviated according to the International System of units (SI).

AC	adenylyl cyclase
Acb	accumbens ncl.
AgRP	Agouti-gene-related protein
AHA	anterior hypothalamic area
AHC	anterior hypothalamic area, central
AMPO	anterior medial preoptic ncl.
AP	area postrema
Arc	arcuate hypothalamic ncl.
BCIP	5-bromo-4-chloro-3-indolyl-phosphate-4-toluidine salt
BSA	acetylated bovine serum albumin
BST	bed nucleus of the stria terminalis
BSTIA	bed nucleus of the stria terminalis, intraamygdaloid div
CART	cocaine- and amphetamine-regulated transcript
CCK	cholecystokinin
CeM	central amygdaloid ncl., med div
CGRP	calcitonin-gene-related peptide
CNS	central nervous system
CRH	corticotropin-releasing hormone
CRLR	calcitonin receptor-like receptor
CT	calcitonin
DA	dorsal hypothalamic area
DAB	3,3 diaminobenzidine tetrahydrochloride
DEPC	diethyl pyrocarbonate
DMH	dorsomedial hypothalamic ncl.
DMSO	dimethyl sulfoxide
DMTg	dorsomedial tegmental area
dNTP	deoxynucleoside triphosphate
DR	dorsal raphe ncl.
DTgP	dorsal tegmental ncl., pericentral
DTT	dithiothreitol
EDTA	ethylene diaminetetraacetic acid
fr	fasciculus retroflexus
GABA	γ-aminobutyric acid
GAD	glutamate decarboxylase
Gi	gigantocellular reticular ncl.
GLP1	glucagon-like peptide 1

GPCR	G-protein-coupled receptor
HEPES	(2-Hydroxyethyl)-1-piperazineethanesulphonic acid
IPTG	Isopropylthio-β-D-galactoside
LA	lateroanterior hypothalamic ncl.
LC	locus coeruleus
LDTg	laterodorsal tegmental ncl.
LH	lateral hypothalamic area
LHb	lateral habenular ncl.
LPB	lateral parabrachial ncl.
LPGi	lateral paragigantocellular ncl.
LRt	lateral reticular ncl.
LSV	lateral septal ncl.
MCH	melanin-concentrating hormone
MdV	medullary reticular ncl., ventral
Me	medial amygdaloid ncl.
MeAD	medial amygdaloid nucleus, anterodorsal
MeAV	medial amygdaloid nucleus, anteroventral
MePD	medial amygdaloid nucleus, posterodorsal
MePV	medial amygdaloid nucleus, posteroventral
MnPO	median preoptic ncl.
MnR	median raphe ncl.
MPA	medial preoptic area
MPO	medial preoptic ncl.
MSH	melanocyte-stimulating hormone
NBT	4-nitroblue - tetrazol - chloride
NPY	neuropeptide Y
NTS	nucleus of the solitary tract
Pa4	paratrochlear ncl.
PaAP	paraventricular hypothalamic ncl., ant parvo
PACAP	pituitary adenylate cyclase-activating peptide
PCR	Polymerase chain reaction
PCRt	parvocellular reticular ncl.
Pe	periventricular hypothalamic ncl.
PeF	perifornical ncl.
PKC	protein kinase C
POMC	pro-opiomelanocortin
PPTg	pedunculopontine tegmental ncl.
PTH	parathyroid hormone
PVN	paraventricular hypothalamic ncl.
RAMP	receptor-activity-modifying-protein

RMg	raphe magnus ncl.
ROb	raphe obscurus ncl.
RPa	raphe pallidus ncl.
RtTg	reticulotegmental nucleus pons
SCh	suprachiasmatic ncl.
SDS	sodium dodecyl sulfate
SFO	subfornical organ
SHy	septohypothalamic ncl.
SPTg	subpeduncular tegmental ncl.
SSC	standard sodium citrate buffer
StHy	striohypothalamic ncl.
SubCD	subcoeruleus nucleus, dorsal
TEA	triethanolamine
TEMED	tetramethyl ethylene diamine
TESAP	3-(Triethoxysilyl) propylamine
TRH	thyrotropin-releasing hormone
Tris	Tris (hydroxymethyl) aminomethane
VGLUT	vesicular glutamate transporter protein
VMH	ventromedial hypothalamic ncl.
VTg	ventral tegmental ncl.
X-gal	5-bromo-4-chloro-3-indolyl-β-D-galactopyranoside
3V	third ventricle

9 Addendum

9.1 Financial support

This project was supported by grant BMB+F 01GS0118 to Prof. Weihe and Dr. Schäfer and DFG grant TE 307/2-1 to Dr. Schäfer.

9.2 Publications

Articles

1. Li Y, **Ji A**, Weihe E, Schafer MK (2004) Cell-specific expression and lipopolysaccharide-induced regulation of TNFa and TNF receptors in rat dorsal root ganglion. ***J Neurosci***. 24(43):9623-9631.
2. Bender F, Schnitzler M, Li Y, **Ji A**, Weihe E, Gudermann T, Schafer MK (2005) The temperature-sensitive ion channel TRPV2 is endogenously expressed in the primary sensory cell line F-11. ***Cellular Physiology and Biochemistry.*** 15:183-194

Abstracts

1. **Ji A**, Li Y, Peter M, Weihe E, Schafer MK (2003). Cell-specific expression of calcitonin receptor isoforms in hypothalamic neurons regulating feeding behaviour. Program No. 49.17. *2003 Abstract Viewer/Itinerary Planner.* Washington, DC: Society for Neuroscience.
2. Li Y, **Ji A,** Bender F, Bette M, Weihe E, Schafer MK (2001) Neuronal and non-neuronal expression of TNF receptors in rat dorsal root ganglion: effects of LPS. Soc Neurosci Abstr 27:52.2.
3. Li Y, **Ji A**, Bender F, Weihe E, Schafer MK (2001). Use of laser capture microdissection to identify cytokine- and cytokine receptor expressing cells in rat dorsal root ganglion. Abstract of European Laser-Capture-Microdissection Symposium, P10.
4. Li Y, **Ji A**, Bender F, Ulke C, Bette M, Weihe E, Schäfer MK (2001). Primary afferent neurons express proinflammatory cytokine receptor genes in rat dorsal root ganglion. Abstract of International Symposium Mechanisms of Neuro-Immune-Endicrine Interactions, P16.
5. Schafer MK, Li Y, **Ji A**, Ulke C, Weihe E (2002) Relevance of presynaptic IL-1 and TNF receptors on rat DRG neurons for immuno-nociceptive signaling. 1090-P6, Abstracts of 10th world congress of pain.
6. Bender F, Schnitzler M, Li Y, **Ji A**, Weihe E, Gudermann T, Schafer MK (2002) Expression and functional characterization of the vanilloid receptor-like trp channel vrl-1 in the primary sensory cell line f-11. program no. 48.23. *2002 abstract viewer/itinerary planner.* Washington, DC: Society for Neuroscience.
7. Li Y, **Ji A**, Schafer MK (2002) Toll-like receptor 4 is expressed by peptidergic presumed nociceptive neurons in rat dorsal root ganglion Program No. 46.19. *2002 Abstract Viewer/Itinerary Planner.* Washington, DC: Society for Neuroscience.

Submissions to GenBank

1. **Ji A**, Li Y., Bender F. and Schafer MK (2003) F-11 rat/mouse fusion cell line TRPV2 protein mRNA, complete cds. GenBank AY487844
2. Li Y **Ji A**, Schafer MK (2002) Rattus norvegicus TNFR2 mRNA, transcript variant 1, AF498039; transcript variant 2, AY191268; transcript variant 3, AY191269
3. Li Y, **Ji A**, Schafer MK (2002) Rattus norvegicus toll like receptor 2 mRNA, transcript variant 1, AY151255; transcript variant 2, AY151256
4. Li Y, **Ji A**, Schafer MK (2002) Rattus norvegicus toll like receptor 9 mRNA, complete cds. GenBank AY191271.
5. Li Y, **Ji A**, Schafer MK (2002) Rattus norvegicus myeloid differentiation primary response gene 88 (MyD88), complete cds. GenBank AY191270
6. Li Y, **Ji A**, Schafer MK (2001) Rattus norvegicus CGRP-receptor component protein mRNA, complete cds. GenBank AF440799.

9.3 Akademische Lehrer

Meine akademischen Lehrer in Marburg waren die Damen und Herren:

Aumüller, Beato, Besedovsky, Cetin, Gemsa, Heeg, Krieg, Müller, Oertel, Schäfer,

Seitz, Steiniger, Suske, Voigt, Weihe, Westermann.

9.4 Lebenslauf

Persönliche Daten

Name	Ailing Ji
Anschrift	Am Richtsberg 88/209, 35039 Marburg E-Mail: ji@staff.uni-marburg.de
Geburtsdatum	10.09.1965
Geburtsort	Luoyang, Henan, VR China
Familienstand	verheiratet

Schulbildung

Grundschule und Weiterführende Schule	*No 3 High School of Luoyang*, Luoyang, Henan, VR China, September 1980 - Juli 1983
Studium	Biologie an *der Henan Normal University*, 09/1983 - 07/1987, Abschluß mit dem Bachelor Degree Aufnahmeprüfung zum Masters-Studiengang am *Beijing Normal University*, 09/1987 - 07/1990 , Abschluß mit dem Masters Degree Titel der Masters-Arbeit: „**A study on the effect of PI turnover in the ts 6m2 cell proliferation and transformation**“
Promotion	March 2003 - April 2005 Experimentelle Untersuchungen zum Thema: „**Pathway-specific expression of calcitonin receptors in hypothalamic and brain stem nuclei regulating food intake and transcriptomic changes in hypothalamic orexin neurons after fasting**“ am *Institut für Anatomie und Zellbiologie der Universität Marburg*

9.5 Acknowledgements

I would like to express my deep gratitude to my mentor, Dr. Martin K.-H. Schäfer. He made great efforts in supporting me during my studies here in Marburg. He has always been available to give me advice founded in his broad professional knowledge and wealth of technical expertise, to discuss critically the research progress, and to help me to tackle all scientific challenges. I really appreciate his care and support he has given me not only to ensure my professional development but also my successful integration in Marburg and his help with the management of all administration matters concerning my status as PhD student, employee of the Philipps-University Marburg and foreign resident.

I am indebted to Dr. Birgit Samans, IMT, formerly at the Institute of Medical Biometry and Epidemiology, Philipps-University Marburg, for performing the analysis of the microarray data, and the productive collaboration during my involvement in the NGFN1 project.

I also thank Jörn Wessels, AG Klingenspor, Department of animal physiology, for teaching me the use of the Affymetrix fluidics station and the chip hybridization procedures.

I am grateful to PD. Dr. Jörg Kämper at the MPI for Terrestrial Microbiology for giving me access to the Fluidics station.

I would like to thank Dr. Joanna Mika for her instructions to use the MCID image analysis software to perform the semi-quantitative analysis of the ISH results, and Dr. Annette Bieller for the very helpful discussions about technical problems regarding molecular biological procedures.

Special thanks should go to Dr. Micheal Bette, Dr. Ulrich Rausch and particularly to Uwe Schneider for their efforts to manage the internet network and keeping me online. This was extremely helpful for preparing this thesis.

My deep gratitude goes to Nadschman Asami, Barbara Wiegand, Romy Weber and Annette Seip for their day to day support in the laboratory work and for managing the ordering of reagents.

I am particularly grateful to Heidi Hlawaty for teaching me cutting cryosections and for her support in the laboratory work and to Michael Schneider for his help the organization of the animal experiments with tissue preparation.

I am grateful to Frau Marion Zibuschka and Frau Elke Rodenberg-Frank for teaching me immunohistochemical procedures and to Frau Petra Lattermann for teaching me cutting paraffin sections.

I would like to thank Frau Heike Reichert-Preibsch for her assistance in the cell culture laboratory and teaching me good laboratory practice and to Frau Heidemarie Schneider for support in the photographic documentation.

I would like to give special thanks to Dr. Johannes Tebbe who taught me how to make the microinjection in rat brain.

Last not least I would like to say a very special thank you to Prof. Dr. Eberhard Weihe, Head of the Department of Molecular Neuroscience, not only for giving me the privilege to work with him and learn from him, but also for his most generous support, his continuous and time-consuming efforts to find financial support for my research activities, his valuable scientific advice and his critical, but most constructive comments of preparing this thesis. I consider myself very fortunate that he taught me critical scientific thinking and that he was willing to share with me his scientific visions on the neurosciences. I have learned a lot from him of the scientific attitude, never give up.